Kristian Olof Ejdfors

Use of in-service data to determine the added power of a ship due to fouling

Master's thesis in Marine Technology
Supervisor: Sverre Steen
June 2019

Master's thesis

NTNU
Norwegian University of Science and Technology
Faculty of Engineering
Department of Marine Technology

NTNU
Norwegian University of
Science and Technology

Kristian Olof Ejdfors

Use of in-service data to determine the added power of a ship due to fouling

Master's thesis in Marine Technology
Supervisor: Sverre Steen
June 2019

Norwegian University of Science and Technology
Faculty of Engineering
Department of Marine Technology

NTNU
Kunnskap for en bedre verden

NTNU Trondheim
Norwegian University of Science and Technology
Department of Marine Technology

MASTER THESIS IN MARINE TECHNOLOGY

SPRING 2019

FOR

Kristian Olof Ejdfors

Use of in-service data to determine the added power of a ship due to fouling

Ships are increasingly equipped with automatic data collection systems to collect a large number of variables describing the performance of the ship and its systems. In a hydrodynamic context, variables such as speed over ground, speed through water, position, wind speed and direction, shaft speed and power, air and water temperature are examples of interesting and commonly collected variables. The collected data are often transferred to the ship operator's office for further analysis, but currently, there is a lack of routines and methods to utilize these data in an efficient way.
It is of interest to ship owners and operators to know which speed they can expect their ship to achieve on different routes and with increasing time since last hull and/or propeller cleaning (the effect of hull and propeller roughness is significant). In this master thesis, methods to determine the added power of a ship due to fouling shall be formulated and tested, using in-service data of real ships.

In the thesis, the in-service data shall be described in detail. The data processing performed shall be described, and methods used in the processing be properly documented. Different methods to determine the added power shall be formulated and the results compared, in order to recommend the best method for the studied case(s).

In the thesis the candidate shall present his personal contribution to the resolution of problem within the scope of the thesis work.

Theories and conclusions shall be based on mathematical derivations and/or logic reasoning identifying the various steps in the deduction.

The thesis work shall be based on the current state of knowledge in the field of study. The current state of knowledge shall be established through a thorough literature study, the results of this study shall be written into the thesis. The candidate should utilize the existing possibilities for obtaining relevant literature.

The thesis shall be organized in a rational manner to give a clear exposition of results, assessments, and conclusions. The text should be brief and to the point, with a clear language. Telegraphic language should be avoided.

The thesis shall contain the following elements: A text defining the scope, preface, list of contents, summary, main body of thesis, conclusions with recommendations for further work, list of symbols and acronyms, reference and (optional) appendices. All figures, tables and equations shall be numerated.

NTNU Trondheim
Norwegian University of Science and Technology
Department of Marine Technology

The supervisor may require that the candidate, in an early stage of the work, present a written plan for the completion of the work. The plan shall include a budget for the use of laboratory or other resources that will be charged to the department. Overruns shall be reported to the supervisor.

The original contribution of the candidate and material taken from other sources shall be clearly defined. Work from other sources shall be properly referenced using an acknowledged referencing system.

The thesis shall be submitted electronically (pdf) in Inspera:

- Signed by the candidate
- The text defining the scope (this text) (signed by the supervisor) included

The candidate will receive a printed copy of the thesis.

Supervisor : Professor Sverre Steen
Start : 15.01.2019
Deadline : 11.06.2019

Trondheim, 15.01.2019

Sverre Steen
Supervisor

Preface

This master thesis takes on the topic of how in-service performance monitoring data can be used to determine the added power due to fouling. It is the final work done in a five years integrated master program in Marine Technology at Norwegian University of Science and Technology (NTNU) in Trondheim. The work has been carried out during the spring of 2019, and it is a part of the hydrodynamic specialization.

The theme for this master thesis was one of many available topics proposed by the Institute of Marine Technology. I chose the topic of performance monitoring of ships because I find it interesting, and I formed it to have a focus on the added power due to fouling. I would like to thank my supervisor, Professor Sverre Steen. He proposed this topic and has helped me with guidance meetings thought out the semester. I would also like to thank Hans Anton Tvete from DNV GL, which provided me with the performance monitoring data and AIS data for the studied vessel.

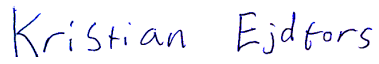

Kristian Olof Ejdfors
June 6, 2019
Trondheim

Summary

The focus on energy efficiency is increasing in the world today, and the shipping industry is no exemption. New and stricter regulations concerning emissions is one clear example of this. Today, ships are increasingly fitted with automatic data collection systems, and the development of information technology and communication allows these data to be communicated to an on-shore team automatically. So that ship owners and operators can utilize this data to ensure more efficient operations of the vessels. In this thesis, the focus is on how to utilize performance monitoring data to determine the added power of a ship due to fouling. The objective is to develop different methods to determine the added power and test them using in-service data from a real ship.

In-service performance data for a 2500 Twenty-foot Equivalent Unit (TEU) container ship are acquired and used for analysis in this thesis. The collected data are from an automatic data collection system with a sampling period of 15 minutes. The vessel is five years old, and performance monitoring data for the whole lifetime of the vessel are acquired. The Automatic Identification System (AIS) database is used to obtain location data, and the European Center for Mid-range Weather Forecasts (ECMWF) database is used to acquire weather data. All the different data sources had various sampling periods, which means that some initial processing had to be done in order to combine the data. Parameters used in the analysis were; timestamp, shaft power, shaft speed, draft, ship speed, significant wave height, wave period, wave direction, wind speed, wind direction, longitude, and latitude.

In this thesis, three methods to determine the added power due to fouling by using in-service performance monitoring data are developed. Method 1 and 2 use different methods to account for environmental effects such as wave and wind resistance, but they both evaluate the change in the Admiralty coefficient and the resistance coefficient over time. Method 1 removes the data points with bad weather, which means wind speeds higher than 5.5 m/s and significant wave heights over 1 meter. Method 2 includes the data point with bad weather but compensates for the wind and wave resistance by applying methods described in the ISO 15016 standard. However, the limitations for the environmental condition in the standard are followed in Method 2, which mean that a maximum significant wave height of 3 meters is implemented. Method 3 is a little bit different than Method 1 and 2. It uses machine learning in order to predict the shaft power based on input data containing information about the loading condition, speed, and environmental condition. Then the change in relative prediction error over time is evaluated to determine the added power rate and the added power due to fouling because the models are trained on a dataset containing values form the first year of operation, where the fouling is assumed to be small. Two different regression models were used, a custom linear regression model and a Gaussian regression process.

The added power was found by determining the trend lines based on the data from the methods. The ship had three propeller cleanings and one hull cleaning in the given period, so trend lines were calculated based on data between each event resulting in five successive trend lines for each model. The different models yielded some variations in the trend lines. However, at the end of the period, all the trend lines gave an added power between 19 and 30 %, which was compared with experimental values for a hull with similar conditions and found to be a reasonable prediction. Most of the lines give a slope (added power rate) that follows the theory as well.

Method 1 had some difficulties regarding the few available data points in some periods, which gave negative trend lines between the two last propeller cleanings. The assumption that the relative prediction error from Method 3 could be interpreted as the added power was not so reasonable, as it was found that the vessel changed operating condition over time. This change provides a larger prediction error regardless of the condition of the hull, as the machine learning model was not adequately trained on the new operating condition. These two concerns gave that Method 2 with the Admiralty coefficient model was recommended as the best model. Further, in order to improve the model, a benchmark model that takes into account different loading conditions should be implemented. It is also recommended that a cost function which takes into account the economic cost of a propeller and hull cleaning, as well as the potential savings in the reduction of the added power is developed. This cost function can then be used by ship owners and operators to decide when a propeller or hull cleaning should be conducted.

Sammendrag

Det er et økende fokus på energi effektivitet i verden og shipping industrien er ikke noe unntak. Nye og strengere regler om utslipp er ett eksempel på dette. Flere og flere skip blir utstyrt med automatiske data samlings systemer og nylig utvikling i informasjons og kommunikasjons teknologi gjør at disse dataene automatisk blir sendt til teamet på land for videre analyser. Dette gir muligheter for redere og skips operatører til å bruke disse dataene til å gi mer effektiv operasjon av skipene. I denne avhandlingen ligger fokuset på hvordan man kan bruke disse dataene til å bestemme tilleggs effekt behovet til et skip på grunn av begroing. Avhandlingen går ut på å utvikle forskjellige metoder for å determinere denne tilleggs effekten og teste de metodene på ytelses data fra ett virkelig skip.

I denne master oppgaven er ytelses data for et 2500 TEU kontainer skip brukt. Dataen kommer fra ett automatisk datasamlings system som logger data hvert 15 minutt. Skipet er 5 år gammelt og ytelses dataen er for hele levetiden til skipet. I tillegg er lokasjons data fra AIS databasen og vær data fra European Center for Mid-range Weather Forecasts (ECMWF) brukt i analysen. Dataene fra de tre forskjellige data kildene ble kombinert og prosessert slik at uønskede verdier, som da skipet akselererer er fjernet. De forskjellige parameterne som ble brukt i analysen var; motor kraft, omdreininger per minutt, dypgang, hastighet, signifikant bølge høyde, bølge periode, bølge retning. vind hastighet, vind retning, lengdegrad og breddegrad.

Tre forskjellige metoder for å determinere tilleggs effekten på grunn av begroing ved bruk av ytelses data ble utviklet. Både Metode 1 og 2 evaluerer endringen i Admiralitets koeffisienten og motstands koeffisienten over tid, men de bruker forskjellige metoder for å redegjøre for vær effektene. Metode 1 tar bort data punkter som kan klassifiseres som dårlig vær, altså at vind styrken er under 5.5 sekundmeter og signifikant bølgehøyde er under 1 meter. Metode 2 inkluderer data punktene med dårlig vær men tar bort ekstra motstanden fra været ved hjelp av metoder beskrevet i ISO 15016. Metode 3 er litt annerledes da den bruker maskin lærings metoder til å predikere motor kraften basert en rekke parameter som beskriver operasjons tilstanden til skipet samt været. Forskjellen i relative prediksjons feil over tid er så analysert til å finne effekten av begroing. To forskjellige regresjons modeller ble bruk, nemlig en egendefinert linjer regresjons modell og Gaussian regresjons prosess.

Tilleggs effekten ble funnet ved å lage trend linjer basert på resultatene fra de forskjellige metodene. Propellen ble vasket tre ganger og skroget en gang i løpet av den gitte perioden. Trend linjene ble derfor funnet basert på dataene mellom disse begivenhetene, dette gave fem trendlinjer per metode. De forskjellige metodene gav forskjellige trend linjer, men alle metodene gav en tilleggs effekt på grunn av begroing mellom 19 og 30 % i slutten av tidsperioden. Detter er i samsvar med erfaringer fra andre skip. De fleste linjene har også et stignings tall som er i samsvar med teorien. Metode 1 har noen problemer med antall data, noe som gir negative trend linjer mellom de to siste propell rengjøringene. Noen av antagelsene Metode 3 er bygget på viste seg å ikke være så bra for dette data settet. Dette gir at Metode 2 basert på Admiralitets koeffisienten er anbefalt som den beste metoden.

Videre er det anbefalt å implementere en ny referanse modell som inkluderer last kondisjonen for å forbedre Metode 1 og 2. Det er også anbefalt å lage en kostfunksjon som baserer seg på resultatene fra metodene gitt i denne master oppgaven til å finne potensielle besparelser en propell eller skrog vask

kan gi. Dette kan da bli brukt til å optimalisere tiden mellom propell og skrog vask og dermed gi store besparelser i form av redusert drivstoff forbruk.

Contents

List of Figures

List of Tables

Abbreviations

Acronyms

AHR Average Hull Roughness

CFD Computational Fluid Dynamics

CWT Circulating Water Tunnel

ECMWF European Centre for Medium-Range Weather Forecasts

EEDI Energy Efficiency Design Index

EU European Union

GPS Global Positioning System

ICT Information and Communications Technology

IMO International Maritime Organization

ISO International Organization for Standardization

ITTC International Towing Tank Conference

MHR Local Mean Hull Roughness

ROV Remotely Operated Vehicle

RPM Rounds per Minute

SOG Speed Over Ground

SPC Self-Polishing Co-polymer

STA-JIP Sea Trial Analysis - Joint Industry Project

STW Speed Through Water

TBT Tributyltin

Greek

Δ Weight Displacement

η_0 Open Water Efficiency

η_D Quasi-Propulsive Coefficient

η_H Hull Efficiency

η_M Mechanical Efficiency

η_R Relative Rotational Efficiency

∇ Volume Displacement

ν Kinematic Viscosity

ν^* Wall Friction Velocity

ω Circular Frequency of Regular Waves

ψ_{WRef} Relative Wind Direction

ρ Density of Seawater

ρ_a Density of Air

ρ_m Density of Water During Model Test

τ_w Friction Stress on the Hull Surface

Lowercase

$\overline{u}$ Mean Longitudinal Velocity on the Boundary Layer

g Acceleration of Gravity

h Water Depth

k Form Factor

k Wave Number

k_s Hull Surface Roughness

k_{yy} Non-Dimensional Radius of Gyration in Lateral Direction

m_0 Zero Spectral Moment

m_1 First Spectral Moment

m_2 Second Spectral Moment

n Rotational Speed

w_j Weight Function

Uppercase

R Resistance due to Environmental Effects

ΔC_F Roughness Allowance

ΔV Speed Loss due to Shallow Water

A_M	Midship Section Area Under Water
A_{XV}	Transverse Projected Area Above the Water Line Including Superstructures
B	Breadth of Ship
C_A	Correlation Allowance
C_B	Block Coefficient
C_F	Frictional Resistance Coefficient
C_W	Wave Resistance Coefficient
C_{AAS}	Air Resistance Coefficient for the Ship
C_{AA}	Wind Resistance Coefficient
C_{Fm}	Frictional Resistance Coefficient for the Model
C_{Fs}	Frictional Resistance Coefficient for the Ship
C_{Tm}	Total Resistance Coefficient for the Model
C_{Ts}	Total Resistance Coefficient for the Ship
D	Draft
F_n	Froude Number
$H_{1/3}$	Significant Wave Height
H_S	Significant Wave Height
L	Characteristic Length
L_{BWL}	Distance of the Bow to 95% of Maximum Breadth
L_{PP}	Length Between Perpendiculars
L_{WL}	Waterline Length
P_B	Break Power or Shaft Power
P_D	Delivered Power
P_E	Effective Power
Q	Shaft Torque
R_e	Raynold Number
R_T	Total Resistance
R_{AA}	Added Resistance due to Wind
R_{AS}	Resistance due to Change in Water Temperature and Density
R_{AWL}	Added Resistance due to Waves

R_{AWML} Added Resistance due to Motion Caused by Inncomming Wave

R_{AWRL} Added Resistance due to Wave Reflection

R_{CW} Calm Water Resistance

$R_{Fouling}$ Resistance due to Roughness of Fouling

R_{Tm} Total Resistance Model Scale

S Wetted Surface Area

S_m Wetted Surface Area Model Scale

S_η Wave Spectrum

T_M draft Midships

T_{02} Zero Crossing Period

T_{AP} draft at Aft Perpendicular

T_{FP} draft at Fore Perpendicular

V_S Vessel Speed

V_G Ship Speed Over Ground

V_m Model Speed

V_{WRef} Relative Wind Velocity

AIS Automatic Identification System

NO_x Nitrogen Oxides

SO_x Sulfur Oxides

Chapter 1

Introduction

1.1 Background

Fouling on ships has always been an important factor for ship performance. Even in the early days of sail were the issues of fouling well known and the vessels were sailed upriver or beached in order to remove the marine growth on the hull. Today ships are docked in dry docks to be cleaned and fitted with new antifouling coating. In between the dry docking, divers or robots are used to clean the hull while the ships are in port. Fouling increases the resistance of the hull and decreases the propeller efficiency, both increasing fuel consumption [1]. The added resistance due to fouling on the hull and propeller varies from 6% to 80 % of the total resistance [2]. On average an added resistance of 30% is common for an ocean-going vessel if no special attention is paid to it [3]. Even a thin slime layer can increase the local skin friction by 25% compared to a clean hull [4]. This shows that fouling is a major contributor to the operational performance of a vessel.

Energy efficiency and reduced emissions have become more and more important in recent years. The International Maritime Organization (IMO) has ratified stricter environmental regulations for emissions from ships, for example restrictions in NO_x and SO_x emissions [5]. With the Energy Efficiency Design Index (EEDI), IMO aims to provoke more energy efficient ship designs [6]. Shipping companies also want to save money on fuel costs and be able to market themselves as a green alternative. It is therefore of interest to ship owners and operators to know the effect of added resistance due to fouling in order to predict the fuel consumption, the attainable speed and optimizing the time between hull cleanings.

More and more ships today are equipped with automatic data collection systems describing the performance of the ship and its systems. It is of interest to utilizing this data to ensures more effective operation. Some of the parameters collected can be used to find the added resistance due to fouling [7]. However, currently there is no standardized way to do this, but some solutions exist such as Propulsion Dynamic´s CASPER [3] and BMT SeaTech´s SMART system [8]. These solutions use collected data to monitor the ship performance by comparing the performance with historical data and sea trial results. Other methods of determining the added resistance due to fouling are to use added resistance diagrams which adjusts the speed power diagram for the effect of fouling based on statistical models [3, 7]. Utilizing performance monitoring data to determine the effect of fouling is also in the interest of companies that specialize in antifouling systems so they can evaluate how well their solution work. Its estimated (based on some broad assumptions) that if the global fleet shift to the best antifouling coating available to the vessels a global saving in fuel consumption and thereby air emissions by 7 to 10 % [6]. As the shipping industry accounts for 3.1 % of the global CO_2 emissions [9], will this result in a significant decrease in the global greenhouse gas emissions.

1.2 Objective

The objective of this thesis is to develop different methods to determine the added power of a ship due to fouling and test them using in-service data from a 2500 TEU container ship. The results from the different methods shall be compared with another in order to recommend the best method for the studied case. The in-service data used shall be described in detail, and the data processing performed and methods used in the processing shall be properly documented.

1.3 Structure

This master thesis consists of 10 chapters with the structure given below. Chapters 2-5 are largely based on work carried out by the author in the project thesis [10].

Chapter 2 presents the theory behind ship resistance and powering. Both the concept of calm water resistance and the effect of environmental factors like wind, waves, and current are presented.

Chapter 3 covers the topic of fouling. It includes a description of the different kinds of fouling, how it can be measured, and how one can determine the resistance due to fouling. A presentation of different antifouling systems is also included.

Chapter 4 takes on the topic of performance monitoring of ships with a focus on how to collect and use the data. At the end of the chapter are some examples of performance monitoring systems used today presented.

Chapter 5 gives a brief introduction to machine learning and how to use it in regression analysis. How to split a data set into a training set and a validation set is presented as well as methods to prevent over and under fitting.

Chapter 6 presents the data used in the analysis. The data set consists of data from three different sources, and a presentation of the different data sources is given as well as a description of the content and how it has been processed.

Chapter 7 presents the methods developed to determine the added power due to fouling.

Chapter 8 presents the results from the analysis.

Chapter 9 gives a discussion about the methods used, the data set, and the results. It also gives a recommendation of the best method based on the results and discussion.

Chapter 10 presents the conclusions and recommendations for further work.

Chapter 2

Resistance and Powering

This chapter describes the basic theory behind ship resistance and powering. The chapter starts by describing calm water resistance and how it can be determined. Then some methods to determine the environmental effects on the ship's resistance is presented. Lastly, some theory about ship powering is presented. The theory described in this chapter is used to develop methods presented in Chapter 7.

2.1 Calm Water Resistance

To be able to determine the added resistance due to fouling, it is necessary to have an understanding of ship resistance. Ship resistance is a complex problem, so it is common to divide it and see what kinds of physical components it consists of. The simplest form of ship resistance is for a ship moving in calm water. Then the resistance can be considered as forces acting on the hull from the fluid, which can be subdivided into frictional resistance and pressure resistance [11] as seen below.

Frictional resistance
The frictional resistance is due to tangential shear forces acting on the hull. The tangential shear forces occur as skin friction between water and the hull, due to the viscosity of the water.

Pressure resistance
The pressure resistance is due to forces acting normal to the hull surface. The major part of the pressure resistance is the resistance caused by the ship's wave-making due to the pressure differences along the hull. Another part comes from viscous effects like 3D flow separation.

There are many different ways one can calculate the calm water resistance. Model testing and scaling the results is a standardized and well-known method [12]. Other methods include utilizing mathematical models based on empirical data from model tests and/or sea trials. Examples of such models are the Holtrop and Hollenbach. Software using CFD solvers have become more and more common as computational power has rapidly increased the recent years. These methods are not used in this thesis and will not be explained further. However, an extensive overview of such methods can be found in Molland's or Carlton's textbooks [11, 7]. In this thesis are some of the principles from model testing used, so an overview of this method is given below.

The main idea behind model testing is to tow a geometrically scaled model of the hull in a towing tank and to measure the towing force for different velocities. For a detailed description of how to execute a resistance test, see ITTC recommended practice [13]. To find the full-scale velocities Froude scaling is applied, which means similarity in Froude number. The Froude number is given by the equation

below.

$$F_n = \frac{V_S}{\sqrt{gL}} \tag{2.1}$$

The measured resistance is then expressed as a dimensionless resistance coefficient C_{Tm}.

$$C_{Tm} = \frac{R_{Tm}}{0.5\rho_m \ S_m V_m^2} \tag{2.2}$$

Where R_{Tm} is the measured towing force, ρ_m is the density of the water, S_m is the wetted surface area, and V_m is the towing speed. By applying the division above the total resistance coefficient for the model C_{Tm} becomes [11].

$$C_{Tm} = C_{Fm}(1+k) + C_{Wm} \tag{2.3}$$

C_{Fm} is the frictional resistance coefficient of the model and can be found according to the ITTC-1957 line, k is the form factor and C_{Wm} is the resistance coefficient for the wave making. When scaling to full scale it is assumed that the resistance due to wave making is the same i.e., the wave coefficient for the model and full scale is the same $C_{Wm} = C_{Ws} = C_W$ [11]. This assumption gives that the resistance coefficient for full scale becomes [12]

$$C_{Ts} = (1+k)C_{Fs} + \Delta C_F + C_A + C_W + C_{AAS} \tag{2.4}$$

Where C_{Fs} is the frictional resistance coefficient of the ship, ΔC_F is the roughness allowance, C_A is the correlation allowance, C_W is the wave resistance coefficient calculated from the model test by $C_W = C_{Tm} - (1+k)C_{Fm}$ and C_{AAS} is the air resistance coefficient for the full-scale ship. The roughness allowance ΔC_F accounts for the roughness of the hull. Since model testing estimates the resistance of a clean hull is the roughness allowance meant to compensate for the roughness of a clean hull. Thus, the surface roughness is assumed to be small (< 230 µm), and is usually set to 150 µm [11]. The flow around a ship hull is usually a fully rough flow. Then the frictional resistance and the roughness allowance $C_F + \Delta C_F$ becomes independent of the Reynolds number and only dependent on the surface roughness. The surface roughness on a fouled hull can be much larger than the estimated 150 µm for a clean hull, which means that other methods have to be used to determine the effect of fouling. A discussion about this is given in Chapter 3. As seen from Equation 2.4, the form factor k is essential when estimating the full-scale resistance based on a model test. There exist different methods to find the form factor and for an extensive overview, see Molland's textbook [11]. For more details about how to scale from model to full scale, see ITTC recommended procedures and guidelines [12].

2.2 Environmental Factors

As vessels are operating at sea, it often experiences conditions where waves, wind, and current are present. In order to separate the resistance due to fouling from the total resistance, it is necessary to account for these environmental resistance components. This compensation is also important for sea trials as a speed-power curve often is contracted for a specific sea state, usually calm water. Different procedures to compensate for environmental effects during a sea trial have been developed. Some examples are the ISO 15016 standard, and ITTC recommended procedures. MARIN [14] through the

STA-JIP project has also developed a set of recommended procedures for sea trials based on the ISO 19019 standard, and ITTC recommended the practice.

However, there exists also other methods to determine environmental effects. As waves usually have the most substantial impact on the added resistance due to environmental factors, are there many different methods to calculate the added resistance of waves. These methods can be split into two main approaches, the far-field and the near field approach. The far-field approach is based on momentum conservation, while the near field approach is based on direct pressure integration. Seo et al. [15] have performed a study where different methods such as strip theory, Rankine panel, and Cartesian grid method to find the added resistance in waves have been compared. A review of all the different methods to calculate added resistance due to environmental factors would be a study in itself and is thereby not performed.

In this thesis, it is chosen to focus on the methods given in the international standard ISO 15016 [16], which is an international guideline for assessment of speed and power performance by analysis of the speed trial data. As the standard is developed for sea trials, it has limitations regarding the magnitude of the sea state. The criteria to carry out a sea trial is for wind – maximum Beaufort 6 for $L_{PP} \geq 100$m and Beaufort 5 for $L_{pp} < 100$m. The Beaufort wind scale is a standard wind scale that relates wind speed to wave conditions. In addition it is limitations regarding the maximum significant wave height – for $L_{PP} \geq 100$m $H_S \leq 0.015 L_{PP}$ or 4 meters and $H_S \leq 1.5$ meter for $L_{pp} < 100$m. The environmental effect on the resistance is corrected in the following way in the standard.

$$R_{CW} = R_T - \Delta R \tag{2.5}$$

Where R_{CW} is the calm water resistance, R_T the total resistance and ΔR is the resistance due to environmental effects. ΔR is given by the equation below.

$$\Delta R = R_{AA} + R_{AWL} + R_{AS} \tag{2.6}$$

Where R_{AA} is the added resistance due to the wind, R_{AWL} is the added resistance due to waves and R_{AS} is the resistance due to water temperature and density deviations. The methods to calculate these parameters given in the ISO 15016 standard [16] are described in the following sections and will be used in the analysis of the performance monitoring data.

2.2.1 Wind Resistance

The added resistance due to the wind is related to the wind speed and cross section area above the waterline. As ships have large volumes above the waterline, the added resistance due to wind can be a significant part of the total resistance. The added resistance due to the wind is defined by the equation below.

$$R_{AA} = 0.5\rho_a \cdot C_{AA}(\psi_{WRef}) \cdot A_{XV} \cdot V_{WRef}^2 - 0.5\rho_a \cdot C_{AA}(0) \cdot A_{XV} \cdot V_G^2 \tag{2.7}$$

Where R_{AA} is the added wind resistance in newtons, ρ_a is the density of the air, $C_{AA}(\psi_{WRef})$ is the wind resistance coefficient for the relative wind direction, ψ_{WRef}, at a reference height (usually 10 meters above the free surface), $C_{AA}(0)$ is for headwind, A_{XV} is the transverse projected area above the waterline including superstructure, V_{WRef} is the wind velocity at the reference height, and V_G is the ship's speed over ground.

The wind velocity and direction changes often, so the input for Equation 2.7 is averaged over a given time. The wind resistance coefficients are either found by model tests in a wind tunnel or by using table data for similar ships, the latter being less accurate. Graphs for C_{AA} values for different relative wind angles and ship types are given in ISO Standard 15016 [16].

2.2.2 Wave Resistance

The ISO Standard 15016 [16] gives two different simplified methods for calculating the added resistance due to waves, STAWAVE-1 and STAWAVE-2. Both methods are based on representing irregular waves as a linear superposition of different regular waves. The first method is only valid for small heave and pitch motions, while the second model takes the effect of these motions into account.

STAWAVE-1

The effects of wave-induced motions are neglected in this method so that the wave reflection determines the added resistance. Equation 2.8 gives the added resistance for head sea (less than ± 45 degrees off the bow).

$$R_{AWL} = \frac{1}{16}\rho g H_{1/3}^2 B \sqrt{\frac{B}{L_{BWL}}} \tag{2.8}$$

Where R_{AWL} is the added resistance due to waves, ρ is the density of the seawater, $H_{1/3}$ is the significant wave height, B is the breadth of the ship and L_{BWL} is the distance from the bow to the 95% of the maximum breadth in the waterline. In order to use this approximation, the significant wave height has to be less than $2.25\sqrt{L_{pp}/100}$, and the heave and pitch motions have a maximum vertical acceleration at the bow less than $0.05g$. The criteria for head sea must also be satisfied, incoming waves less than ± 45 degrees off the bow.

STAWAVE-2

In this approach, the ship's heave and pitch motion due to the waves are taken into account. Thus, the total wave resistance is split into two components, R_{AWRL} due to wave reflection and R_{AWML} due to the motions.

$$R_{Wave} = R_{AWML} + R_{AWRL} \tag{2.9}$$

The reflection component is dominant for short waves while the motion component is dominant for longer waves as illustrated by the STA project [17] in Figure 2.1.

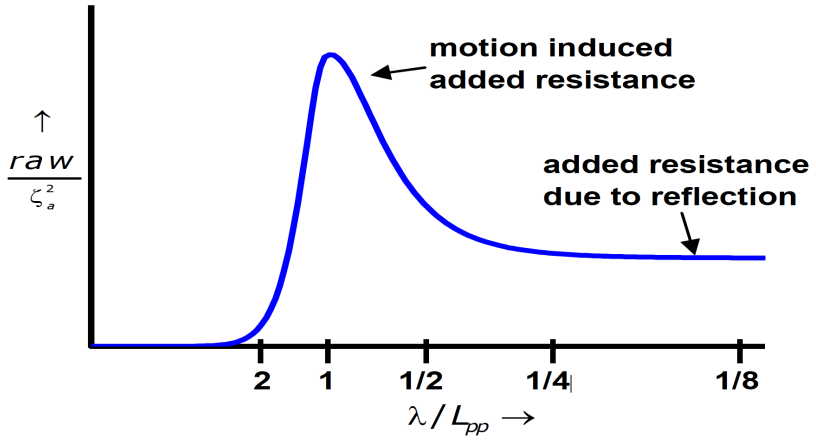

Figure 2.1: Added resistance in waves as a function of wave length over ship length [17]

The following equation calculates the motion component.

$$R_{AWML} = 4\rho g \zeta_A^2 \frac{B^2}{L_{PP}} \overline{r_{aw}}(\omega) \tag{2.10}$$

Where ζ_A^2 is the wave amplitude and $\overline{r_{aw}}(\omega)$ is defined by Equation 2.11.

$$\overline{r_{aw}}(\omega) = \overline{\omega}^{b_1} \exp\left[\frac{b_1}{d_1}\left(1 - \overline{\omega}^{d_1}\right)\right] a_1 F_n^{1.50} \exp\left(-3.50 Fn\right) \tag{2.11}$$

$\overline{\omega}$ is defined by the Equation 2.12, b_1 by Equation 2.13, a_1 by Equation 2.14 and d_1 by Equation 2.15

$$\overline{\omega} = \frac{\sqrt{\frac{L_{PP}}{g}}\sqrt[3]{k_{yy}}}{1.17 F_n^{-0.143}} \omega \tag{2.12}$$

Where k_{yy} is the non-dimensional radius of gyration in the lateral direction, and ω is the circular frequency of regular waves in radians per second.

$$b_1 = \begin{cases} 11 & for\ \overline{\omega} < 1 \\ -8.50 & elsewhere \end{cases} \tag{2.13}$$

$$a_1 = 60.3\ C_B^{1.34} \tag{2.14}$$

C_B is the block coefficient of the ship.

$$d_1 = \begin{cases} 14. & for\ \overline{\omega} < 1 \\ -566\left(\frac{L_{PP}}{B}\right)^{-2.66} & elsewhere \end{cases} \tag{2.15}$$

The reflection component R_{AWRL} is given by Equation 2.16.

$$R_{AWRL} = 0.5\rho g\zeta_A^2 B\alpha_1(\omega) \tag{2.16}$$

Where $\alpha_1(\omega)$ is defined by Equation 2.17

$$\alpha_1(\omega) = \frac{\pi^2 I_1^2(1.5kT_M)}{\pi^2 I_1^2(1.5kT_M) \ + \ K_1^2(1.5kT_M)} f_1 \tag{2.17}$$

I_1 is the modified Bessel function of the first kind of order 1, K_1 is the modified Bessel function of the second kind of order 1, k is the wave number, T_M is the draft midships, and f_1 is defined by the equation below.

$$f_1 = 0.692 \left(\frac{V_s}{\sqrt{T_M g}} \right)^{0.769} + 1.81 C_B^{6.95} \tag{2.18}$$

R_{Wave} is an empirical transfer function for the mean increase of resistance in regular waves. To obtain the mean increase of resistance in irregular waves, R_{AWL}, Equation 2.19 is applied.

$$R_{AWL} = 2 \int_0^{\inf} \frac{R_{Wave}}{\zeta_A^2} S_\eta(\omega) d\omega \tag{2.19}$$

S_η is the frequency wave spectrum in m^2/s, it depends on the location, but the Pierson-Moskowitz spectra is used for wind-generated waves. For the North-Sea it is common to use the JONSWAP spectra. These are two different standardized wave spectra. The limitations of the STAWE-2 method is that it is only valid for had sea, incoming waves less than $\pm$ 45 degrees of the bow. The following criteria must also be satisfied.

- $L_{PP} > 75$ m
- $4.0 < \frac{L_{PP}}{B} < 9.0$
- $2.2 < \frac{B}{T_M} < 9.0$
- $0.10 < F_n < 0.30$
- $0.50 < C_B < 0.90$

2.2.3 Effect of Current

The current will affect the ship's speed through water relative to the speed over ground. The ship resistance is proportional with speed through water squared [13], which means that the effect of current can be significant. One can take the difference between the vessel speed obtained from the GPS signal and the measured speed through water to find the speed of the current in the direction of the ship's movement. However, the sensors that measure the speed through water can be unreliable [18], and this difference should be checked with tables for current for the given area if it is available. If the difference between the speed through water and speed over ground is found to be caused by the current and not a faulty sensor. Then the speed through water measurements can be used in an analysis, and it is not necessary to compensate for the current. As the effect of the current on the ship's speed is measured directly by the speed through water sensor. In this thesis, the speed through water measurements was found to be reliable, and the effect of current is therefore not needed to be taken into account.

2.2.4 Effect of Water Temperature and Density

Water temperature and density affect the viscosity of water, which affects the ship resistance. The ISO standard [16] operates with a standard seawater temperature of 15 °C and density of 1026 $[kg/m^3]$. The effect of change in water temperature and density is defined in the ISO standard by the following equation.

$$R_{AS} = R_{T0}\left(\frac{\rho_s}{\rho_{s0}} - 1\right) + R_F\left(\frac{C_{F0}}{C_F} - 1\right) \tag{2.20}$$

Where ρ_s is the density of seawater for the actual temperature and salt content, ρ_{s0} is the standard density, C_F is the frictional coefficient for the actual water temperature and density, C_{F0} is the frictional coefficient for the reference temperature and density and R_{T0} is the total resistance for the reference water temperature, and density is given by Equation 2.21 and R_F is the frictional resistance for the actual water temperature and density given by Equation 2.22.

$$R_{T0} = 0.5\rho_{s0}SV_S^2 \cdot C_{T0} \tag{2.21}$$

$$R_F = 0.5\rho_s SV_S^2 \cdot C_F \tag{2.22}$$

However, as temperature measurements were not available in the performance monitoring data set was the above method for compensation for temperature and density deviations not used.

2.2.5 Effect of Shallow Water

If the ship operates in shallow water, the effect of shallow water will decrease the ship's speed. Therefore it is common to account for this during sea trials [17]. The ISO standard proposes the following method to account for the speed loss due to the effect of shallow water.

$$\frac{\Delta V}{V_S} = 0.124 \cdot 2\left(\frac{A_M}{h^2} - 0.05\right) + 1 - \left(tanh\left(\frac{gh}{V_S^2}\right)\right)^{0.5} \qquad for\ \frac{A_M}{h^2} \geq 0.05 \tag{2.23}$$

Where ΔV is the speed loss due to shallow water, A_M is the midship section area under water, and h is the water depth. However, as the vessel operates deep sea and water depth measurements were not available in the performance monitoring data set was the above method for compensation for shallow water not used.

2.3 Powering

The resistance as a force is not measured on board a ship, so it is necessary to relate the resistance as a force to the power and speed of the vessel. This relationship is established by defining the effective power P_E as the product of the total ship resistance R_T and the ship's speed V_S, as given by Equation 2.24.

$$P_E = R_T \cdot V_S \tag{2.24}$$

The effective power is the power needed to tow the vessel at the given speed. The delivered power P_D is the power delivered to the propulsion unit at the tail shaft [11]. A performance monitoring system can measure this by measuring the torque and rotational speed and using the relationship given in Equation 2.25.

$$P_D = 2\pi\ nQ = \frac{P_E}{\eta_D} \tag{2.25}$$

Where Q is the torque delivered by the shaft, n is the rotational speed of the shaft. It is also shown by Equation 2.25 that the delivered power can be found by using the relationship between the effective power P_E and the quasi-propulsive efficiency coefficient η_D [11]. η_D depends on the efficiency of the propulsive-device and the hull-propeller interaction. So, η_D defines the losses that occur between the actual towing power P_E and the power delivered at the tail shaft P_D. It is determined by

$$\eta_D = \eta_0\ \eta_H\ \eta_R \tag{2.26}$$

where η_0 is the open water efficiency, η_H is the hull efficiency, and η_R is the relative rotational efficiency. A detailed description of how these efficiency coefficients are calculated can be found in Molland's and Carlton's textbooks [11, 7] . Another important relationship is the relationship between the brake power P_B and the delivered power P_D, and it is given by

$$P_B = \frac{P_D}{\eta_M} \tag{2.27}$$

where η_M is the mechanical efficiency, which contains the losses in the transmission between the engine and the tail shaft i.e., the gear and shaft, both the brake power and the delivered power can be measured by the aboard performance monitoring system. The aboard performance monitoring systems often give something called the shaft power, which can be placed somewhere in between P_D and P_B based on how it is obtained. If the shaft power is based on fuel consumption measurements, then it is the brake power P_B that is measured. If it is based on torque and rotational speed measurements, then it depends on where the torque measurement is placed, as there is a small loss in the shaft between the measurement location and the tail shaft.

Chapter 3

Fouling

In this chapter takes on the topic fouling. First, different kinds of fouling are presented followed by different methods to determine the surface roughness due to fouling. Methods to determine the resistance due to fouling are presented as well as some types of antifouling systems.

3.1 Types of Fouling

Fouling also called biofouling is due to colonization of a surface by living organisms [4]. Fouling will increase the roughness of the surface, which will give an increase in the frictional resistance of the hull and a decrease in propeller performance. As stated in the previous chapter, the flow around a ship can be described as fully rough, which gives that the frictional resistance is a function of the surface roughness and independent of the Raynolds number. The surface roughness of the hull can be divided into two separate components, permanent and temporary roughness. The permanent roughness is the surface of the hull after the hull is cleaned and a fresh layer of coating is applied. Some factors that influence the permanent roughness are corrosion, mechanical damage, a build-up of old coating, poor cleaning before re-painting, etc. [7]. The temporary roughness is due to fouling organisms, Townsin [1] divides fouling organisms into three categories based on their properties, namely slime, weed, and shell.

3.1.1 Slime

A slime film is the first fouling type to develop on the hull. This layer is easily cleaned off by soft brushes that usually does not hurt the antifouling coating. However, it can resist relative high shear stresses caused by high speeds and cause a significant increase in the frictional resistance of the vessel. Bohander performed a full-scale experiment on a frigate in 1991 [1], where a mature slime layer had developed without the presence of weed or shells. Speed and power trials were performed before the ship was drydocked and cleaned. New speed and power trials were conducted after new antifouling coating had been applied, and it was measured a decrease in total propulsive power between 8 to 18 %. This full-scale experiment shows that a slime layer has a significant contribution to the added resistance. Figure 3.1 and 3.2 shows two different examples of slime fouling on a hull.

Figure 3.1: Continuous slime layer [19]

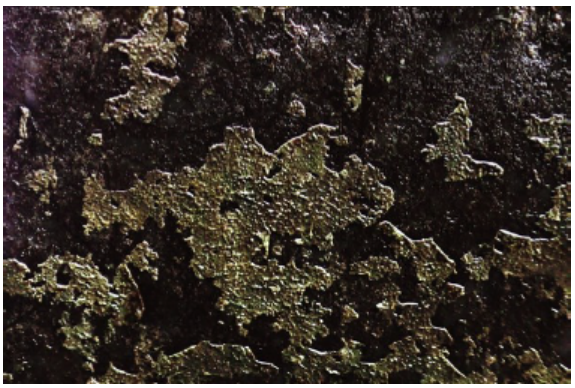

Figure 3.2: Interspersed slime [19]

3.1.2 Seaweed

Seaweed, together with slime, is often referred to as soft fouling and consists of filamentous algae that have a root attached to the hull while the rest will move with the flow. It is difficult to estimate the added resistance due to seaweed since it is hard to determine the influence seaweed has on the boundary layer. Some research has been done by Schultz [20], who performed experiments with different filamentous algae in a Circulating Water Tunnel (CWT). He found that the two species tested gave an average increase in frictional resistance coefficient of 125 % and 110 % compared to the smooth surface. This increase in frictional resistance shows that seaweed gives a significant added resistance. Two examples of seaweed fouling are shown in Figure 3.3 and 3.4.

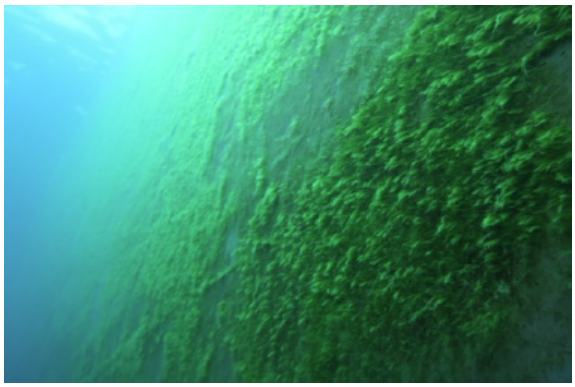

Figure 3.3: Filamentous algae [19]

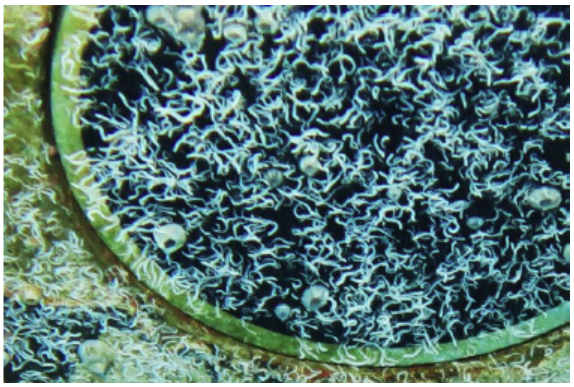

Figure 3.4: Tubeworms [19]

3.1.3 Shell

Shell and barnacle fouling is often referred to as hard fouling as it is not moving with the water like seaweed. The fouling penalty is determined by the characteristic like height, diameter, and distribution density. If these parameters are known, the fouling penalty can be calculated. However, it is not always easy to determine these characters. As discussed in the next section. Shells and barnacles are important for the added resistance. It has been shown that for a 120 meter long vessel with 75 % coverage of shells with a height of 4.5 mm, the increase in skin friction was 85 % [1]. An example of barnacle fouling is shown in Figure 3.5 and 3.6.

Figure 3.5: Barnacle fouling [19]

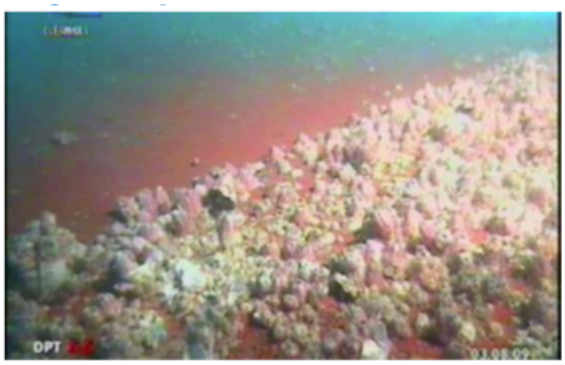

Figure 3.6: Dense barnacle fouling [21]

3.2 Measuring Methods

Fouling will increase the surface roughness of the hull. For clean and freshly painted hulls, the surface roughness is measured by a Hull Roughness Analyser, which measures the maximum difference in height over a given length [18]. The surface roughness is noted as $R_{t(50)}$ if measured over a 50 mm sample length. Figure 3.7 shows how $R_{t(50)}$ is defined, it also shows that surface roughness has an arbitrary shape, and it is only the maximum peak height that is measured. However, the shape of the surface has a huge influence on the flow over the surface and consequently, the boundary layer. Hence, the equivalent sand-grain height k_s is a popular parameter to use instead. It expresses the surface roughness as a height, which is the height of sand grains covering a surface that would give the equivalent surface roughness. So, the parameter k_s accounts for the shape of the surface as well.

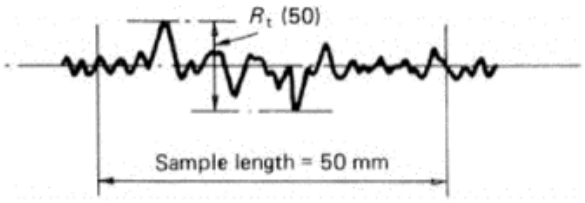

Figure 3.7: Definition of $R_{t(50)}$ [7]

To find the Average Hull Roughness (AHR) is the local Mean Hull roughness (MHR) measured at different locations around the hull. MHR can be expressed as either $R_{t(50)}$ or k_s [7], then AHR is expressed as

$$AHR = \frac{\sum_{j=1}^{m} (w_j(MHR))}{\sum_{j=1}^{m} w_j} \tag{3.1}$$

where w_j is a weight function depending on the localization of the measured surface. w_j is not standardized and has many different shapes [7]. For example, added roughness at the bow has the most influence on the resistance of the hull, but parameters such as distribution density and fouling type also play a significant part and must be considered when determining w_j. For the hard fouling like shells and barnacle, the characteristics such as height, diameter, and distribution density are measured to express the AHR. The following relationship is purposed to express the equivalent sand-grain height for barnacle fouling [19].

$$k_s = 0.059\ k_t\ (\%cover)^{0.5} \tag{3.2}$$

Where k_t is the height of the largest barnacle. The Naval Ship's Technical Manual, used by the US Navy, provides a different method to determine the fouling with a rating index ranging from 0-100. The parameter is based on visual observation of the fouling before a ship is cleaned. An explanation of the NSTM rating is provided by Schultz [2] and given in Table 3.1.

Table 3.1: The NSTM rating [2]

Description of condition	NSTM rating	$k_s(\mu m)$	$R_{t(50)}$
Hydraulically smooth surface	0	0	0
Typical as applied AF coating	0	30	150
Deteriorated coating or light slime	10 - 20	100	300
Heavy slime	30	300	600
Small calcareous fouling or weed	40 - 60	1 000	1 000
Medium calcareous fouling	70 - 80	3 000	3 000
Heavy calcareous fouling	90 - 100	10 000	10 000

There are other methods to determine the fouling rate, especially related to the weight function w_j in Equation 3.1, but it will not be discussed further in this thesis.

3.3 Resistance Due to Fouling

The roughness increases the boundary layer around the hull, which causes more fluid to be dragged along with the vessel, which gives more kinetic energy to the fluid. The added surface roughness may also change the wave pattern of the hull, which may increase the wave resistance [22]. In order to understand how the surface roughness of the hull influences the resistance, it is common to study the roughness of a flat plate and scale up the results [2, 22]. The mean longitudinal velocity on the boundary layer for a rough surface $\overline{u}$, is derived in the same way as for a smooth plate. It is expressed as [23]

$$\frac{\overline{u}}{\nu^*} = f\left(\frac{y}{k_s}\right) \tag{3.3}$$

where ν^* is the wall friction velocity given as $\sqrt{\tau_w/\rho}$, τ_w is the frictional stress on the hull surface and k_s is the equivalent sand-grain height. For closely spaced sand grains and if the flow can be considered fully rough, Equation 3.3 can be expressed as

$$\frac{\overline{u}}{\nu^*} = 2.5ln\left(\frac{y}{k_s}\right) + 8.5 \tag{3.4}$$

For a fully rough flow $k_s\nu^*/\nu > 60$ the frictional coefficient for the flat plate can be expressed by

$$C_F = \left(1.89 + 1.62log_{10}\left(\frac{L}{k_s}\right)\right)^{-2.5} \tag{3.5}$$

Equation 3.5 is only valid for a fully rough flow otherwise, the friction coefficient is dependent on the Reynolds number [23]. However, as stated in Chapter 2, the flow around a full-scale ship can almost always be considered as fully rough. The International Towing Tank Conference (ITTC) [12] gives another method to determine the frictional coefficient for a rough surface. ITTC uses Equation 3.6 to calculate the roughness allowance, ΔC_F.

$$\Delta C_F \cdot 10^3 = 44 \left[\left(\frac{k_s}{L_{WL}} \right)^{\frac{1}{3}} - 10(R_e)^{-\frac{1}{3}} \right] + 0.125 \tag{3.6}$$

The problem with this equation is that it is only valid for $k_s < 230$ µm and AHR ($R_{t(50)}$) for fouled ships is often larger than this as given in Table 3.1. The added resistance can be calculated by Equation 3.7.

$$R_{Fouling} = 0.5\rho \; S \; V_S^2 \cdot \Delta C_F \tag{3.7}$$

Where ρ is the density of seawater, and S the area of the wetted surface. C_F from Equation 3.5 is actually $C_F + \Delta C_F$, where C_F is for a smooth plate. So, in order to use C_F from Equation 3.5 in Equation 3.7 the effect of the smooth plate has to be removed. However, it is difficult to measure the roughness of the hull when fouling is present, as discussed in the previous section. Schultz made some predictions of the resistance due to fouling on a US Naval ship by scaling results for an equivalent flat plate and compared those to experimental values. Table 3.2 shows these results and that the added resistance is a significant part of the total resistance.

Table 3.2: The effect of fouling for a US Naval ship [2]

Description of condition	$\%\Delta R_T$ @ $V_s = 7.7$ m/s	$\%\Delta R_T$ @ $V_s = 15.4$ m/s
Hydraulically smooth surface	-	-
Typical as applied AF coating	2	4
Deteriorated coating or light slime	11	10
Heavy slime	20	16
Small calcareous fouling or weed	34	25
Medium calcareous fouling	52	36
Heavy calcareous fouling	80	55

It is important to note that even though the percentage is lower at a higher velocity, the value of the resistance is larger because the frictional resistance is a smaller part of the total resistance for higher speeds. Oliveira et al. [22] discussed how the form factor could be applied in the scaling of the flat plate result by comparing Schultz's method with CFD calculations. He concluded that "*...the hypothesis of a form factor affecting hull penalties due to roughness cannot be generalized for all speeds, since the effect of hull roughness on wave pattern cannot be neglected*" [22]. This statement means that hull roughness affects both the frictional resistance and the wave resistance.

3.4 Types of Antifouling Systems

Today almost all ships are fitted with an antifouling paint coating covering the underwater surface of the hull. This coating is to limit the occurrence of biofouling. During the 1800s wooden ships were protected by cobber sheathing, mainly to protect the wood from teredo worm, but it also showed effectiveness against biofouling [1]. This led to attempts where iron ships were cladded with copper, but it had an undesired side effect of increasing the corrosion of iron. Because iron works as a sacrificial anode for copper according to the galvanic series [24]. Copper cladding was not the only antifouling system at the time, the first patent on antifouling coating was issued already back in 1625 to William Beale, and in 1865 more than 300 antifouling paints were patented [1]. In the 1960s a new super effective coating system was introduced, namely Self-Polishing Copolymer (SPC) with Tributyltin (TBT) [1, 2]. The TBT coatings could ensure a foul-free hull for up to 5 years. Vessels are required by classification societies to dock each 5th year for the renewal survey, so in practice, the TBT coating system could ensure foul-free hulls. However, because of the environmental impact the TBT coating systems had on the marine coastal environment, especially oysters, it was partially banned in 2003, and a total worldwide ban came in 2008 [25]. Since the ban on TBT coating, the primary replacement has been copper based SPC systems [2]. Other available solutions are non-toxic surfaces, hydrogels, and low energy surfaces [26]. The problem with today's solutions is that they are not as effective as the TBT coating and some coating types give a rough hydrodynamic surface after it is applied. So there are many different considerations to take into account when choosing an antifouling coating. Claire Hellio and Diego Yebra [26] give an extensive overview of the development of antifouling systems and the different solutions available.

In addition to antifouling paint coating, other control methods such as hull cleanings and propeller polishing are popular. The benefit of these methods is that they can be performed while the ship is doing cargo handling operations in port, which means it does not cause downtime for the vessel. Both divers and ROVs can perform hull cleanings. The procedure is to use special brushes or high-pressure water jets to remove marine growth. A diver can clean approximately 200-400 m^2 per hour [27] while a ROV can clean 800-1000 m^2 per hour [21]. The drawback of a hull cleaning is that if it is not done properly, it may damage the antifouling paint, which will result in a decrease in ship performance over time [3]. Propeller cleaning follows the same procedure as a hull cleaning, where a diver polishes the propeller manually. It is more common to use divers for propeller cleaning as the geometry makes it harder to use an ROV.

Chapter 4

Performance Monitoring of Ships

In this chapter, a brief review of performance monitoring systems is presented. First, a little motivation for performance monitoring is given. Then different data collection methods are discussed, followed by a description of the parameters typically collected. Lastly some examples of current solutions what they are used for.

4.1 Motivation for Performance Monitoring of Ships

Martin Stopford [28] states that we are now undergoing the fourth revolution of shipping.

"*I'm going to call it Smart-Shipping and it is different from previous waves. Its focus is on managing and improving every aspect of sea transport by using systems made possible by recent advances in Information and Communications Technology (ICT).*"

By this, he means that the increasing usage of sensors, data collection, and cloud technology can be seen as a huge change in how the shipping industry operates. He divides the revolution into three segments:

Smart Ships
Ships are fitted with more and more sensors that communicate data to both the on-shore team and the crew. These data are used to improve the ships performance, management, and automation.

Smart Fleet Management
By utilizing the data from different ships, the shipping companies can work across the fleet to improve the efficiency of the entire fleet.

Smart Shipping Logistics
Increasing communication and specialization between sea transport, cargo handling, and land transport systems will increase efficiency.

Performance monitoring of ships is an important factor in all these segments, especially the first two. The main motivation behind the digitization of the world fleet is to improve ship performance and thereby decrease the operation and maintenance costs. The fuel cost for a ship can account for as much as 50% of the total operational costs [29]. Another benefit of reduced fuel consumption is a reduction in greenhouse gas emissions. The performance monitoring data of the equipment aboard a ship can be used to optimize maintenance schedules and repairs. Classification societies can also benefit from this by evaluating the utilization of the hull and optimize surveys accordingly. Automation of different

ship functions can reduce the number of crewmembers and thereby, the operation cost.

4.2 Data Collection Methods

There are different practices of how performance data is collected. More and more vessels have automatic data logging that logs data continuously, which then is stored typically as an average over a period between 1 to 15 minutes. Another common method is daily performance monitoring, which often means that the crew registers a daily average of the performance data collected. This average is called noon-data. Other solutions are to log data less frequently like weekly or monthly [3].

Continuous logging excludes the possibility of human error as the logging is done automatically, but creates an extensive data set with many data points. This has both positive and negative sides. A positive side is that there are many data points that can be analyzed, which makes it easier to compare data with similar operating conditions. A negative side is the storage of the amount of data collected, and that it is difficult to work with large data sets.

The crew typically reports the noon-data. It is useful for many things, such as predicting the estimated time of arrival, fuel consumption, and calculating the emissions produced by the ship. Since the noon-data is averaged over one day, it is not that reliable for added-resistance calculations as the operating conditions seldom are the same over a 24h period. Noon-data reporting is still the most used reporting system in 2014 [18].

4.3 Examples of Parameters Typically Collected

Carlton [7] provides a table of traditionally recorded parameters in ship logbooks, the table is given below. The parameters are divided into two categories Deck log and Engine log.

Table 4.1: Traditionally recorded parameters in ship log books [7]

Deck log	Engine log
Ship drafts (fore and aft)	Cooling sea water temperature at inlet and outlet
Time and distance travelled (over ground)	Circulating freshwater cooling temperature and pressures for all engine components
Subjective description of the weather	Lubricating oil temperature and pressures
Ambient air and sea water temperature	fuel lever, load indicator and fuel pump settings
Ambient air pressure	Engine/shaft revolution count
General passage information	Turbocharger speed
	Scavenge and injection pressures
	Exhaust gas temperatures
	Main engine fuel and lubricating oil temperatures
	Bunker data
	Generator and boiler performance data
	Evaporator and boiler performance data
	Torsion meter reading

Parameters from both categories are of interest in this thesis but not all. Automated collection systems lead to an increase in the parameters collected. With more parameters, one has more information, but the time it takes to review the data set increases, which makes it harder to work with. Figure 4.1 shows the location of 15 automatic logging sensors of an example ship.

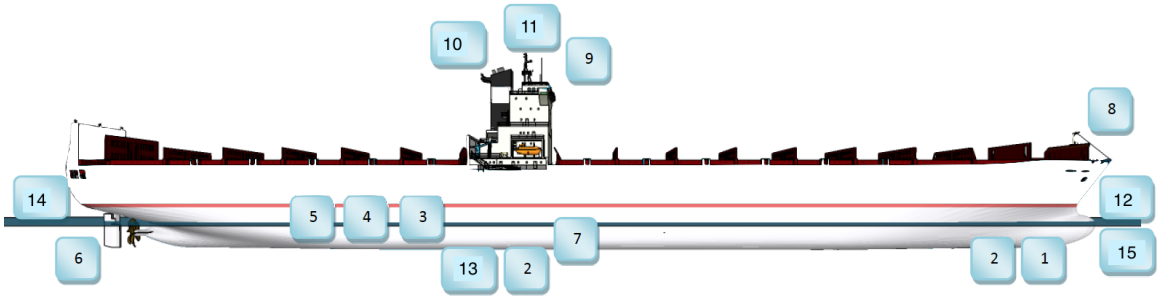

Figure 4.1: Location of sensors on an example ship [30]

1. Speed log 2. Echo sounder 3. RPM and torque meter 4. Shaft motor 5. Thrust meter 6. Rudder indicator 7. Stabiliser fins 8. Wind anemometer 9. GPS 10. Air temperature 11. Gyrocompass 12. Accelerometer 13. Sea water temperature 14. draft aft 15. draft forward

As shown above, there are many parameters collected by a performance monitoring system. A discussion about how some of these parameters are collected and their usage is given below. The discussion is based on Pedersen's [18] and Hansen's [30] PhD thesis.

4.3.1 draft and Trim

The draft and trim can be measured in different ways. The simplest way is a visual observation of the markings on the ship side before the vessel leaves the port. The trim is then obtained by calculating the difference between the draft aft and fore. All ships are also fitted with a loading computer which gives the ship draft and trim based on the weight and placement of the cargo, ballast water, fuel, etc. The draft calculated by the loading computer is derived based on ship particulars, which means that it can be less accurate than the visual observation. The advantage of the loading computer is that it can automatically update the draft based on the daily consumption of fuel, oil, and water. Another method is to use pressure gauges at the fore and aft, which measures the hydrostatic pressure. These sensors need to be robust to withstand environmental forces. The advantage of these sensors is that in addition to measuring the draft can it be used to measure the wave elevation. However, since the pressure gauges need to be sensitive to be able to cope with large pressure fluctuations from waves in rough sea are they usually unreliable.

Both the draft and trim changes the wetted surface of the ship and the wetted surface is proportional to the frictional resistance and thus the fouling resistance of the ship. The draft and trim will also affect the wave resistance of the ship, especially when a bulbous bow is present. However, this effect is difficult to determine. The draft and trim are also an important factor for the ship safety as it determines the restoring forces and moments for the ship.

4.3.2 Speed

The ship's speed is usually measured through both a speed log and a GPS signal. The speed log is mounted near the bow to reduce the effect of non-laminar flow over the sensor. It uses the Doppler

principle to measure the acoustic reflection in the water and thereby finds the speed of the vessel. Environmental factors such as water density, aeration, eddy currents, and sea states may influence the speed log measurements. It is an accurate sensor as long as it is regularly calibrated, as the measurements tend to drift over time. The speed measured through GPS signal is usually a very reliable source. The difference between the two methods is that the speed log measures the speed through water while the GPS measures the speed over ground, which means that when there is no current present the two should show the same speed. Usually, the first filtering of a data set is done by comparing these two values and disregard points where the difference is much larger than what a reasonable current would be. The ship resistance is proportional with the speed through water squared, which means that speed measurements are an important factor.

4.3.3 Wind

A wind anemometer is a standard way of measuring the relative wind speed and direction. A propeller measures the wind speed, and it rotates so it is facing the wind head-on, which gives the relative wind direction. To reduce the influence of the ship's superstructure and deck cargo on the wind measurements, the anemometer is usually mounted in the bow high above the deck. In addition to cause air resistance, the normal component of the wind force may create a moment that results in a rudder angle that gives an increased resistance. Another method to find wind speed and direction is the usage of hindcast data. These data are often coarse and an average for a large area. An example of a hindcast database is The European Centre for Medium-Range Weather Forecasts (ECMWF).

4.3.4 Waves

Waves cause a significant increase in resistance, but unfortunately, it is difficult to measure by an aboard measuring system. A wave radar can measure the wave environment given as the wave specter around the vessel. However, this system is costly and only mounted on special purpose ships e.g., research vessels and some special vessels for the offshore industry. Traditionally the sea state is visually estimated by experienced crew members. Hindcast data is also available for waves and can be used to estimate the sea state the vessel has experienced. There are also methods to estimate the wave height based on the accelerations in the ship bow. The motions of the vessel can be measured by a Motion Reference Unit which gives the vessels six motions, represented as statistical parameters. These statistical parameters provides a motion specter, and the spectral moments of the motion specter can be used to describe the waves. The first spectral moment m_0 describes the energy of the specter, and by combining these for all the motions, an estimate of the energy in the wave specter can be found. Through the relationship $H_S = 4\sqrt{m_0}$ the significant wave height of the sea state is estimates and the period is estimated by $T_{02} = \sqrt{m_0/m_2}$, this is described by Vanem and Brandsæter [31, 32].

4.3.5 Shaft Power

The best way of estimating the shaft power is to measure the shaft thrust, torque, and rotational speed. The rotational speed is often given as an engine output, but optical sensors can also measure it. The thrust and torque can be measured by strain gauges glued directly to the shaft or by commercial power meters using optical sensors. The shaft power can also be estimated based on fuel consumption, but it is not a good alternative as it depends on the efficiency of both the fuel, engine, and propulsion system.

4.4 Example of Performance Monitoring Systems

There are many different performance monitoring systems today, which use different approaches and data for analysis of the ship's performance. Some systems monitor different components of the engine to be used in maintenance decisions. Other systems are more complex and monitor the ships overall performance. Some systems are also used for fleet monitoring, which uses data collected from multiple vessels. Systems and parameters that are used to monitor the hydrodynamic performance of a vessel are of interest in this thesis, and some examples are given below.

The Admiralty coefficient A_C, is a parameter which traditionally has been used in performance analysis. The coefficient uses the relationship between the weight displacement Δ, ship speed V_S, and shaft power P_S.

$$A_C = \frac{\Delta^{2/3}\ V_S^3}{P_S} \tag{4.1}$$

This relationship accounts for different loading conditions, but not for environmental effects. In calm water for a smooth hull A_C is assumed to be constant [32]. So, when the environmental conditions are accounted for, the added resistance can be found by the decrease in A_C over time. Added resistance diagrams based on the Admiralty coefficient are made and used to monitor the vessel's performance over time. An example of an added resistance diagram is given in Figure 4.2.

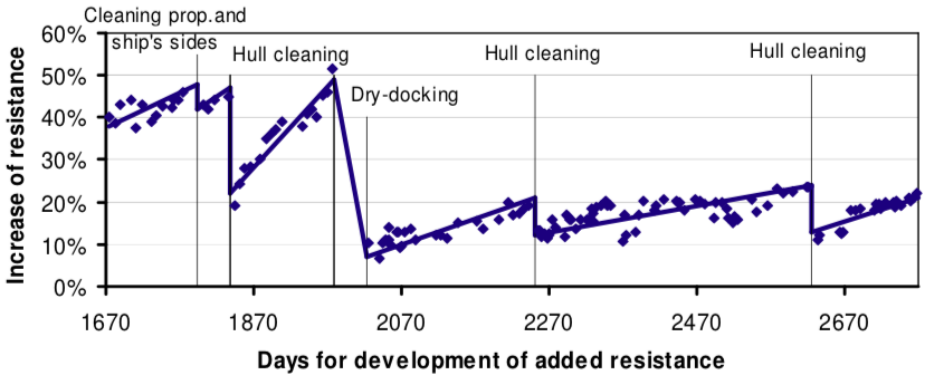

Figure 4.2: Added resistance diagram [3]

Here, it is shown that propeller and hull cleanings decrease added resistance significantly. Initially, the vessel had a high added resistance and the first hull cleaning, after approximately 1850 days, had a remarkable effect. It reduced the added resistance with about 20%. However, it damaged the antifouling coating as seen by the steep increase in resistance after the cleaning.

Propulsion Dynamics [33] has developed the CASPER (Computer Analysis of Ship PERformance) system. The system utilizes noon-data for hull and propeller performance monitoring. The procedure is to calculate the speed through water from propeller revolutions, the power delivered to the propeller and propeller design. Then corrections for the sea state are made before the performance data is compared with sea trial data, and the added resistance is reported as a percentage of the total resistance [34]. These results can then be used in economic analysis, such as speed loss and increased fuel consumption.

SMART (Ship-board Monitoring, Analysis, and Recording Technologies) is another performance monitoring system which is developed by BMT SeaTech [8]. The system is built up by three subsystems, $\text{SMART}^{\text{POWER}}$, $\text{SMART}^{\text{STRESS}}$, and $\text{SMART}^{\text{SHORE}}$. $\text{SMART}^{\text{POWER}}$ monitors the ship's speed, fuel consumption, RPM, and torque together with navigational and environmental parameters in order

to analyze the trends by applying different mathematical models which account for trim, draft, and environmental factors. SMART$^{\text{STRESS}}$ monitors and logs stress at different locations on the hull in real time. This provides the ship owners with information about the ships operation and fatigue utilization, which again can be used by class societies to make surveys more effective. SMART$^{\text{SHORE}}$ gathers the data from the two other systems, together with data from the other vessels managed by the ship manager so that extensive analysis of fleet can be performed. For example, the performance of two sister vessels are compared.

In addition to these two commercially available systems, performance monitoring of ships is an interesting research topic. Benjamin Pedersen [18] wrote his PhD thesis about how one can utilize noon reports combined with machine learning methods to evaluate the ship propulsion performance. Søren Hansen [30] has also written a PhD about performance monitoring of ships where he focuses on automatic data logging, data filtering, and performance evaluation based on the data. More recently Soner, Akyuz and Celik [35] used data from a 2h ferry route over two months, for ship operational performance based on statistical learning methods Ridge and Lasso.

Chapter 5

Machine Learning

This chapter aims to give a brief overview of the concepts of statistical learning, also called machine learning and how this can be applied to a data set of performance monitoring data. The chapter starts with a section about the basic concept of machine learning, followed by an introduction to regression. Then an introduction of how to split a data set into a training and validation set, and different methods to evaluate the model's performance. The theory in this chapter is mainly based on the textbook "Elements of statistical learning" by Hastie, Tibshirani, and Friedman [36] and "Pattern recognition and machine learning" by Bishop [37].

5.1 Basic Theory

Machine learning is fitting data based on statistical models with the usage of computers. The aim is to develop a model that can learn to perform a task based on a set of data without being specifically programmed to perform that task. So, based on a data set the program makes predictions for similar data sets. Machine learning can be split into two main categories, supervised learning and unsupervised learning.

Supervised learning
The model is first trained with a data set that contains input data with corresponding output data. This means that the program is given both the variables and the response. Based on the chosen statistical model, the program captures the relationship between the output and input data. Then this relationship is used to predict the response for a similar data set only containing input variables.

Unsupervised learning
In unsupervised learning, there is no specified output data, so the aim is for the model to cluster the data in groups of similar characteristics. Unsupervised learning is used to find hidden structures in the data.

The concept of unsupervised learning will not be discussed further in this thesis, as it is not used. Supervised learning can be used for both classification problems and regression problems. Trying to predict the added resistance due to fouling is most sensibly posted as a regression problem. Thus, it is natural to present some different methods of regression. A regression problem can be generalized by Equation 5.1 [18].

$$\mathbf{y} = \mathbf{f(x)} + \boldsymbol{\epsilon_{tr}} \tag{5.1}$$

$\mathbf{y}$ is the response variable and $\mathbf{f(x)}$ is the function or model that uses the input variables $\mathbf{x}$ to predict the response, $\boldsymbol{\epsilon_{tr}}$ is the training error or noise, which is assumed to be standard Gaussian distributed. The aim of is to choose a model that minimizes the error between the predicted response and the given response. By training the function $\mathbf{f(x)}$ with a data set where both $\mathbf{x}$ and $\mathbf{y}$ are known and testing it on a different test set also containing inputs with corresponding output values. In order to understand the theory given in this chapter better are an explanation of the notation used given below.

The notation used in theis thesis is the same used by Bishop [37]. The data set consists of training data from D different sensors and each sensor have N samples. The input variables is noted as $\mathbf{X}$ and it consists of N samples of input variables $\mathbf{x}$, which gives us in mathematical terms $\mathbf{x} = (x_1, x_2, \ldots, x_D)^T$ and $\mathbf{X} = (\mathbf{x}^{(1)}, \mathbf{x}^{(2)}, \ldots, \mathbf{x}^{(N)})^T$. The training set will also have some response variables corresponding to the input sample. The response variables will be noted as $\mathbf{y}$, where $\mathbf{y}$ is a vector of dimension N such that we have a response for each input, which gives us in mathematical terms $\mathbf{y} = (y^{(1)}, y^{(2)}, \ldots, y^{(N)})^T$.

5.2 Regression Methods

For linear regression, it is assumed that there is a linear relationship between the input and output variable. It is the simplest form of regression. The main idea is that the output $\mathbf{f(x)}$ is a function of weight parameters here noted as w.

$$\mathbf{f(x)} = w_0 + w_1\mathbf{x}^{(1)} + w_2\mathbf{x}^{(2)} + \cdots + w_N\mathbf{x}^{(N)} \tag{5.2}$$

ω_0 is called bias, if we introduce a dummy variable $\mathbf{x}^{(0)} = 1$ we can rewrite Equation 5.2 to matrix form.

$$\mathbf{f(x)} = \boldsymbol{w}^T\mathbf{X} \tag{5.3}$$

As mentioned above the model uses the training set to estimate the wight parameters by minimizing the prediction error. It is most common to use the sum of squared errors to express the error. This minimization of the error is also referred to as the cost function ($C(\cdot)$). The sum of squared errors is given by the equations below.

$$C(\boldsymbol{w}) = \sum_{i=0}^{N} \left(y^{(i)} - \hat{\boldsymbol{f}}(\boldsymbol{x}^{(i)}) \right)^2 \tag{5.4a}$$

$$C(\boldsymbol{w}) = \sum_{i=1}^{N} \left(y^{(i)} - \sum_{j=0}^{D} x_j^{(i)} w_j \right)^2 \tag{5.4b}$$

$$C(\boldsymbol{w}) = (\mathbf{y} - \mathbf{X}w)^T(\mathbf{y} - \mathbf{X}w) \tag{5.4c}$$

Equation 5.4a to 5.4c expresses the same, in 5.4b is Equation 5.2 used to express the estimated values $\hat{\boldsymbol{f}}(\boldsymbol{x})$, note that the dummy variable $\mathbf{x}^{(0)} = 1$ is included. Equation 5.4c is the cost function written in vector form. The estimated output based in the $\boldsymbol{w}$ parameters is noted as $\hat{\boldsymbol{f}}(\boldsymbol{x})$ in Equation 5.4a and y is the true response given in the training set. By differentiating Equation 5.4c with respect to

w and setting the first derivative equal to zero, we obtain the unique solution for the best estimate of $\boldsymbol{w}$.

$$\hat{\boldsymbol{w}} = (\mathbf{X}^T\mathbf{X})^{-1}\mathbf{X}\mathbf{y} \tag{5.5}$$

An easy way to extend the linear regression model is to introduce a basis function $\Phi(x)$. The basis function can be non-linear which means that $\mathbf{f(x)}$ is non-linear. However, it still has a linear form as it is linear in $\mathbf{w}$.

$$\mathbf{f(x)} = \sum_{i=0}^{N} (w_i \ \phi_i(\mathbf{x})) = \mathbf{w}^T\phi(\mathbf{x}) \tag{5.6}$$

As stated above can the basis functions have many different forms. For polynomial regression we have $\Phi(x) = x^j$ other popular functions is different forms of exponential functions. These functions can be customized to fit the data set, based on the knowledge the user has of the data set [18]. The cost function in Equation 5.5 is modified to fit the basis function by the following equation.

$$\hat{\boldsymbol{w}} = (\boldsymbol{\Phi}^T\boldsymbol{\Phi})^{-1}\boldsymbol{\Phi}\mathbf{y} \tag{5.7}$$

The problem with the least square method is that the full data set is processed at once, which is very costly for large data sets. It is therefore common to use sequential learning for large data sets. Here the data points are considered one at the time, and the weight function is updated simultaneously using the principle of gradient descent given below.

$$\mathbf{w}^{(\tau+1)} = \mathbf{w}^{(\tau)} - \eta\nabla C(\mathbf{w}^{(\tau)}) \tag{5.8}$$

where τ is the iteration number, η is the learning rate parameter and ∇C is the gradient of C with respect to the parameters in $\mathbf{w}$. By using the cost function defined by the least square method in Equation 5.5, Equation 5.8 expands to

$$\mathbf{w}^{(\tau+1)} = \mathbf{w}^{(\tau)} + \eta\left(y_n - \mathbf{w}^{(\tau)T}\boldsymbol{\Phi}(\boldsymbol{x_n})\right)\boldsymbol{\Phi}(\boldsymbol{x_n}) \tag{5.9}$$

These are some of the many statistical models that may be used in a statistical learning algorithm.

5.3 Splitting the Data Set

As mentioned above is the basic idea of supervised learning to split the available data set into a training part and a testing part. There is no standard way to split the data set, but it is common to use the largest part for training and a smaller part for testing/validation. Pedersen [18] splits his data so that 20 % of the data are the test/validation part and 80 % are for training the model. One can also split the training and test sets into smaller parts for cross-validation [31, 32], then one can utilize all the data for both training and testing.

It is important to have in mind that the model makes predictions based on the training set. So, if one wants to predict the performance of a ship at a given state, it is important that the model has been trained with data for a similar state. Otherwise, the model will not be able to predict the performance

correctly. This means that one can use the model as a benchmark for how the ship should perform and compare it with the true value to see the increase/decrease of the performance [18]. Because machine learning methods use regressions based on known data, it is essential to know the states the ship has experienced in the training data, in order to be able to use a model correctly.

5.4 Model Selection

The concept of linear regression is given above together with the extension where the input parameter is given as a function Φ. This section will focus on how to choose the right model. To illustrate this, the example provided in Bishop´s textbook [37] is used. In this example, the aim is to find a polynomial model that best fits points that follows the function $sin(2\pi x) + \epsilon$, where ϵ is some noise which is standard Gaussian distributed. Ten points are used in the example to represent one wave, as shown by Figure 5.1.

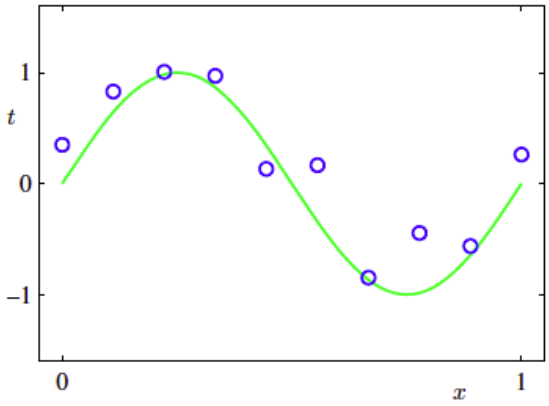

Figure 5.1: Sample data with underlying function [37]

The blue points are the observed sample data, and the green line is the underlying function that is not known by the model. The aim is to predict new values of t for a given x value based only on the blue points. Four polynomial functions of a different order, M, are investigated to see which gives the best prediction. , and the expressions are found by minimizing the cost function described by Equation 5.4a. The resulting predictions are given in Figure 5.2.

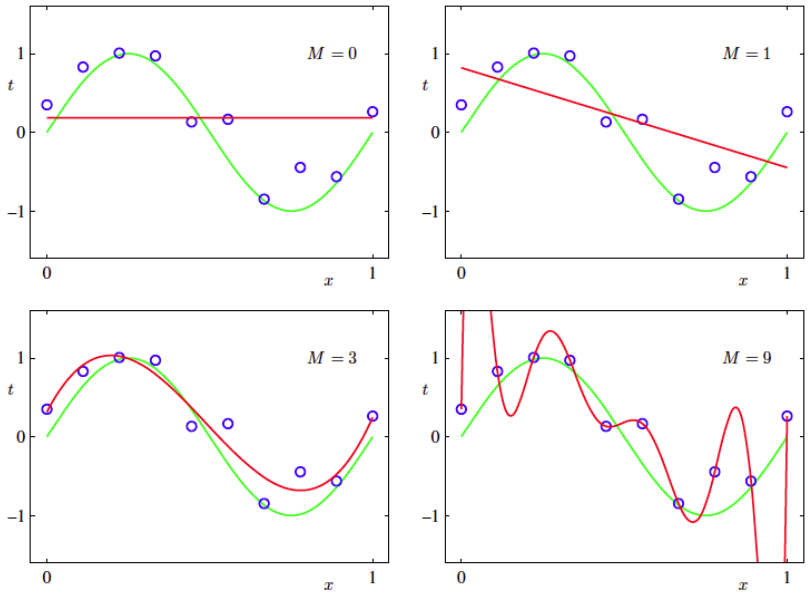

Figure 5.2: Polynomial prediction functions of different degree M [37]

It is shown that for the polynomial functions with order $M = 0$ and $M = 1$ are too simple for predicting the data. The error is large and they do not capture the underlying function well, which is an example of underfitting. The model was too simple. The polynomial function of order $M = 3$ is a good estimate for both the underlying function and data. For the polynomial function of order $M = 9$, an interesting phenomenon occurs. The regression fits the data perfectly, but the underlying function is not captured in a good way. Thus, the model is too complex, which is called over-fitting. By this, its shown that finding the regression which captures the data best is not always easy, and one has to be careful not to have under- and over-fitting. Some strategies of how to choose the right model are presented below.

Another approach to finding the best regression is to plot the root mean square error, for the different polynomial functions for both the training and testing set, as shown in the figure below.

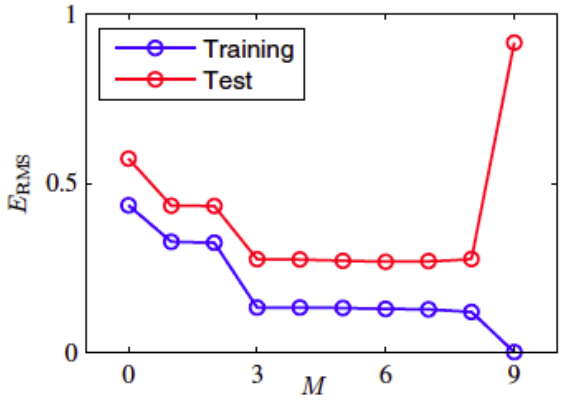

Figure 5.3: Error vs. complexity [37]

Here it is shown that the error decreases for both the test and training set between $M = 0$ to $M = 3$, which indicates that the model gives a better prediction of the data set. For $M = 9$ is it seen that the

training error goes to zero while the test error is large. This indicates that the model only makes a good (perfect) estimate for the training set, but it does not capture the underlying function indicated by the large error for the test/validation set. A plot like Figure 5.3 can be used to evaluate if the model is over-fitting. Another method for reducing the over-fitting problem is to increase the size of the data set as shown by Figure 5.4. Both the red lines are a polynomial with order $M = 9$ but the number of data points is 15 on the left and 100 on the right, and it is clearly shown that the regression captures the underlying function best for the larger data set.

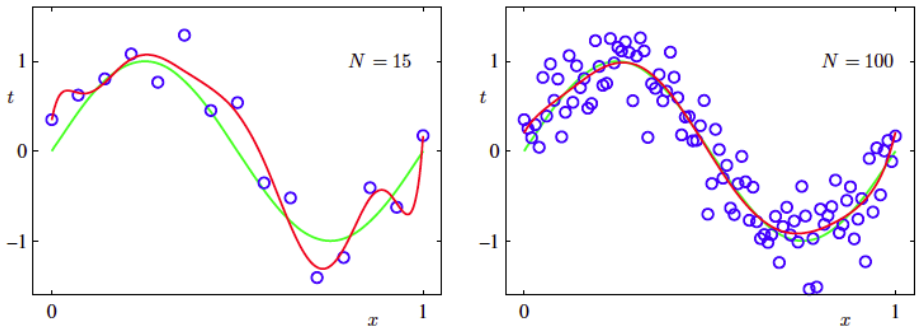

Figure 5.4: Polynomial regression $M = 9$ with varying sample size [37]

Another method to reduce over-fitting is to introduce a regularization coefficient, λ, which penalizes large parameter values. It is known that large values in the weight vector $\mathbf{w}$ tend to overfit the data, especially for linear regression. To handle this problem the cost function from Equation 5.4 is modified to include the regularization coefficient.

$$C(\mathbf{w}) = \frac{1}{2}\left(\sum_{i=1}^{N}\left(y_i - \mathbf{w}^T\Phi(\mathbf{x}_i)\right)^2 + \lambda\mathbf{w}^T\mathbf{w}\right) \tag{5.10}$$

Chapter 6

Data Set

This chapter describes the data sets used in the further analysis. The vessel used in the analysis is a five years old 2500 TEU container vessel. The data set contains data from three different sources, all with different sampling rates. The vessel's performance data are from the aboard performance monitoring system, information about the weather condition is re-analysis of hindcast weather data from the ECMWF database, and the location data are obtained from the AIS system. The main characteristics of the container vessel are given in Table 6.1

Table 6.1: Ship particulars (Design condition)

Parameter	**Abbreviation**	**Magnitude**	**unit**
Length overall	L_{OA}	208.9	[m]
Length between perpendiculars	L_{PP}	196.9	[m]
Breadth	B	29.8	[m]
Draft	D	10.1	[m]
Displacement	∇	37 718	[m^3]
Block coefficient	C_B	0.64	-

The first three sections describe the different data and data sources, while the last section describes the processing of the data.

6.1 Performance Monitoring Data

The performance monitoring data set consists of data logged by the aboard performance monitoring system. The data set contains values from vessel delivery in March 2014 to the beginning of 2019. The sampling period for this system is approximately 15 minutes. Figure 6.1 gives a bar chart over how many measurements that are available per day.

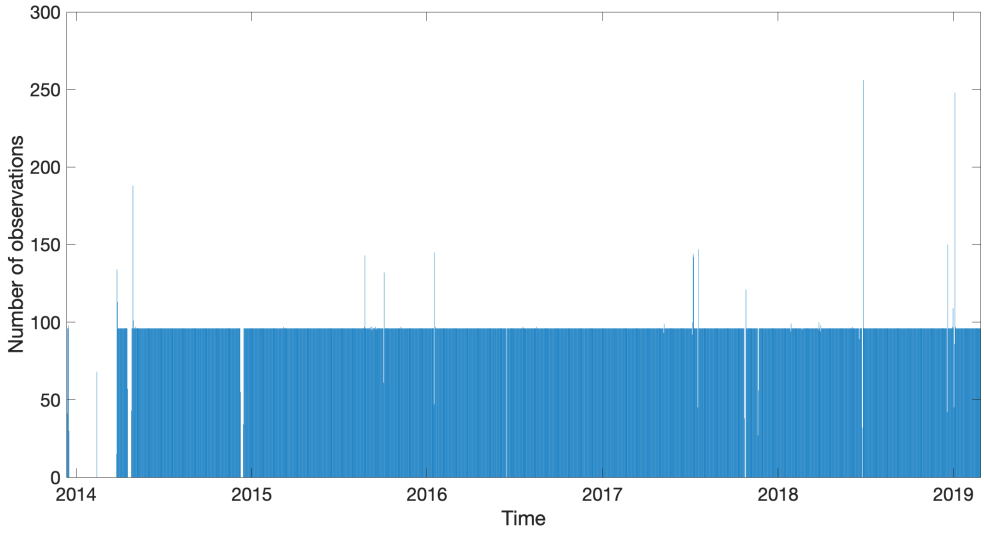

Figure 6.1: Available Performance data per day

From the figure, it is shown that most dates have 96 samples are available, which corresponds to the sampling period of 15 minutes. It is not known why the sampling rate for some dates is different from 15 minutes. It may indicate that something was wrong with the data and to make it simpler in the analysis were all data points with sampling rates of less than 10 minutes have been removed. There are 34 different parameters in the ship performance monitoring data set, they are listed in Table 6.2.

Table 6.2: Parameters sampled from the aboard monitoring system

Parameter	**unit**	**Parameter**	**unit**
Date	yyyy-mm-dd	ME Fuel Mass Tot In	kg
Time	hh:mm:ss	ME Fuel Mass Tot Ret	kg
ME Fuel Mass Net	kg/hr	ME Fuel Mass In	kg/hr
AE Fuel Mass Net	kg/hr	ME Fuel Mass Ret	kg/hr
Ship Speed Log	knot	AE Fuel Mass Tot In	kg
Ship Speed GPS	knot	AE Fuel Mass Tot Ret	kg
Ship Course	deg	AE Fuel Mass In	kg/hr
ME Shaft Power	kW	AE Fuel Mass Ret	kg/hr
ME Shaft Speed	rpm	ME Fuel Temp In	°C
Wind Speed Abs.	knot	ME Fuel Density In	kg/m3
Wind Speed Rel.	knot	ME Fuel Temp Ret	°C
Wind Dir. Rel.	deg	ME Fuel Density Ret	kg/m3
Draft Fwd	m	AE Fuel Temp In	°C
Draft Aft	m	AE Fuel Density In	kg/m3
ME Fuel Vol Tot In	l	AE Fuel Temp Ret	°C
ME Fuel Vol Tot Ret	l	AE Fuel Density Ret	kg/m3
AE Fuel Vol Tot In	l	AE Fuel Vol Tot Ret	l

It is some uncertainty in how the data are measured, and a full investigation of how all the different parameters are measured has not been conducted, which means that the uncertainty related to the measurement of the data is unknown and assumed not to have a great impact on the analysis. However, a general overview of how some of the most critical parameters are usually sampled is given in Chapter 4. The data are processed in order to identify false values. A discussion of how the data are processed is given in Chapter 6.4. Not all the data in Table 6.2 were used further in the analysis, Table 6.3 states which parameters that are used in further.

Table 6.3: Parameters used in further analysis

Parameter	**unit**	**Comment**
DateTime	yyyy-mm-dd hh:mm:ss	Date and time in UTC
Timestamp	s	Epoch time, calculated from DateTime
Ship Speed Log	knot	Speed through water
Ship Speed GPS	knot	Speed over ground
Ship Course	deg	-
ME Shaft Power	kW	-
ME Shaft Speed	rpm	-
Wind Speed Abs.	knot	Only compared with ECMWF data
Wind Speed Rel.	knot	Only compared with ECMWF data
Wind Dir. Rel.	deg	Only compared with ECMWF data
Draft Fwd	m	-
Draft Aft	m	-
Draft mid	m	Calculated from draft Aft and Fwd
Trim	m	Calculated from draft Aft and Fwd

6.2 Weather Data

The weather data used in this thesis are obtained from the European Center for Medium-Range Weather Forecasts (ECMWF). ECMWF is a research and 24/7 operational institute providing weather predictions and other weather-related services. It has one of the worlds largest databases of meteorological data. The archived data are continuously reanalyzed using updated weather forecast models and observations. The data used in this thesis are a part of their ERA-Interim re-analysis data set which has data available from 1979 to present. A detailed description of the re-analysis process and data set can be found in [38].

To obtain the data from the ECMWF's database, one has to specify which parameters that are of interest, the area, spatial and temporal resolution. As the vessel operates worldwide was the area set to cover the whole globe, the spatial resolution used was 0.75x0.75 degrees, and the temporal resolution was 6 hours. The downloaded files contain information about the wind and wave conditions. The parameter used in the analysis is given in Table 6.4.

Table 6.4: Description of ECMWF parameters

Parameter	**Unit**	**Description**
10 metre eastward wind component	m/s	The eastward horizontal wind component 10 meter above the sea surface
10 metre northward wind component	m/s	The northward horizontal wind component 10 meter above the sea surface
Absolute wind velocity	m/s	Calculated from the 10 metre eastward and northward wind component
Wind direction	m/s	Calculated from the 10 metre eastward and northward wind component
Significant wave height	m	4 times the square root of the integral over all directions and all frequencies of the two-dimensional wave spectrum
Mean wave direction	degrees	The mean wave direction over all frequencies and directions of the two-dimensional wave spectrum
Mean wave period	s	The mean wave period over all frequencies and directions of the two-dimensional wave spectrum

6.3 Location Data

Automatic Identification System (AIS) is mandatory and it is an automatic tracking system that gives the vessel's position, speed, course, and identification. It is mostly used to avoid collisions between ships. The location data in this thesis are obtained from the AIS database. The AIS data consists of a timestamp and the GPS coordinates (longitude and latitude). The sampling rate is not constant and varies from a couple of seconds to several hours, even days. Figure 6.2 shows a bar chart of how many samples that are available for the vessel each day. From the figure, it is shown that the sampling rate is fluctuating. This fluctuation gave that the main source of loss in data comes from the location data set.

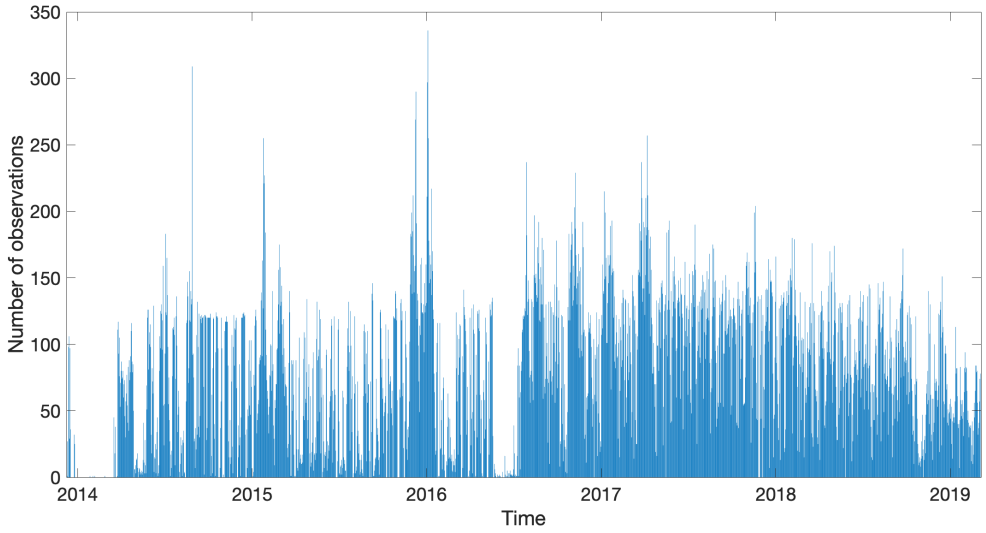

Figure 6.2: Available AIS data per day

6.4 Processing of Data

In this section, the processing of the data is described. A data point is removed by removing all the variables with the corresponding timestamp.

6.4.1 Combining Different Data Sources

The first step in the data processing was to collect the data from the three different sources and combine them into readable data files. The performance monitoring data were obtained as one .csv file per day, while the AIS data was given as one large unsorted .csv file. In order to combine these, the AIS data were sorted and split into one file per year, and the performance data were combined into one file per year. The AIS data and performance monitoring data were connected by linearly interpolating the AIS data in time to match the performance monitoring data. A restriction was set so the difference between the timestamp in the performance data and AIS data was smaller than 1 hour. The MATLAB script Save_Variable.m was used to combine the performance monitoring and AIS data, the script is given in Appendix A.1.

A .m file containing both AIS data and performance data were made for each year. In order to combine the weather data to this data set, the weather data were linearly interpolated both in time and space. As mentioned above the temporal resolution for the weather data are 6 hours while the temporal resolution for the performance data is 15 minutes. The weather data have a spatial resolution of 0.75x0.75 degrees, which means that the data set only contains information about the weather conditions in the corners, as illustrated in Figure 6.3. The blue points are the grid position, which contains information about the weather condition, and the red points represent the vessel's position. In order to obtain the weather condition at the vessels location, the weather condition at the blue points are linearly interpolated to the vessels position in space for both the time instant before and after the timestamp. Then the weather condition is linearly interpolated in time. The longitude values in the AIS data had values between -180 to 180 while the ECMWF operates with longitude from 0 to 360, so the longitude form the AIS data had to be converted in order to obtain the correct weather condition.

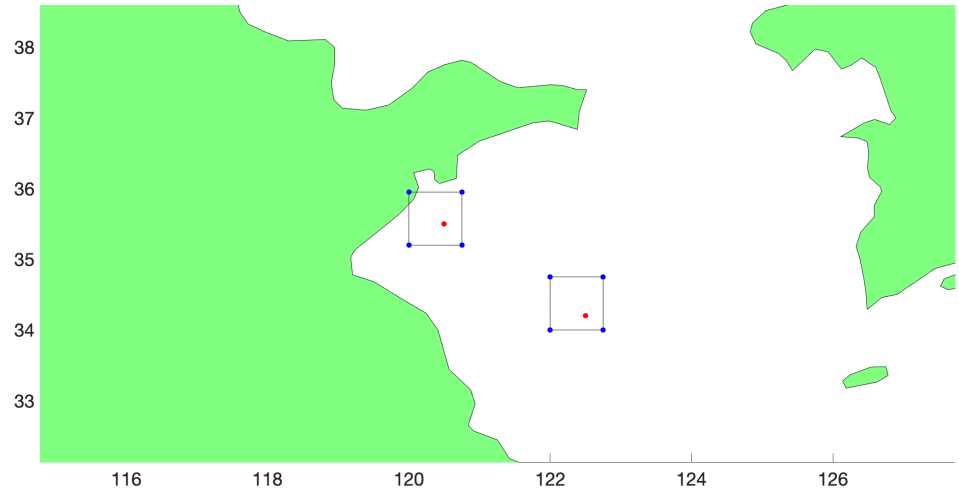

Figure 6.3: Definition of ECMWF grid

Figure 6.3 shows two different vessel positions. For the position to the right, all the grid points are at sea, so all contain information about both wind and wave conditions. For the position to the left, the grid point over land does not contain information about the wave condition, which is natural since there are no waves on land. The wave condition for this grid point is therefore set to be the mean of the other points. The mean value was chosen because it represents the wave condition better than setting the values to zeros as this might be artificially low. How this processing of the weather data and combining it with the performance monitoring data was done are given in Appendix A.2 and A.3. Figure 6.4 gives a bar chart over the number of available data points per day for the combined data set, the total amount is 77 738.

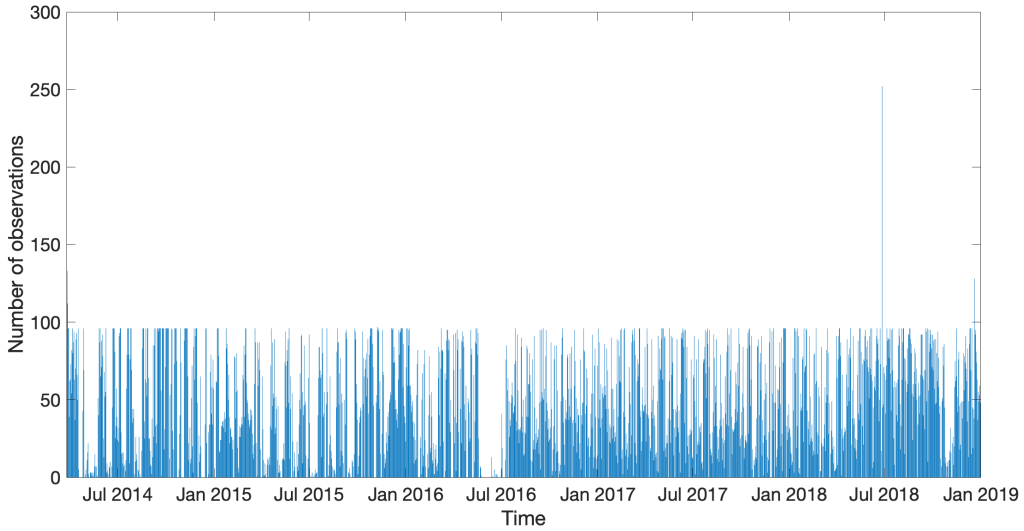

Figure 6.4: Data samples per day after processing

The figure shows that the number of available data points is nicely spread over in time, but there are

more data points available in the end than the beginning. There are a lot of missing values in July 2016. This is due to a lack of AIS data for that period, as shown in Figure 6.2. The vessel operates worldwide, as shown in Figure 6.5, which gives the complete travel history of the vessel.

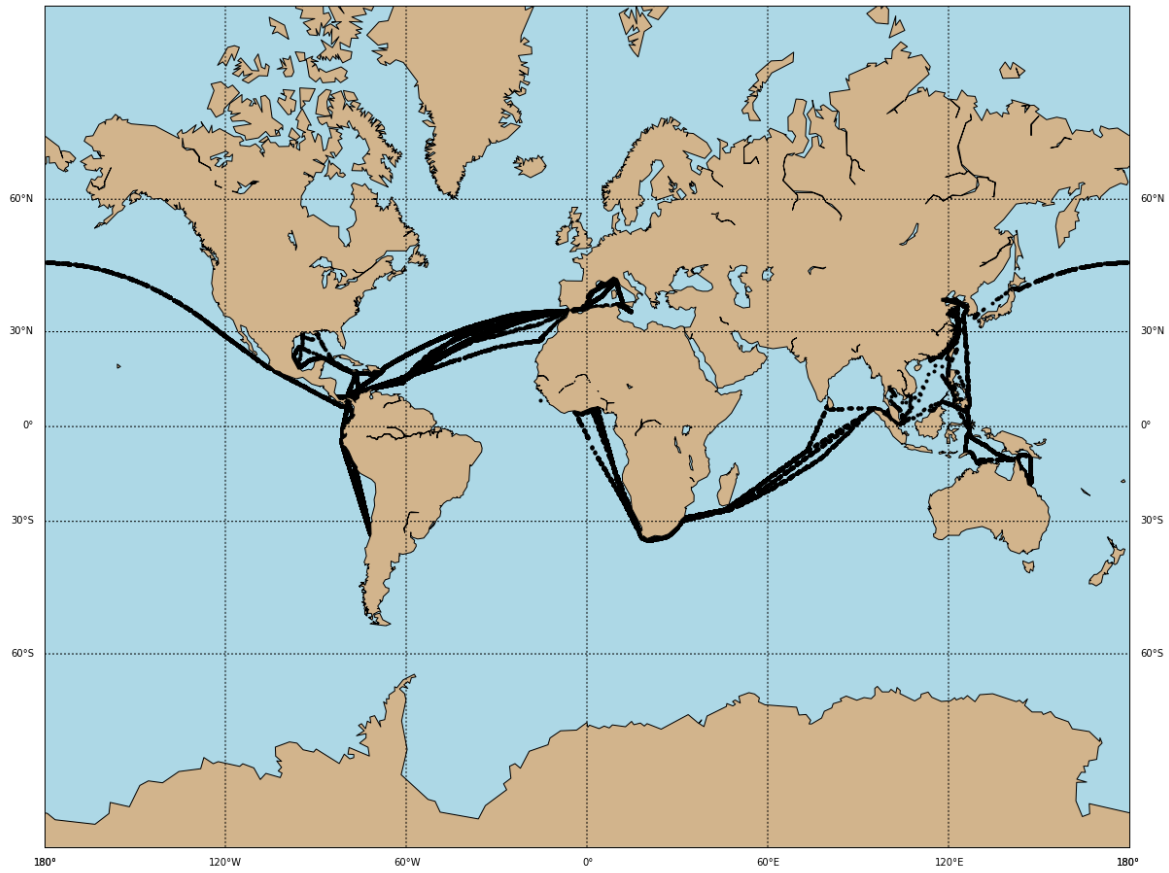

Figure 6.5: Complete travel history of the vessel

6.4.2 Draft and Trim

The performance monitoring data contains values for the draft fore and aft. The draft midships is calculated as the mean of these two drafts, and the trim is the difference. It was observed that the draft measurements for the vessel in transit were scattered, which is assumed to be caused by the fact that the draft measuring sensors are sensitive to the ship velocity. In order to reduce the measurement error, the drafts were averaged. First, the vessels speed below 8 knots, and data points where the vessel was accelerating were removed. This initial processing was done, so the vessel always was in transit and not undergoing loading operations at the port. Then the drafts were averaged over time so that the maximum time difference between two succeeding measurements was two hours. Figure 6.6 illustrates how this was done by showing a scatter plot of the original draft and the mean values for a short time window. The velocity of the vessel was between 16 and 20 knots in the given time window. In addition to averaging the draft measurements over time were data points for drafts below 6 meters removed because the draft in ballast condition is 6.2 meters, so drafts below this are either considered as false or un-normal operation. About one percent of the measurements were below 6 meters.

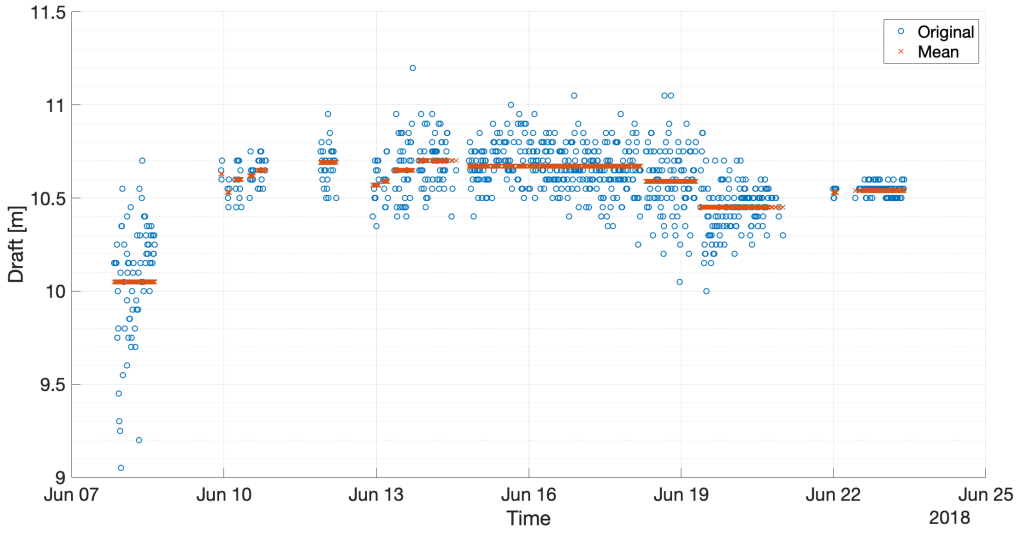

Figure 6.6: Draft

The calculated trim was also averaged as explained above. Trim values above 4 meters were also considered to be false and thereby removed from the data set. It is also observed that the trim and draft have some correlation, as shown by Figure 6.7.

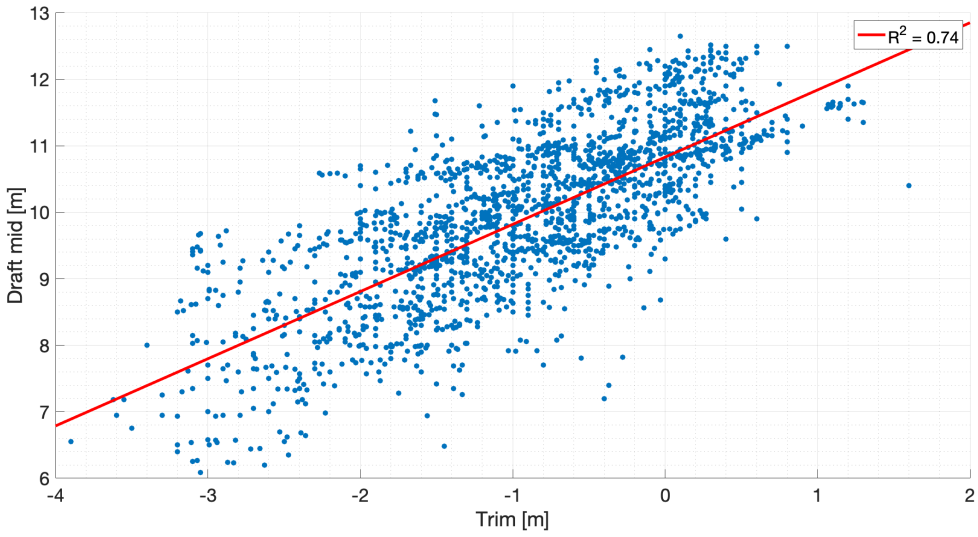

Figure 6.7: Correlation between draft and trim

Most of the measurements gave a draft of around 10.7 meters and trim around -0.4 meters.

6.4.3 Speed

There are two different speed measurements for the vessel, speed over ground and speed through water. A description of how these parameters usually are measured is given in Chapter 4.3.2. As the vessel

is mostly operating deep sea, it is expected that the currents are small. So, it is expected that the speed through water and speed over ground should be approximately the same. It was found that the difference in speed through water and speed over ground was smaller than 1.5 knots for 96.5 % of the data, which means that the accuracy of the speed through water sensor is good. Further analysis of the speed measurements gives that the ship's speed is zero for 40 % of the measurements. Figure 6.8 shows how the speeds is distributed.

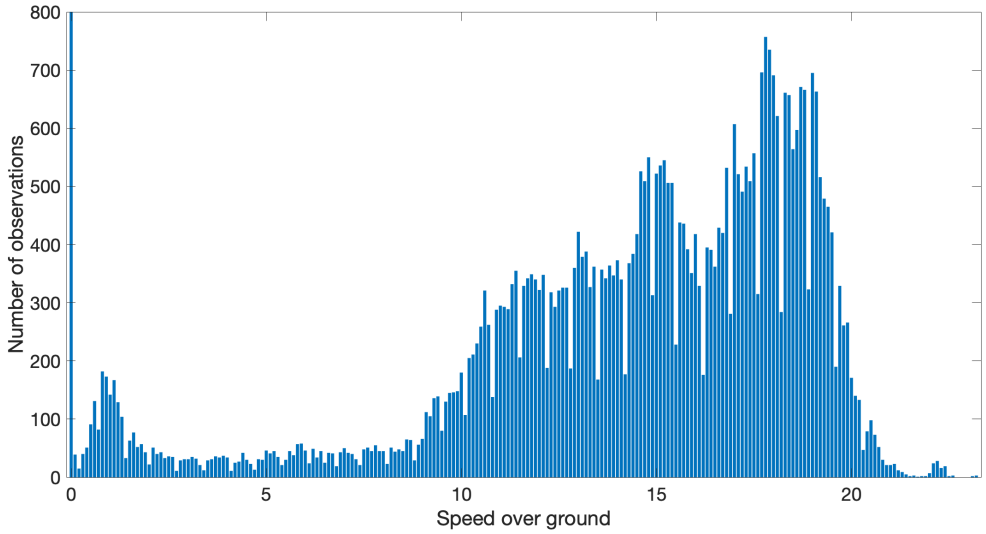

Figure 6.8: Distribution of speed over ground

Figure 6.8 does not show the top of the bar for speeds equal to zero as it contains over 31 000 measurements. The added power in transit is of interest, so the data points for speeds below 8 knots, both speed over ground and speed through water, were removed. Also, the data points where the difference between the speed over ground and speed through water was greater than 1.5 knots were disregarded. When the vessel is accelerating is the speed-power ratio different than for normal operation, therefore are the data points where the vessel is accelerating removed. This is done by letting the maximum difference in vessel speed between two measurements be 0.5 knots. By applying these requirements, about 60 % of the total data were removed.

It was also found that before February 2016 the vessel was operating at a significantly lower speed than after February 2016 as shown by Figure 6.9. The mean speed before was 13.5 knots while the mean speed after was 16.4 knots. This is believed to be correlated with the oil price, which had a drop around the same time. The spread in draft and trim were also smaller at the end of the time period.

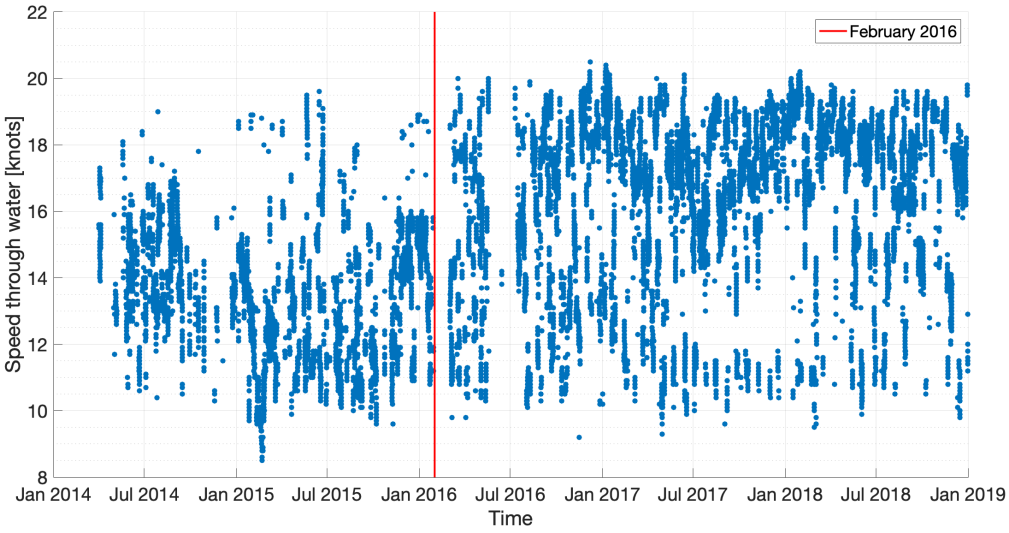

Figure 6.9: Speed variations over time

6.4.4 RPM

In addition to the above-mentioned data processing was the RPM values evaluated. It was found that the RPM data had some negative values, so all these were removed. This was done by removing all RPM values below 50 as these correspond to vessel speed below 8 knots.

Chapter 7

Methods

This chapter describes the methods used in this thesis to determine the added power of a ship due to fouling by using in-service performance monitoring data. As previously stated, this is a complex problem where different loading conditions, speeds, and environmental conditions have a significant influence on the power need. There are therefore necessary to compensate for these factors in order to compare the different data points and evaluate the change in power need over time. In this thesis, three methods are developed to determine the added power due to fouling.

The first two methods aim to produce data sets where the environmental effects such as wind and waves are accounted for. Then both the Admiralty coefficient and resistance coefficient are used to account for different loading conditions and speeds. The last method uses machine learning trained on data from the first year of operation to predict the shaft power. Then the relative prediction error is analyzed over time, to find the added power due to fouling. Appendix B shows how the methods presented below were implemented in MATLAB.

7.1 Benchmark

To be able to determine the added power due to fouling, it is necessary to have a reference for what the expected power need for a clean hull is. Usually, this benchmark is obtained during the speed-power test at the sea trial. However, for this vessel, the speed-power test was conducted for higher speeds than achieved during normal operation. Therefore, was it necessary to make another benchmark model. An exponential fitted curve was made to fit the lower part of the speed-power curve, for calm water. The values for calm water were found by filtering the data set by a maximum Beaufort number of 3 and a maximum significant wave height of 1 meter, as explained in Chapter 7.4. The line was calculated using the curve fitting toolbox in MATLAB. Figure 7.1 shows a scatter plot of the speed-power for calm water with the orange line representing the fitted curve that will be the benchmark model.

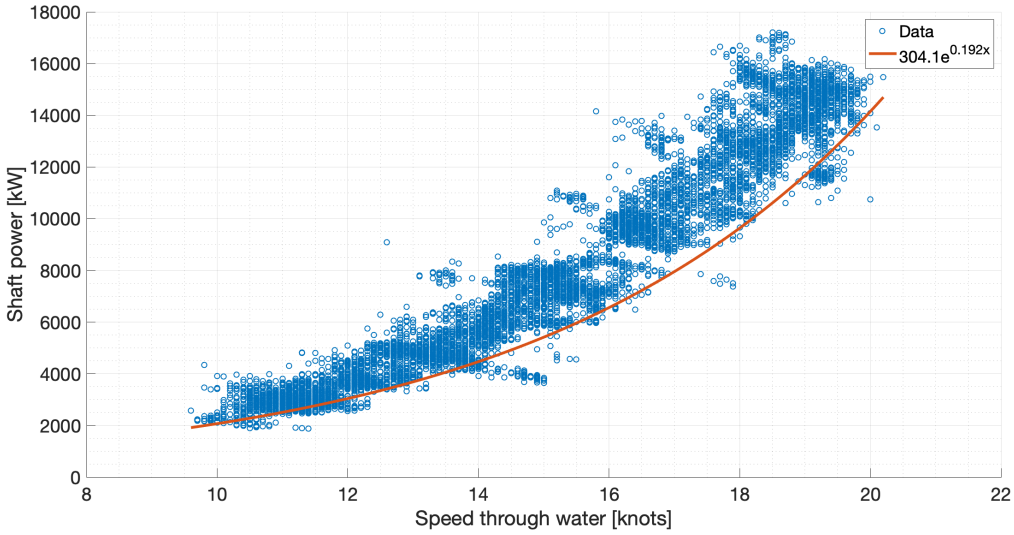

Figure 7.1: Speed-power data for calm water with benchmark line

The benchmark model is given by Figure 7.1 and describes the following relationship between the shaft power and speed through water. The speed through water is in knots and the shaft power in kilowatts.

$$Shaft\ Power = 304.1e^{0.192 \cdot STW} \tag{7.1}$$

In order to check how the drafts influence the speed-power model, the data in Figure 7.1 are split into two different groups, drafts higher and lower than 10 meters. The result is shown in Figure 7.2.

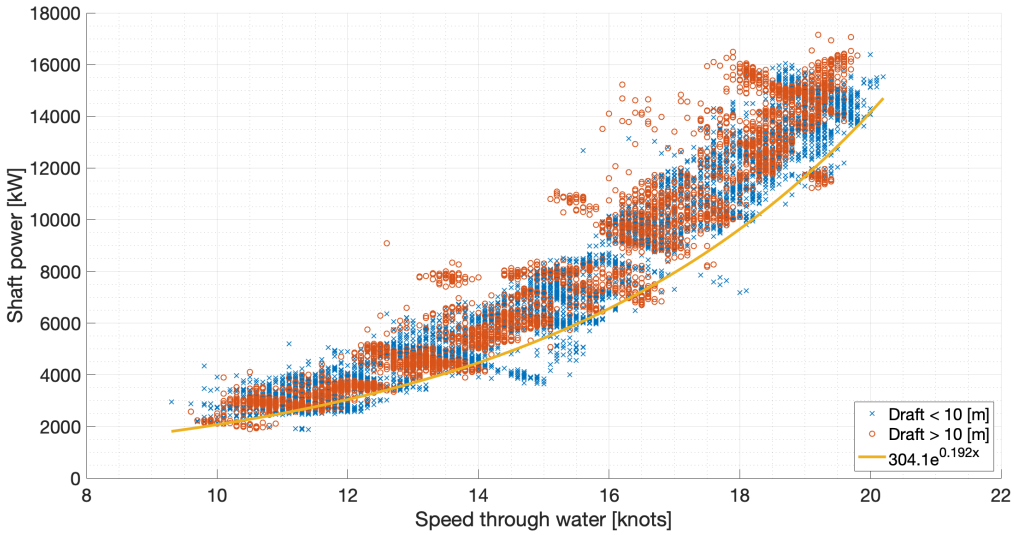

Figure 7.2: Speed-power data with benchmark line for different drafts

Drafts above 10 meters require more power to obtain the same speed as a draft below 10 meters, but the difference is small. For speeds below 18 knots is the difference minimal, and the benchmark

model gives a reasonable estimate for all loading conditions. Above 18 knots is the difference more significant between the benchmark and drafts above 10 meters. However, the difference is still small, so the benchmark model is considered to be a reasonable estimate for the power need of a clean hull.

7.2 Admiralty Coefficient

As explained in Chapter 4.4, the Admiralty coefficient is a traditional parameter used for performance analysis. It is a simple formula that accounts for different loading conditions and speeds, but not for different sea states. The Admiralty coefficient A_C uses the following relationship between the weight displacement Δ, ship speed V_S, and shaft power P_S.

$$A_C = \frac{\Delta^{2/3}\ V_S^3}{P_S} \tag{7.2}$$

The weight displacement Δ is not logged by the aboard performance monitoring system and needs to be estimated. It is estimated based on the mean draft T, which is a logged parameter. Then the following relationship was used to estimate the weight displacement.

$$\Delta = \rho \cdot B \cdot L_{WL} \cdot T \cdot C_B \tag{7.3}$$

Both the block coefficient C_B, water density ρ, breadth B, and length in waterline L_{WL} were all assumed to be constant in lack of better information. This assumption gives a linear relationship between the weight displacement and the draft. However, all of these parameters will change with the draft and trim because of the submerged hull's geometry changes. A more accurate relationship between the displacement and draft and trim can be obtained by using drawings or a 3D model of the vessel. However, this was not available. The water density will change with the seawater temperature, which means that there is also some error related to the assumption of constant density.

The Admiralty coefficient is assumed to be constant in calm water [32], for ships with small variations in speeds and loading conditions. Then the variation over time is caused by fouling. Then the shaft power can be estimated based on the Admiralty coefficient with a given weight displacement and speed, as shown by Equation 7.4.

$$P_{Estimate} = \frac{\Delta^{2/3}\ V_S^3}{A_C} \tag{7.4}$$

Then the estimated power is compared with the benchmark and the added power due to fouling is found by Equation 7.5. The benchmark is the expected power for the given loading condition and speed for a clean hull in calm water.

$$P_{Added} = \frac{P_{Estimate} - P_{Bench}}{P_{Bench}} \cdot 100\% \tag{7.5}$$

The added power P_{Added} is plotted over time to obtain trend lines, and these trend lines determine the added power due to fouling.

7.3 Resistance Coefficient

The difference between the resistance coefficient based on the measured performance data and the resistance coefficient based on the benchmark will give the added power. The following equation gives the resistance coefficient, as given in Chapter 2.

$$C_{TS} = \frac{R_{TS}}{0.5\rho V^2 S} \tag{7.6}$$

Where R_{TS} is the total resistance of the vessel given by Equation 7.7, ρ is the density of the seawater, V is the vessel speed, and S is the wetted surface area. Here the different loading conditions are accounted for by the wetted surface area.

$$R_{TS} = \frac{P_B \cdot \eta_D}{V} \tag{7.7}$$

P_B is the measured shaft power given by the performance monitoring system, and η_D is the propulsion efficiency, which is assumed to be constant and 0.7. The propulsion efficiency is assumed to be the same for both the benchmark and performance data. The propulsion efficiency η_D is not constant and usually changes with the load on the propellers. However, there is no information given about the propulsion efficiency, and as it is assumed to be the same for the benchmark, the error related to the propulsion efficiency is assumed to be small. Equation 7.8 estimates the wetted surface area

$$S = k \cdot \sqrt{\nabla L_{WL}} \tag{7.8}$$

where k is given by Figure 7.3, ∇ is the volume displacement and L_{WL} is the vessel´s waterline length.

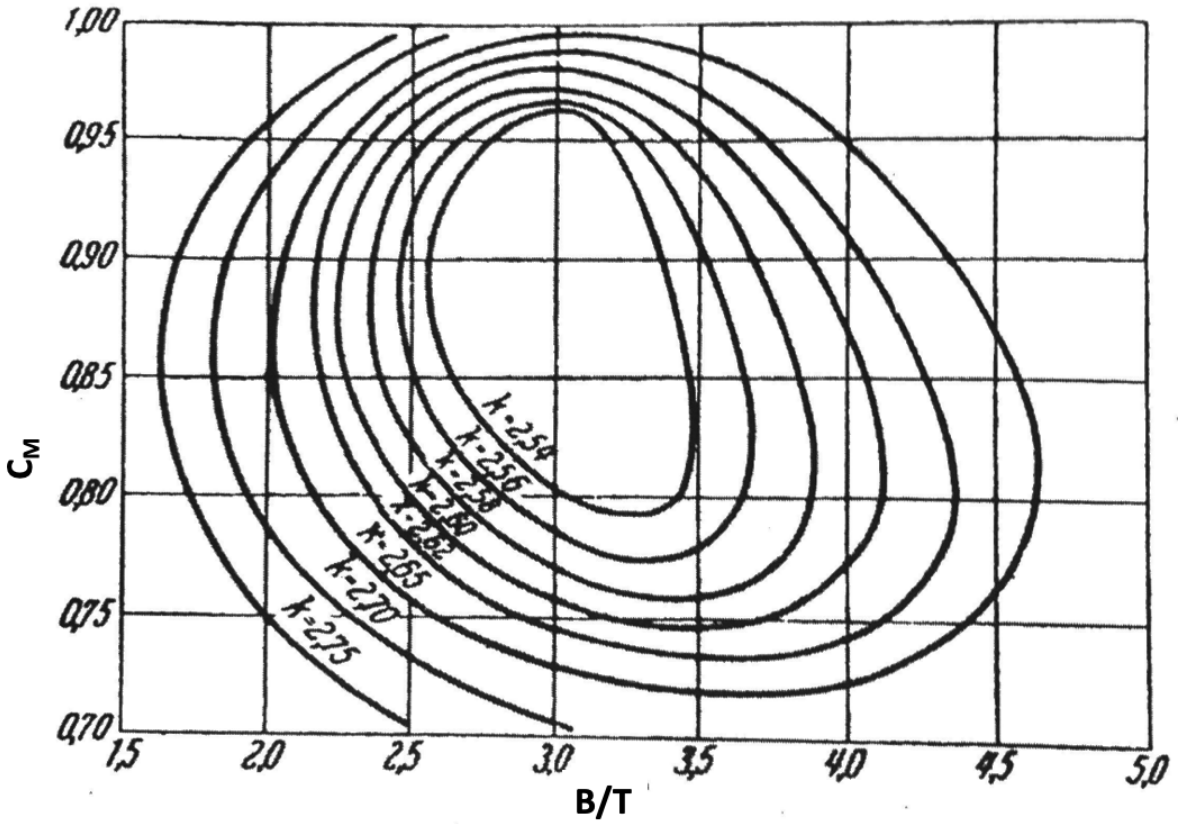

Figure 7.3: Diagram for determination of k used to estimate the wetted surface of a ship [39]

In order to determine the wetted surface constant k of the ship are both the midship coefficient C_M and the breadth of the ship assumed to be constant, while the draft changes. C_M is assumed to be 0.90, which is a reasonable assumption for modern container ships. When estimating the volume displacement ∇, both the block coefficient and the length in waterline are also assumed to be constant. The difference between the total resistance coefficient based on performance monitoring data and the benchmark is assumed to be caused by fouling. So, the change in frictional coefficient ΔC_F can be found by Equation 7.9. If all the other parameters in Equation 2.4 are assumed to be the same for the fouled and clean hull.

$$\Delta C_F = C_{TS_{Measured}} - C_{TS_{Bench}} \tag{7.9}$$

The resistance due to fouling can be expressed by Equation 3.7 as discussed in Chapter 3, which gives that the following equation can estimate the added power due to fouling.

$$P_{Added} = \Delta C_F \frac{0.5\ \rho\ S\ \eta_D\ V^3}{P_{Bench}} \cdot 100\% \tag{7.10}$$

The added power P_{Added} is plotted over time in the same way as for the Admiralty coefficient to obtain trend lines.

7.4 Method 1: Removing Data With Bad Weather

The first method used to compensate for the environmental effects was to filter out the data points with bad weather, by establishing criteria for bad weather and then remove every point, which is classified as bad weather. This filtering reduces the size of the data set. The Beaufort wind scale is a standardized scale that describes the weather condition [16]. In this thesis, a Beaufort number of 3 or less, which means wind velocity between 0 and 5.5 m/s, are classified as calm water. In addition, was a limit of 1 meter significant wave height applied. When these conditions have been removed the wind and wave resistance are assumed to be small compared with the calm water resistance and thereby neglected. That data points left are then dominated by calm water resistance, and the increased resistance over time is caused by fouling. Then both the Admiralty and resistance coefficient are used to compensate for different speeds and loading conditions. In addition to the wind and wave resistance will the density and temperature of the water and air influence the resistance of the vessel. The water depth will also influence the resistance of the vessel. However, nighter the temperatures or the water depth was measured, so these resistance components are not taken into account in this thesis. As the speed through water measurement is found to be reliable is the effect of current handled by using this measurement instead of the speed over ground.

7.5 Method 2: Including Environmental Effects

The second method used was to calculate the environmental effects, i.e. wind and wave resistance. These resistance components are removed from the total resistance so that only calm water resistance is left. This method aims to obtain a calm water data set that contains more data points than in Method 1.

7.5.1 Wind Resistance

The added power due to the wind resistance is calculated according to ISO 15016 standard for sea trails [16]. This procedure is explained in Chapter 2.2.1. The wind data obtained from the ECMWF database are found to be more reliable than the wind data from the performance monitoring system. The wind data from the ECMWF database are therefore used to determine the wind resistance. Equation 2.7 is modified so that the last part of the equation is removed. This gives Equation 7.11 which is used to determine the added wind resistance.

$$R_{AA} = 0.5\rho_a \cdot C_{AA}(\psi_{WRef}) \cdot A_{XV} \cdot V_{WRef}^2 \tag{7.11}$$

Both the transverse projected area above the waterline A_{XV} and the wind resistance coefficient C_{AA}, for all angles, needs to be known in order to use this procedure. The wind resistance coefficient was estimated based on Figure 7.4, which is given in the ISO standard [16].

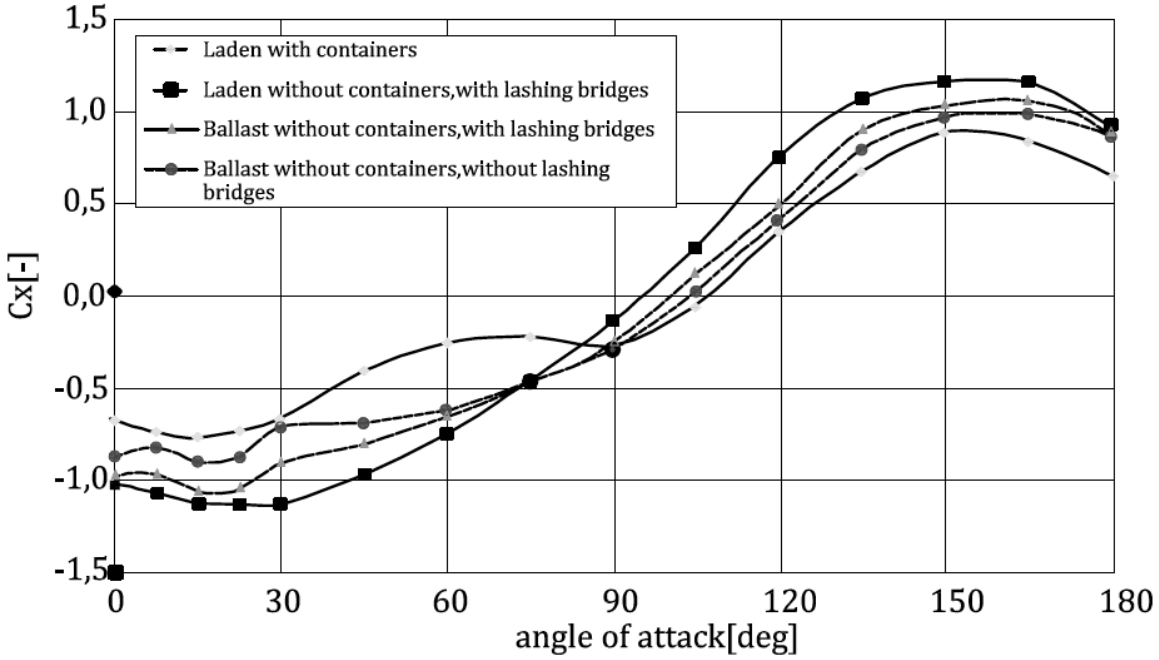

Figure 7.4: Wind resistance coefficient [16]

This figure is based on a 6800 TEU container ship. The ship analyzed in this thesis is a 2500 TEU container ship, which means that it is smaller than the ship Figure 7.4 is based on. However, this is the best available estimate for the wind resistance coefficient, and the error is assumed to be small as the form of the ships is similar. The vessel is always assumed to be loaded with some containers, so the dashed line is used to determine C_X. Then C_{AA} is determined as $C_{AA} = -C_X$. The transverse projected area above the waterline was estimated based on the height above the waterline and the width of the vessel. It was estimated to be 580 m^2.

7.5.2 Wave Resistance

The added power due to the wave resistance was also calculated according to ISO 15016 and is explained in Chapter 2.2.2. The limitations of this procedure mean that the wave resistance only be accounted for in small waves, waves with significant wave height less than three meters. This method only accounts for effects of waves in head sea ± 45°off the bow. The resistance for the waves that are not classified as head sea is set to 0. This is not a good assumption as beam sea might give large roll motions which will influence the vessel considerably and following sea might even give the vessel a boost.

7.6 Method 3: Machine Learning

The third method used to determine the added power due to fouling is to apply machine learning on the data set. The basic principles of how to use machine learning in regression analysis are given in Chapter 5. The machine learning models in this thesis are used to predict the shaft power based on a set of input parameters. They are trained on data for the first year of operation, where the fouling on the hull and propeller is assumed to be small. The data for the first year of operation is split into a training set and a validation set. The split is done randomly in time (within the first year) so that the training set has 80 % of the data and the validation set has the remaining 20 %. After the training

of the machine learning model, the model is fed with the remaining data, and the relative prediction error is calculated. The increase in the relative prediction error over time is assumed to be caused by fouling [18]. Three different machine learning models were tested, linear regression, custom linear regression, and Gaussian process regression.

7.6.1 Linear Regression

Linear regression is the simplest form for regression and can be used on any regression problems. The model assumes that there is a linear relationship between the parameters so that a weighted sum of explanatory variables can explain the desired variable.

$$y = \omega_0 + \sum_{i=1}^{N} \omega_i x_i \tag{7.12}$$

Where y is the shaft power, determined by the sum of weight parameters ω and input parameter x. As previously explained the shaft power, speed through water, and loading condition are not linearly dependent and therefore will this model probably be too simple (under fit) for the problem at hand.

7.6.2 Custom Linear Regression

A custom linear regression model allows the designer to assign non-linear dependencies to the model by using prior knowledge about the problem. A custom non-linear model can be made to predict the shaft power, based on previous knowledge about the relationship between the shaft power, speed and loading condition.

Speed

From the relationship between the ship resistance and the resistance coefficient, it is given that the ship resistance is proportional to the speed squared. It is also known that the shaft power is proportional to the resistance times the ship's speed. This gives the following relationship between power and speed, $P \propto V^3$. The Admiralty coefficient also gives this relationship. From this, the following relationship is applied in the custom regression model.

$$\omega_i V^3 \tag{7.13}$$

Draft

The draft influences both the displacement and wetted surface of the vessel. It is previously stated that it is assumed that the displacement is proportional with the draft, $T \propto \nabla$. From the Admiralty coefficient it is given that $P \propto \nabla^{2/3}$ which gives $P \propto T^{2/3}$. Then the following relationship is applied in the custom regression model.

$$\omega_i T^{2/3} \tag{7.14}$$

Trim

The trim will also influence both the displacement and wetted surface of the vessel. As the vessel has a bulbous bow will the effect of the bulbous bow change with the trim as well. Since the changes in trim have such a complex influence on the resistance of the vessel, it is difficult to determine the relationship between the trim and power. However, a trim optimization test can be carried out in

order to find out how the trim influences the resistance. Results from a trim optimization test are not known for this vessel, so the relationship between trim and power is therefore not known. Thus, the trim will not have a custom regression parameter but are assumed to be linearly. Which gives the following input used in the model.

$$\omega_i Trim \tag{7.15}$$

Time

The power will change in time due to fouling of the hull and propeller. This influence are as previously stated assumed to be linear.

$$\omega_i Time \tag{7.16}$$

Final Model

By including the custom model in Equation 7.12 it becomes

$$y = \omega_0 + \omega_1 V^3 + \omega_2 T^{2/3} + \omega_3 Trim + \omega_4 Time + \sum_{i=5}^{N} \omega_i x_i \tag{7.17}$$

where $i = 5\ to\ N$ are other input parameters for the environmental condition given in table 7.1, where a custom relationship have not been made. Figure 7.5 gives a scatter plot of the different custom models against the shaft power to see how well the data fit a linear relationship.

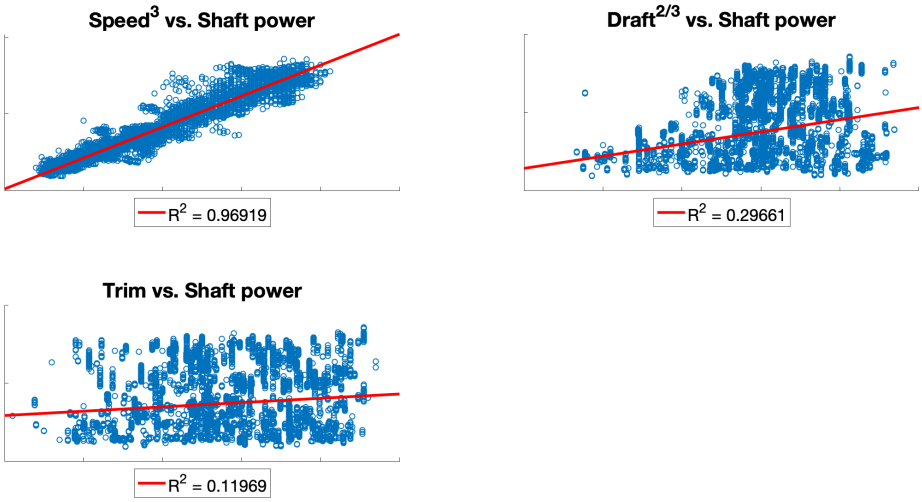

Figure 7.5: Linear correlation for custom model

The figure shows that the model for the ship's speed gives an excellent linear relationship with a R^2 almost 0.97 while the model for the trim and draft does not represent a linear relationship very well.

7.6.3 Gaussian Process Regression

The Gaussian process for regression analysis is built on a complex mathematical and statistical framework, so only a few sentences about the method are given here. For a detailed description, see "Gaussian Process for Machine Learning" by Rasmussen and Williams [40]. A Gaussian process is a generalization of the Gaussian probability distribution where the Gaussian probability distribution describes the variables in the process [18]. Then the input variables for the regression model have a joint Gaussian distribution, and the parameters of these distributions can be obtained by training the input set with a corresponding output set. Then these joint distributions are used to predict new values for similar input sets.

7.6.4 Input analysis

Since this problem is best solved by supervised learning, it is necessary first to choose which variables that shall be the input for the model. An analysis of different input sets was conducted in order to choose the set of input variables that gave the smallest prediction error. The different input sets are given in Table 7.1.

Table 7.1: Input sets

Variable	**Set 1**	**Set 2**	**Set 3**	**Set 4**	**Set 5**	**Set 6**	**Set 7**
Draft midship	x	x	x	x	x	x	x
Trim	x	x	x	x	x		x
Seed through water	x	x	x	x	x	x	x
Time					x		x
Rel. wind direction		x		x			x
Wind speed		x		x			x
Rel. wave direction			x	x			x
Significant wave height			x	x			x
Wave period			x	x			x

The table above is split into three parts. The first part contains parameters with information about the loading condition and speed, the middle part is time from delivery, and the last part contains information about the environmental condition. The draft and speed through water are the most important parameter for determining the shaft power, therefore are these input parameters in all the data sets. The input sets 2, 3, 4, and 7 contain information about the environmental condition as well. Time is included in two of the input sets to see if it will have a large impact on the accuracy of the model. In order to find the best input set, the mean prediction error is evaluated. The mean prediction error is calculated based on the results obtained by applying the trained models on the validation set. It is defined by Equation 7.18.

$$Mean\ prediction\ error = \frac{1}{N}\sum_{i=1}^{N}\left|\frac{True_i - Predicted_i}{True_i}\right| \cdot 100\% \tag{7.18}$$

Figure 7.6 gives the mean prediction error for the different input sets and models.

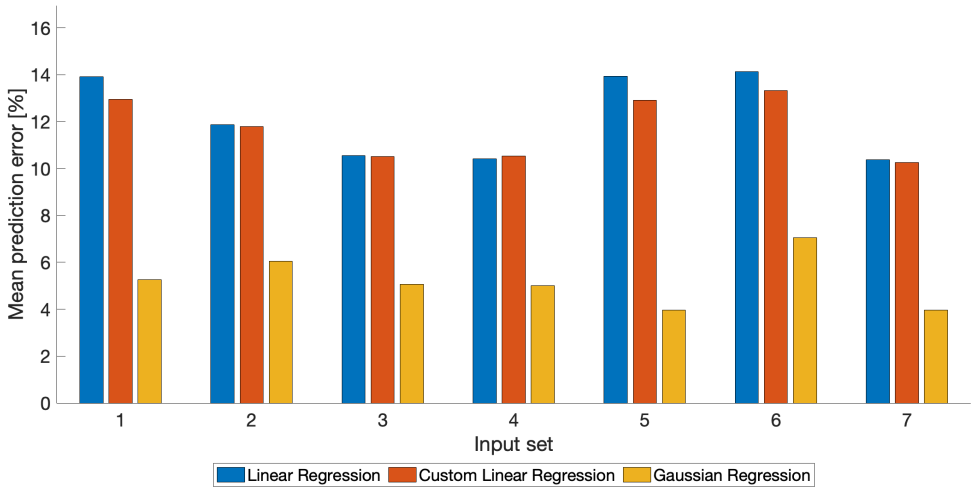

Figure 7.6: Mean prediction error for different input sets

It is given from the figure that the custom linear regression model gives the same or a better prediction than the linear regression model, which indicates that the changes applied to the linear model were good. However, they both have a higher prediction error than the Gaussian regression model. The difference between the three fist input sets is the environmental condition, and here it is shown that as expected, that the wave condition has the most significant influence on the prediction error. By comparing input set 1 with 5 and 4 with 7, it is shown that the time variable has a positive influence on the Gaussian regression model, but a negative influence on the linear and custom regression model. Input set 4 contains information about both the loading condition, speed, and environmental condition. It also gave the least mean prediction error for the three regression models without containing a time variable. It is therefore chosen as the input set to be used in the analysis. Since the custom linear regression model gives better or the same result as the linear regression model, the linear regression model is disregarded in further analysis.

Chapter 8

Results

The following chapter presents the results obtained by the methods described in the previous chapter. The results are presented in figures, and results from different models are compared. This will provide a discussion about the reliability of the models a recommendation of the best model given in the next chapter. The results in this chapter use the data set described in Chapter 6.

8.1 Method 1: Removing Data With Bad Weather

The first method used to determine the effect of fouling is to filter the data set by the weather condition. As previously stated was all the data points where the Beaufort number was higher than 3 and the significant wave height higher than 1 meter removed. By filtering out these conditions, approximately 70 % of the data points were removed.

8.1.1 Power Over Time

The simplest method to determine the added power due to fouling is to choose a speed, then plot the power over time. The calm water data set contains about 11 000 values, and Figure 8.1 shows how these are spread over the different speeds.

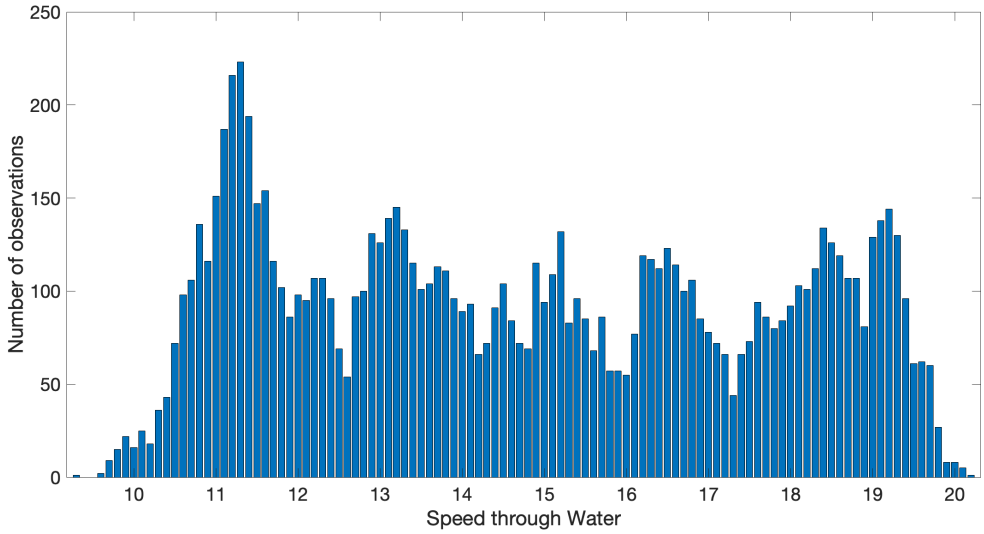

Figure 8.1: Distribution of speeds for the calm water data set

As shown by the figure are the speeds quite evenly distributed. It is also shown that the number of data points rapidly decreases when a speed is selected. For example, if a speed between 17.9 and 18.1 knots is chosen, then the number of data points is reduced to 279, without filtering the loading condition. If different loading conditions are filtered as well, there are almost no data points left. A plot of the added shaft power relative to the benchmark given by Figure 7.1 for velocities between 17.9 and 18.1 over time is shown in the figure below.

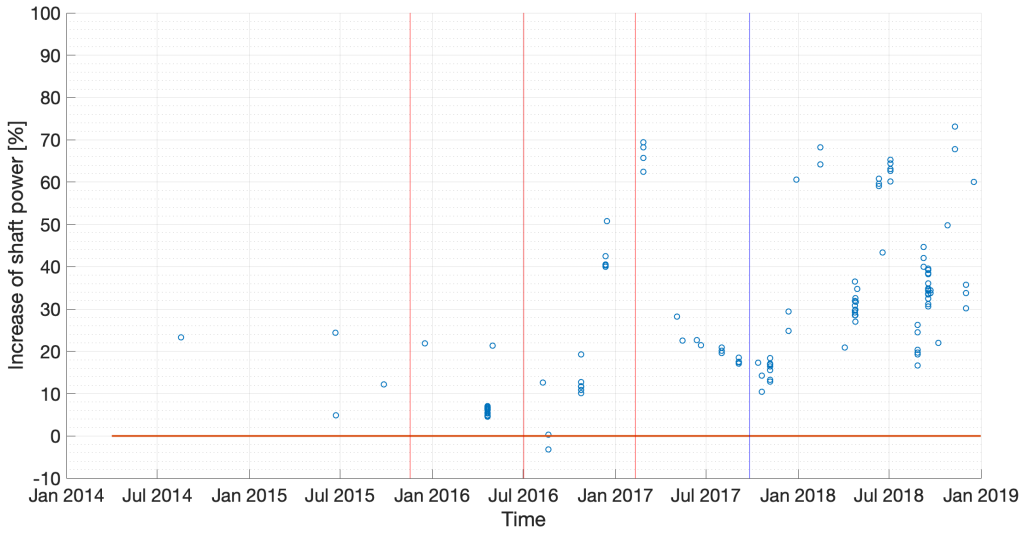

Figure 8.2: Power over time for 18 knots, calm water

It is clearly shown by Figure 8.4 that there are not enough sample points to draw any conclusions about what the added power is. This method is therefore disregarded. However, it shows that there is a trend that the power increases towards the end of the time series.

8.1.2 Admiralty Coefficient

Following the method described in Chapter 7.2, the Admiralty coefficient for the calm water data set is calculated. Figure 8.3 shows a scatter plot of the Admiralty coefficient for the calm water data. The thick red lines are the trend lines between the events marked by the vertical lines. The trend lines are assumed to be linear and calculated by minimizing the root mean square error. The vertical red lines indicate dates where the propeller was cleaned, and the vertical blue line indicates the date when the hull was cleaned.

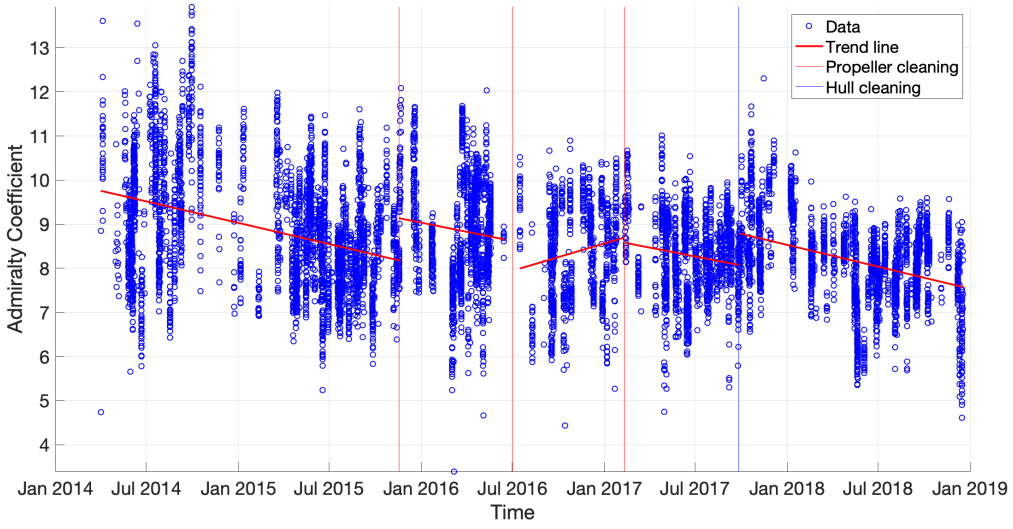

Figure 8.3: Admiralty coefficient over time for Method 1

A decrease in the Admiralty coefficient is a decrease in vessel performance. From the figure, it is shown that from vessel delivery and to the first propeller cleaning, the trend for the Admiralty coefficient is decreasing. It has decreased by approximately 16%. The first propeller cleaning has an obvious effect, as shown by the second trend line. It restores the Admiralty coefficient to a 6% decrees relative to the first value. The second propeller cleaning gives a decrease according to the trend line, while the data points right after the cleaning show an increase in the Admiralty coefficient. The third propeller cleaning gives no effect on the Admiralty coefficient, according to Figure 8.3. However, the hull cleaning shows a significant increase in the Admiralty coefficient, from about a decrease of 20% up to a decrease of 13% relative to the first value.

An estimate for the shaft power for design loading condition and a speed of 18 knots was calculated based on the Admiralty coefficients in Figure 8.3. The shaft power used as a benchmark was calculated based on the line in Figure 7.1.

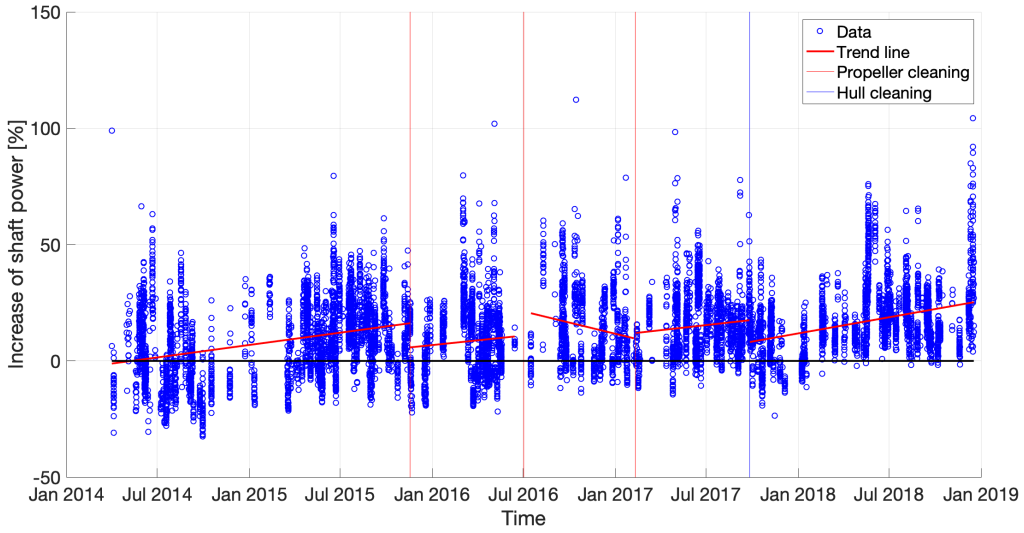

Figure 8.4: Added power based on Admiralty coefficients for design loading condition and speed 18 knots, Method 1

To show the trend lines more clearly are the limits on the y-axis set to be -50 to 150 %, so there are a few data points outside these limits. Form the trend lines in the figure it is given that at vessel delivery, the added power is almost zero, which is expected. Right before the first propeller cleaning the increased power was approximately 16 % and the first propeller polishing had a significant effect, with a 10 % drop to an increased power of 6 %. Between the two last propeller cleanings, the trend lines show an increase in vessel performance, which is not as expected. The hull cleaning had a good effect and as expected are the slope of the trend line more steep after the hull cleaning. At the end of 2018, the increased power according to this method was 25%, which implies that there is significant fouling present.

This method is fast, simple and easy to implement, but as shown by Figure 8.3 and 8.4 the data has much spread which means that there is some uncertainty in the method. To cope with this one needs a lot of data, which means that to be able to use this method to determine the added power due to fouling one has to see the trend over a long period at least a couple of months to be able to draw any conclusion.

8.1.3 Resistance Coefficient

The resistance coefficient was also used to determine the added power due to fouling. Following the procedure explained in Chapter 7.3. Figure 8.5 shows the estimated resistance coefficient plotted against time.

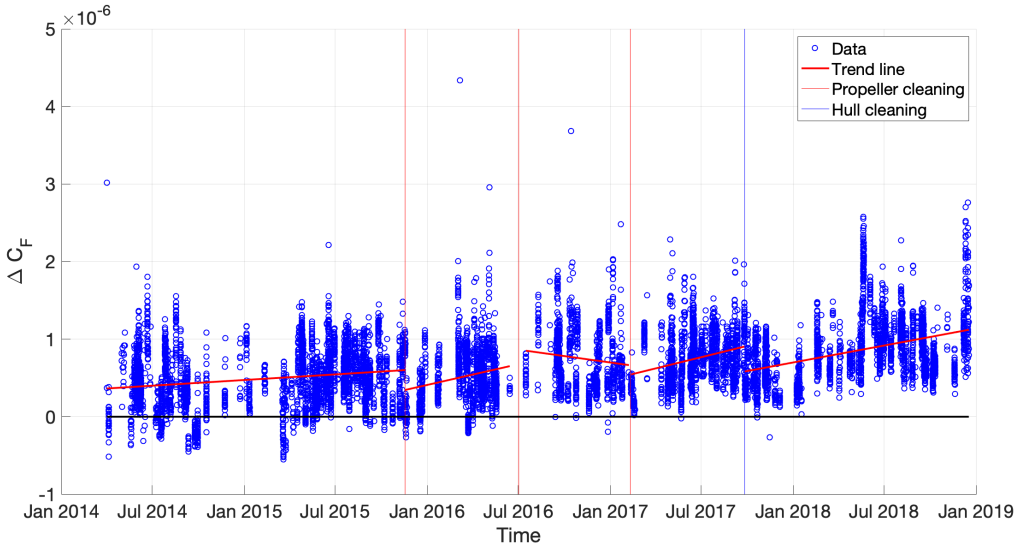

Figure 8.5: Resistance coefficient over time for Method 1

An increase in the resistance coefficient will increase the power needed. The figure clearly shows from the trend lines, that the resistance coefficient increases over time and that there is a drop after each event as expected. Except between the two propeller cleanings in July 2016 and February 2017, where the resistance coefficient decreases over time, which is the same that was shown by the Admiralty coefficient. Based on the resistance coefficient given in Figure 8.5 were the added power due to fouling estimated and are shown in Figure 8.6.

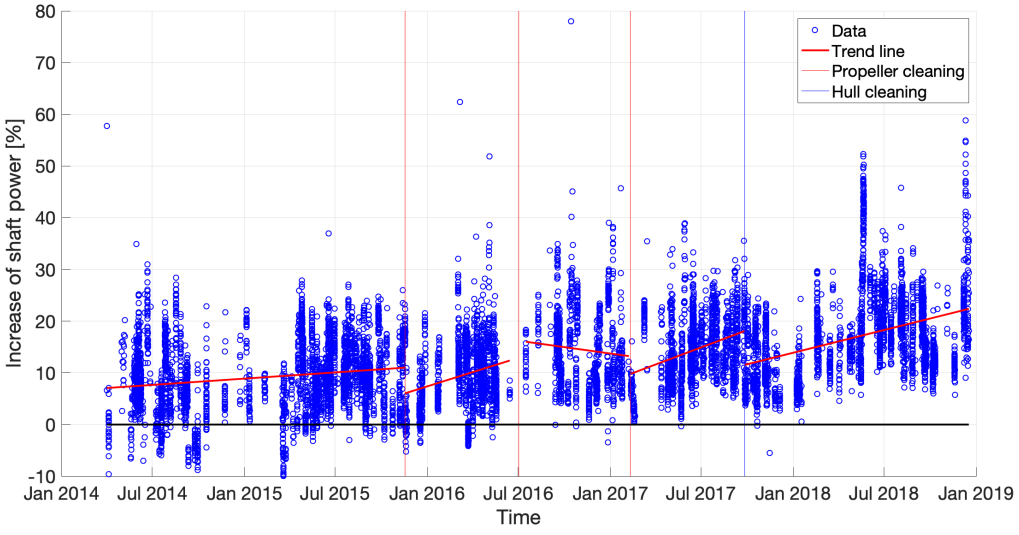

Figure 8.6: Added power based on the resistance coefficients for Method 1

The first thing to notice is that the limits on the y-axis are different than for Figure 8.4, because there is less spread in the data for this method, and all the data points are within the limits. Less spread in the data implicates that this might be a more accurate method. The results are also as expected with an increase of power over time, except between the last two propeller cleanings. However, from

the first trend line, it is shown that the vessel starts with an increase of the shaft power about 6 %, this is higher than the expected zero. The last trend line gives that the added power due to fouling at the end of 2018 is estimated to be 22 %, which is lower than what the added power estimation based on the Admiralty coefficient. However, it still implies a significant added power due to fouling.

8.1.4 Comparison

Figure 8.7 gives a comparison of the trend lines calculated based on the Admiralty and resistance coefficient given in Figure 8.4 and 8.6.

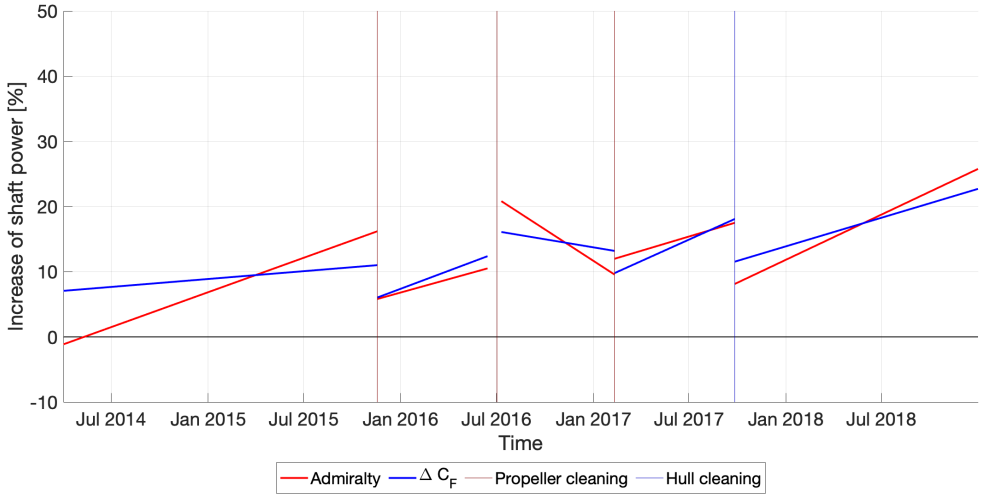

Figure 8.7: Comparison of trend lines for Method 1

The red line gives the added power based on the Admiralty coefficient, and the blue line gives the added power based on the resistance coefficient. From the figure, it is shown that the resistance coefficient gives a more conservative estimate than the Admiralty coefficient. The slope of the trend lines for the resistance coefficient is lower than for the Admiralty coefficient for most of the lines. The difference between the models is small except before the first propeller cleaning. It is also shown that between the two last propeller cleanings the slope of the trend lines is negative for both methods. This is the opposite of what is expected, and both methods even give that the power needed increases after the second propeller cleaning. It was found that the number of data points available between the two last propeller cleanings was lower than between the other events. In addition, there were few data points right after the second propeller cleaning, which influences the results and is believed to be the reason why the trend line has a negative slope. Figure 8.8 shows how the number of available data points per day for Method 1 are distributed. The propeller and hull cleaning events are marked with vertical red and blue lines.

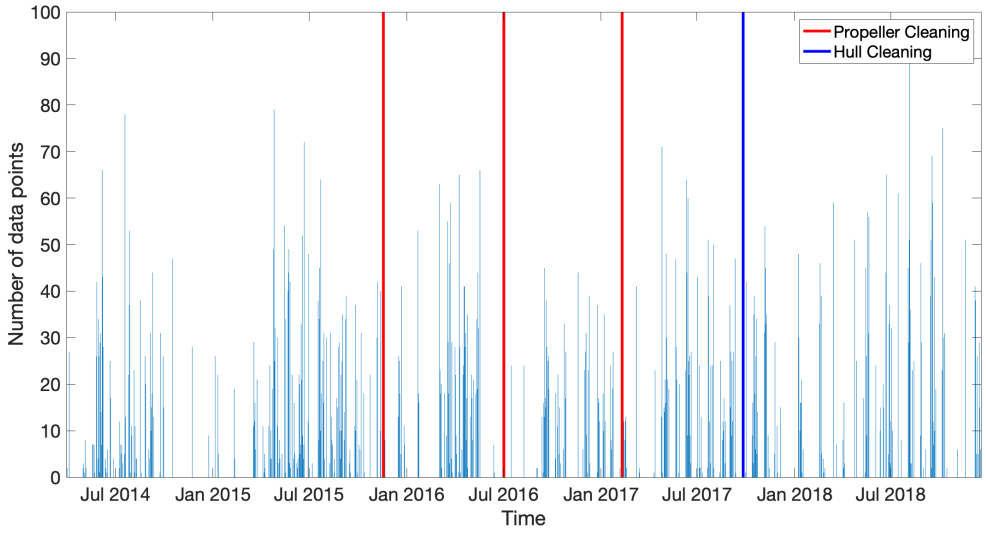

Figure 8.8: Number of data points per day for calm water data set

The holes represent the missing data points due to bad weather (or other data possessing criteria given in Chapter 6). When these holes are close to a propeller or hull cleaning event, it influences the result, so the effect of these events is not captured well. It is shown that around the second propeller cleaning, there are two big holes in the data points both before and after.

8.2 Method 2: Including Environmental Effects

The second method used to determine the added power due to fouling was to calculate the wind and wave resistance and remove them from the total ship resistance, as explained in Chapter 7.5. All data points with significant wave height above 3 meters were removed as the model used to calculate the wave resistance is only valid for small waves. This accounted for approximately 4 % of data, which gives that the total amount of data for this method is much more than for Method 1. The determination of the environmental conditions is however based on some assumptions stated in Chapter 7.5, which gives some uncertainty in the results.

8.2.1 Admiralty Coefficient

After the added power due to wind and wave resistance were accounted for was the Admiralty coefficient calculated. The calculated Admiralty coefficients are given in Figure 8.9.

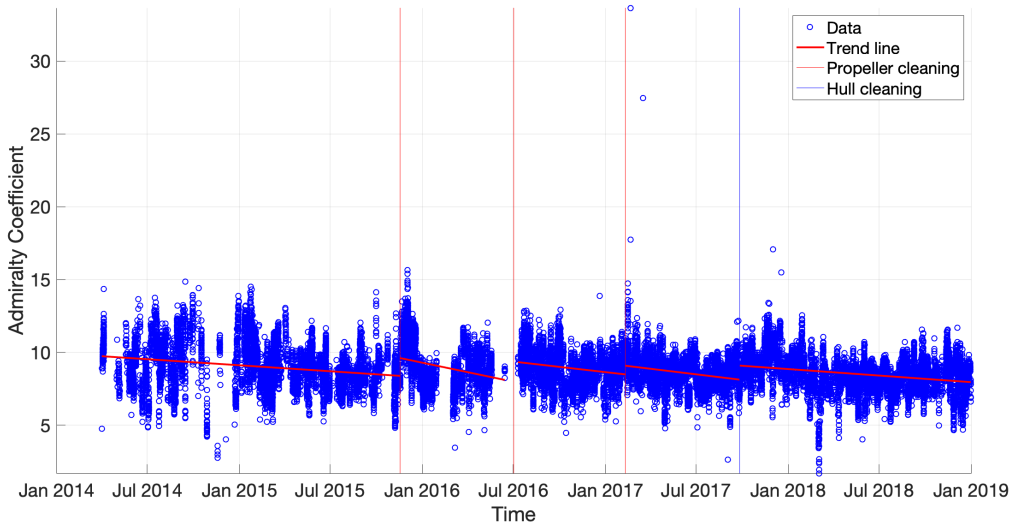

Figure 8.9: Admiralty coefficient over time for Method 2

It is shown here that the Admiralty coefficient is decreasing between each event and that each event gives a positive effect on the performance, which is the expected behavior of the Admiralty coefficient. From the figure, it is also shown that there are some outliers and that the spread is larger than for Method 1. It implies that not all the weather effects were accounted for. Following the same procedure as in Method 1, the shaft power was estimated based on the calculated Admiralty coefficient. Figure 8.10 gives the added power for the design loading condition and speed of 18 knots, the same condition as Method 1.

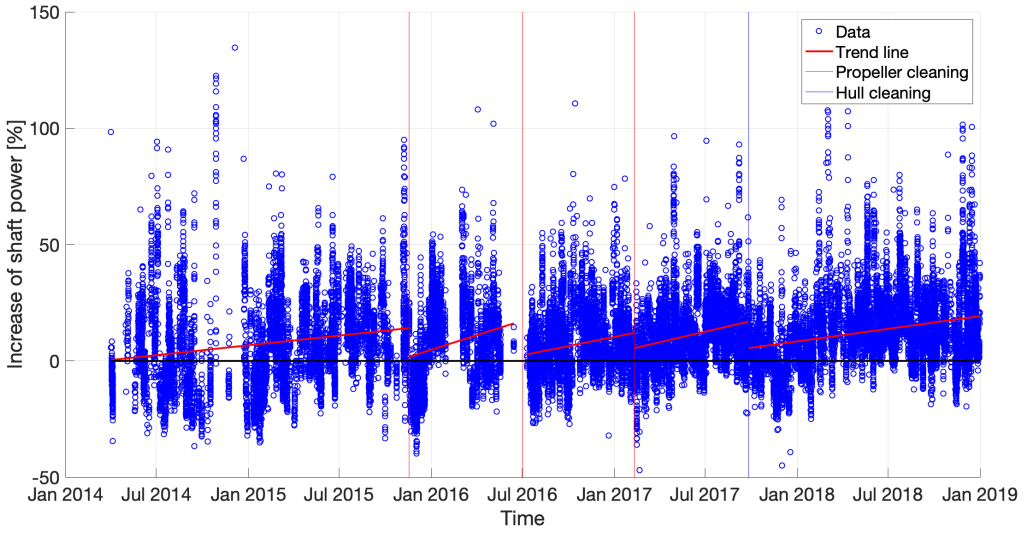

Figure 8.10: Added power based on Admiralty coefficient for design loading condition and speed 18 knots, Method 2

The y-limits are fixed to show the trend lines better and which means that some outliers are not shown in Figure 8.10. It is given form the trend lines that the added power starts at zero, which is the expected value. Right before the first propeller cleaning the increased power was approximately

14%, which is 2 % less than the added power Method 1 gave. The added power after the first propeller cleaning is almost reset to zero. The trend lines increase between all events, which indicates that more data points around the cleaning dates have helped the model to capture the effect of the cleaning. At the end of 2018 gives this model an increased power due to fouling of 19 %, this is 5 % less than Method 1 gave.

8.2.2 Resistance Coefficient

The resistance coefficient was also calculated for this data set. Figure 8.11 shows the calculated resistance coefficient.

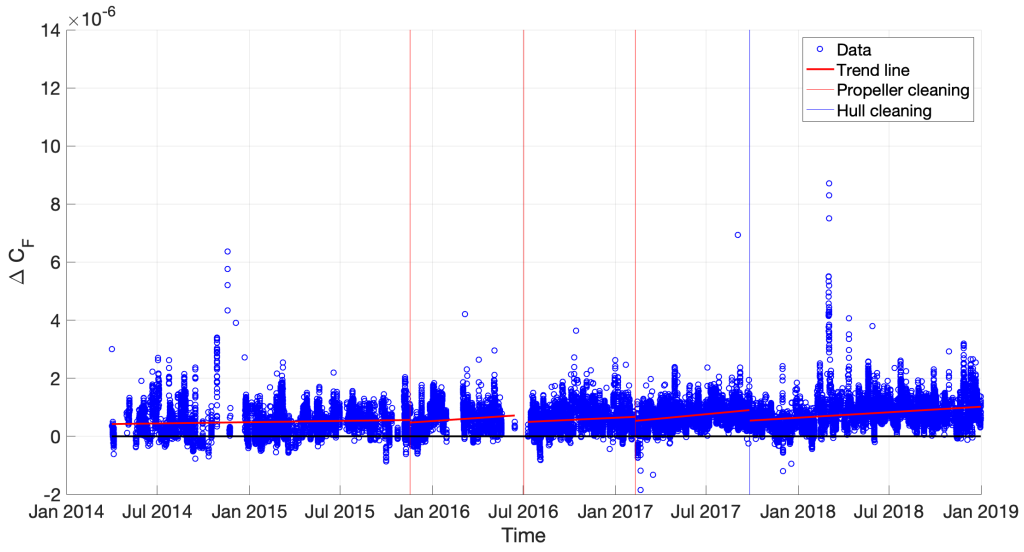

Figure 8.11: Resistance coefficient for Method 2

The figure shows that the spread in the resistance coefficient is larger for Method 2 than Method 1. When comparing Figure 8.11 with Figure 8.5 it is important to notice that the y-limits are different. The trend lines are hard to see in this figure, but they show that the resistance coefficient has a slight increase between all events. The effect of the propeller cleanings are however not identified well, but a little decrease is shown. Based on the resistance coefficients given Figure 8.11 the added power due to fouling was determined and are shown in Figure 8.12.

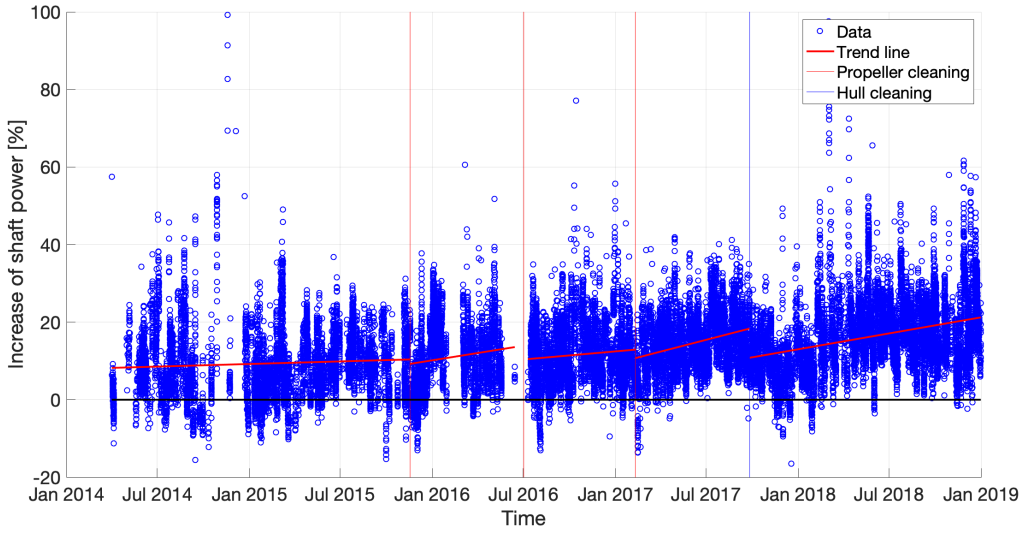

Figure 8.12: Added power based on resistance coefficients for Method 2

From the figure, it is given that the added power at vessel delivery is 8 %, which is much more than expected. The resistance coefficient gave a large initial added power for Method 1 as well, which indicates that something is wrong with the benchmark for this model. The added power increases between all the events, as expected. However, the slopes are small, and the effect of the first and last propeller cleaning gives a small drop in added resistance of about 1 %, which is smaller than expected. The analysis identifies a clear drop of 8 % in added power after the hull cleaning and lands on an added power of 21 % at the end of 2018 which is approximately the same that the Admiralty coefficient gave.

8.2.3 Comparison

A comparison of the trend lines given by the two models for Method 2 is given in Figure 8.13.

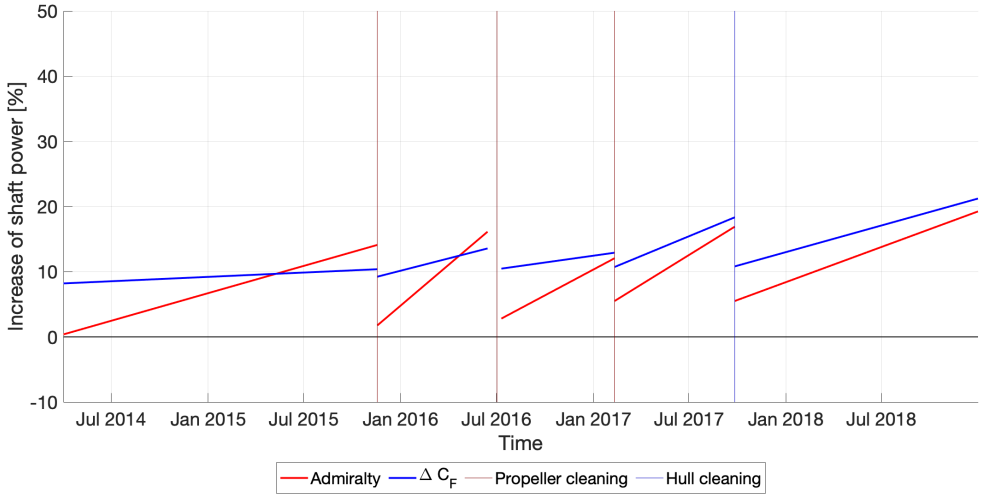

Figure 8.13: Comparison of trend lines for Method 2

The red lines give the added power based on the Admiralty coefficient, and the blue lines are based on the resistance coefficient. Here, the slope of the trend line for the admiralty coefficients all are steeper. The Admiralty coefficient clearly shows the effect of each event. It is also shown that the difference between the two methods is significant right after an event and small right before, which indicates that the resistance coefficient fails to identify a cleaning event. The Admiralty coefficient gives the expected zero added resistance at vessel delivery as well as identifying all events that indicate that this is the most accurate model between the two.

8.3 Method 3: Machine Learning

The third method used to determine the added power due to fouling is to apply machine learning the data set. As explained in Chapter 7.6 is the machine learning models trained on a data set containing values form the first year of operation. It is assumed that the fouling on the hull and propeller during the first year of operation are small so that the increase in the relative prediction error over time is caused by fouling. Input set 4 from Table 7.1 are used. The mean relative prediction error shown in Figure 7.6 is based on the absolute value, which means that it can not be directly compared with the trend lines in this section.

8.3.1 Custom Linear Regression

The custom linear regression model is explained in Chapter 7.6.2 and the modifications are done to the draft and speed through water. The relative prediction error over time for input set 4 are shown in Figure 8.14.

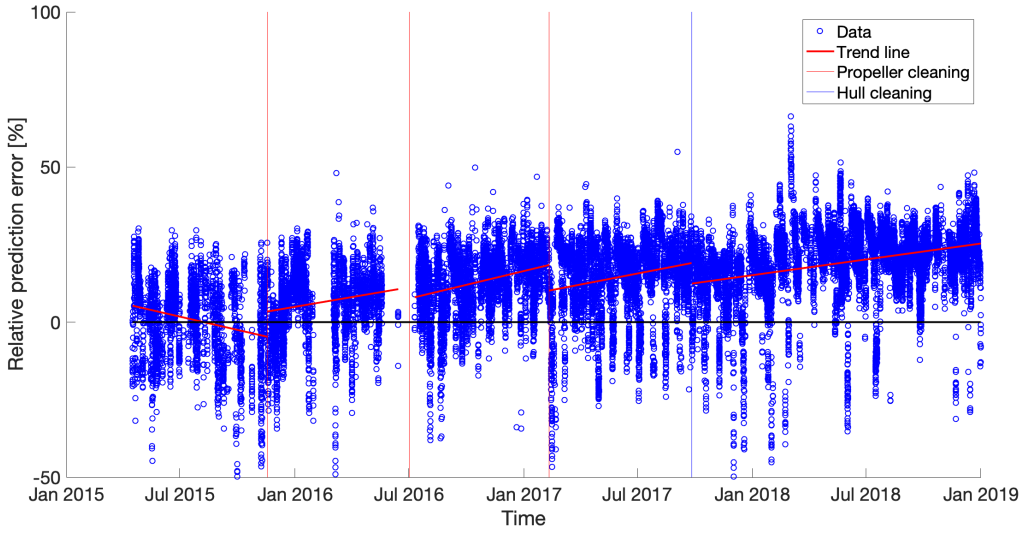

Figure 8.14: Relative prediction error, custom linear regression

The data starts in April 2015 and not at vessel delivery, so the training data are not used in the analysis. It is shown by the figure that before the first propeller cleaning the slope of the trend line is negative. This negative trend is unexpected as it is assumed that fouling on the hull will increase the prediction error. After the first propeller cleaning all the trend lines shows an increase in the relative prediction error. The effect of each event is also clearly shown by a drop in the relative prediction error. This drop indicates that the condition of the hull after an event is more similar to the condition of the hull during the first year of operation than before an event. If one assumes that the model is perfect, the expected relative prediction error for a clean hull is zero. Then the relative prediction error gives the added power due to fouling. Then the added power due to fouling based on this model at the end of 2018 is 25.33 %, which is very close to the result for Method 1 and a little bit higher than the result for Method 2. However, the model is not perfect as shown by Figure 7.6. The expected relative prediction error was calculated to be -2.10 %, by calculating the mean prediction error without absolute value. Adding this value to the data in Figure 8.14 gives a better estimate of the increase of shaft power. Then the added power due to fouling by the end of 2018 becomes 23.23 %, which is close to what both Method 1 and 2 gave.

8.3.2 Gaussian Regression

Gaussian regression was also used to find the effect of fouling. The relative prediction error over time for input set 4, and the Gaussian regression model is shown in the figure below.

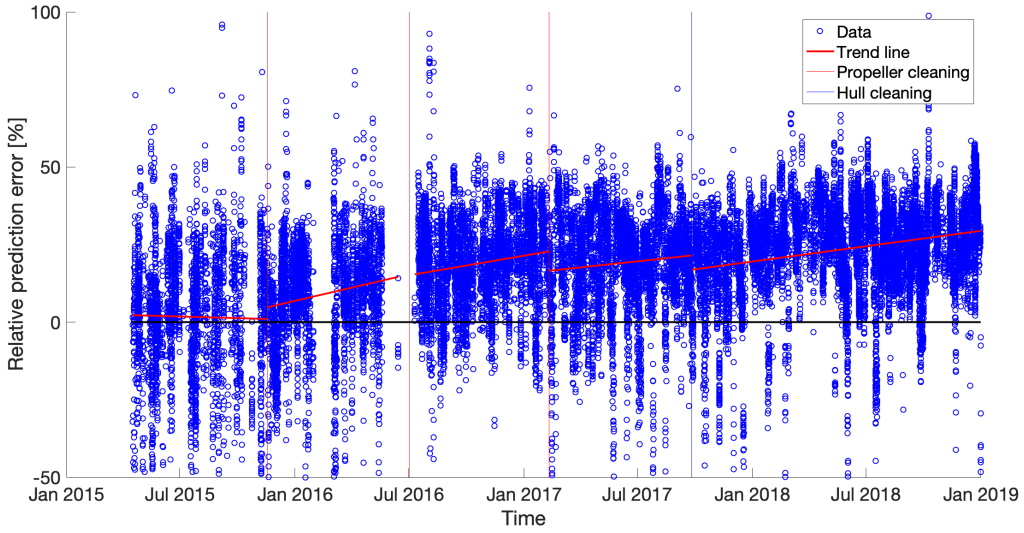

Figure 8.15: Relative prediction error, Gaussian regression

The figure shows that the data points are more scattered for the Gaussian regression model than for the custom linear regression model, which was not expected as the mean prediction error for the Gaussian regression model was almost half that for the custom regression model. The first trend line for this method is also decreasing. All the other trend lines show the expected positive slope. The effect of the last propeller cleaning and the hull cleaning gives the expected drop in relative prediction error, while the second propeller cleaning gave no effect on the relative prediction error according to the figure. At the end of 2018, the relative prediction error was 29.44 %, which is larger than what the custom regression model gave. The expected relative prediction error for the Gaussian regression model was -0.33 %, which gives that the relative prediction error is a reasonable assumption for the increased shaft power.

8.3.3 Comparison

A comparison between the trend lines for the custom linear regression and Gaussian regression is given in Figure 8.16.

Figure 8.16: Comparison of trend lines Method 3

The red lines give the trend for the relative prediction error based on the custom linear regression model while the blue lines give the trend based on the Gaussian regression model. It shows that both trend lines before the first propeller cleaning have a negative slope, while the rest of the lines have a positive slope. The Gaussian regression model gives a larger relative prediction error than the custom regression model, but the slopes for the custom regression model are steeper except for the last line where the slopes are almost identical. The slope of the trend lines determines the fouling rate, which means that the custom regression model predicts a higher fouling rate than the Gaussian regression model.

Chapter 9

Discussion

The different methods give different results, as seen in the previous chapter. In this chapter, the reliability of the different methods are discussed, and a comparison of the different results are given in order to recommend the best method. Some of the points discussed in this chapter have already been discussed in previous chapters. This part will then be a summary to support the recommendation of the best method.

9.1 Benchmark

The benchmark model is given as a relationship between speed through water and shaft power for the un-fouled ship in calm water. The benchmark was obtained as the lower part of the speed-power curve for calm water, based on the sampled performance monitoring data. As mentioned earlier, this model does not account for different loading conditions. Figure 7.1 shows that there is a lot of scattering in the data, with a difference in shaft power up 50 % for some speeds. A study of how the draft influenced the speed power cure was conducted and as shown in Figure 7.2. The drafts were split into two groups, above and below 10.1 meters. Here, it shows that for low speeds the influence the draft had was smaller than for higher speeds. However, the differences were small. Since the vessel has a bulbous bow will the trim also influences the speed power relationship. This influence was difficult to determine as the correlation between the trim and shaft power was low. The correlation between the draft and trim is shown in Figure 6.7, the R^2 value was 0.74 which means that there is some correlation, but the draft alone cannot be used to determine the whole loading condition. The ISO 15016 [16] standard for sea trails requires adjustment of the speed power curve if the displacement changes with more than 2 % during the speed power trail. For the trim is the limit set to 0.1 % of the ship's length. These requirements indicate that both the draft and trim have an influence on the speed power curve, and the benchmark model should compensate for different loading conditions in order to get more accurate results. Thus, the benchmark model may be too simple and therefore cause spread in the result and give wrong trend lines, which again gives wrong added power estimation.

9.2 Admiralty Coefficient

The Admiralty coefficient is a useful parameter to evaluate the vessel's performance over time. It accounts for different speeds and displacements, but only when the changes are small. If the vessel usually operates around the same loading condition and speed, the Admiralty coefficient is constant,

in calm water. However, when the changes in speed and loading conditions are large, the Admiralty coefficient will no longer be constant. So, the benchmark Admiralty coefficient for a clean hull also will change with the loading condition and speed. As presented in Chapter 6, the case ship operates at many different loading conditions and speeds. This is also seen in Figure 8.3 and 8.9, which gives a lot of scatter in the Admiralty coefficient. However, the trend lines give the expected decrease in the Admiralty coefficient over time. As the benchmark Admiralty coefficient changes with large changes in speed and displacement, will the results presented in the previous chapter change when another operating condition than 18 knots and design loading condition are used as the benchmark. The Admiralty Coefficient model only gives the added power based on a specific operating condition.

9.3 Resistance Coefficient

The main uncertainty in the resistance coefficient model lies in the estimation of the wetted surface. The estimation of the wetted surface is based on the assumption that the midship coefficient is 0.9 and that it is constant for all drafts. The trim of the vessel will also influence the wetted surface, but as stated in Chapter 7.3 is the effect of trim not included in the estimation. A better estimation of the wetted surface can be done based on the drawings of the ship or a 3D model. However, this was not available for the case ship. From Figure 8.6 and 8.12 it is shown that the added power at vessel delivery are around 7.5 % which is much higher than expected. However, it may be correct as fouling could have developed on the hull and propeller while the vessel was at the yard, but according to the sea trial test was this not the case. This indicates that the benchmark for the resistance coefficient model is wrong.

9.4 The Data

There is also some uncertainty in the data used in the analysis. As previously stated, the data comes from three different sources, the aboard performance monitoring system, the AIS, and the ECMWF database. The location data from the AIS database have changing sampling rate, which influences the available data points per day. It is shown from Figure 6.2 that there are more location data towards the end of the period than in the beginning. This influenced the data set, as seen in Figure 6.4, which shows the available data points per day for the combined data set. The regression lines are made by reducing the mean square error, which means that a cluster of data points will have more influence than single data points even though the time difference between the data points in the cluster is small. These data clusters have a greater influence on the trend lines than it should. This problem is illustrated in Method 1, especially for the trend line between the two last propeller cleanings. Here, there are almost no data points right after the second propeller cleaning while there are more data before the third propeller cleaning, shown in Figure 8.8.Figure 8.4 and 8.6 shows that the few data points right after the second propeller cleaning are represented poorly by the trend line. However, this problem was reduced significantly for Method 2 when more data points were available, but the lack of data around July 2016 (the second propeller cleaning) is still a problem.

Another problem with the data set is related to environmental data. The environmental conditions, especially waves and wind conditions, have a significant impact on the ship's performance. Thus, it is necessary to have accurate information about the actual weather conditions. The environmental data have a temporal resolution of 6 hours and a spatial resolution of approximately 83x83 km (0.75x0.75 degrees). However, the local weather condition at the vessels location can change a lot during 6 hours and be significantly different from the observed condition at the grid points. Therefore, may weather conditions used in this thesis not be accurate, which can explain some of the spread in the results. The most accurate method to determine the local environmental conditions is to measure them aboard the ship. It is common to measure the wind conditions, and it was measured by the aboard performance

monitoring system. The wave conditions are however more difficult to determine by an aboard system. The wind sensor is sensitive to the location and things around it that may influence the flow of the wind. As there was no information available of the location of the wind sensor and the environment around it, was the reliability of the sensor challenging to determine. The data from the sensor was compared with the data from the ECMWF database, and the differences were not too substantial. Besides, the wave conditions had to be determined by the ECMWF or similar databases, so it was therefore decided to use the ECMWF database to determine the environmental conditions.

The operational profile of the vessel changes significantly after February 2016. The speed increases as shown by Figure 6.9 and the spread in drafts and trim decreases. The mean speed increases from 13.5 to 16.4 knots after February 2016. The Admiralty coefficient is sensitive to large changes in speed and displacement, so when the operational profile of the vessel changes over time will this influence the result. Method 3 is also sensitive to these changes as the training data consists of data for the first year of operation where the vessel has a different main operational profile than after February 2016. The machine learning model is thereby trained on data that does not represent the full data set in the right way. Then the prediction error is expected to increase because of the change in operation profile as the models have not been properly trained on these operational profiles, which may explain why the relative prediction error is so high for Method 3 towards the end of the time series.

9.5 Results

The characteristics of the trend lines for the different methods are given in Table 9.1. ΔC_F means that the trend lines are based on the resistance coefficient model. Line 1 is the trend line before the first propeller cleaning, Line 2 is the trend line between the first and second propeller cleaning and so on. V1 and V2 give the increase of shaft power in percent at the beginning and end of the trend lines. In order to get the best estimate for the increase of shaft power based on the relative prediction error, the expected relative prediction error is subtracted from the relative prediction error for V1 and V2 for Method 3. The expected relative prediction error is -2.10 % for the custom regression model and -0.33 % for the Gaussian regression model. α is the slope of the trend lines. The slopes are given as percent increase in shaft power per year, $\frac{added\ power\ [\%]}{year}$.

Table 9.1: Summary of trend lines

		Method 1: Admiralty	**Method 1: ΔC_F**	**Method 2: Admiralty**	**Method 2: ΔC_F**	**Method 3: Custom**	**Method 3: Gaussian**
Line 1	V1	-1.13	7.07	0.39	8.21	-	-
	V2	16.21	11.01	14.11	10.38	-6.82	0.69
	α	10.64	2.41	8.42	1.33	-16.97	-2.10
Line 2	V1	5.81	6.04	1.77	9.24	1.33	4.46
	V2	10.51	12.38	16.14	13.57	8.53	14.29
	α	8.20	11.08	25.10	7.57	12.58	17.17
Line 3	V1	20.82	16.10	2.81	10.47	7.92	15.08
	V2	9.57	13.20	12.06	12.91	16.32	22.48
	α	-19.15	-4.94	15.74	4.15	17.70	12.59
Line 4	V1	11.99	9.79	5.51	10.72	8.07	16.24
	V2	17.50	18.08	16.90	18.34	16.96	21.16
	α	8.83	13.29	18.26	12.21	14.24	7.88
Line 5	V1	8.12	11.54	5.51	10.82	10.34	16.59
	V2	25.77	22.71	19.25	21.22	23.23	29.11
	α	13.97	8.84	10.87	8.24	10.20	9.91

Table 9.1 shows that the different methods give different results, but there are some similarities worth mentioning. Line 1 shows that both the Admiralty coefficient model and the resistance coefficient model gives almost the same line for Method 1 and 2. However, the difference between the two models is large. For Line 2 is the slope for Method 1, Admiralty and resistance coefficient, Method 2 resistance coefficient and Method 3 custom regression model similar with a minimum value of 7.57 % per year and maximum value of 12.58 % per year. While Method 2 Admiralty coefficient and Method 3 Gaussian regression model gives a much larger estimate. For Line 3, Method 1 gives a negative slope while Method 2 Admiralty and Method 3 gives a large positive slope between 12.59 % per year and 17.7 % per year. The slopes of Line 4 varies from 7.88 % per year to 18.26 % per year. However, four of the trend lines end at an increased shaft power between 17 and 18.4 %. The slopes of Line 5 are very similar with a minimum value of 8.24 % per year and a maximum of 13.97 % per year. Four of the lines also estimate an added power at the end of 2018 between 19 and 23 %. The trend lines given in Table 9.1 are plotted in Figure 9.1 to show the similarities graphically.

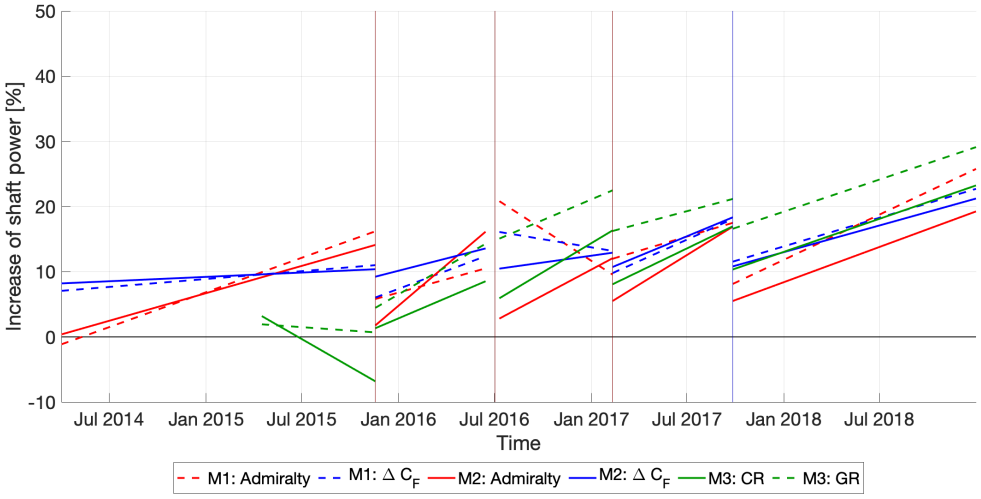

Figure 9.1: Comparison of trend lines for Method 1, 2 and 3

It is seen from Table 9.1 and Figure 9.1 that the added power due to fouling lies between -1 and up to 30 % for all models. The power is proportional to the resistance, which means that they can be compared. According to Munk [3], approximately one-third of all ships have an added resistance under 20 % and half of the world's ships have an added resistance between 20 % and 40 %. Munk also states that the added resistance rate normally is between 0.5 % and 2 % per month, which gives a rate between 6 % and 24 % per year. From Table 9.1 most of the slopes are between these estimations. As mentioned above, Method 1 has some problems with available data points per day, and the benchmark for the resistance coefficient method seems to be wrong. The slopes give the rate for the added power for Method 3, but to interpret the relative prediction error as the added power directly may not be the best assumption. The regression models are trained on data from the first year of operation with the assumption that the added power due to fouling is small. However, the results for Method 1 and 2 estimates an added power at the end of the first year of approximately 10 %, which is significant. The change in operating condition over time also gives that the relative prediction error is expected to increase. So the assumption Method 3 is built on is not that good. The best method is then Method 2 based on the Admiralty coefficient. It is also important to mention that these methods are based on the assumption that the added power over time is only caused by fouling, this is however not correct as other factors influence the performance over time as well. For instance, wear and tear on the engine and damages to the hull and propeller.

9.6 Dry Dock March 2019

The vessel was dry-docked in March 2019, and the condition of the hull was investigated. The fouling on the hull are shown in Figure 9.2 and 9.3.

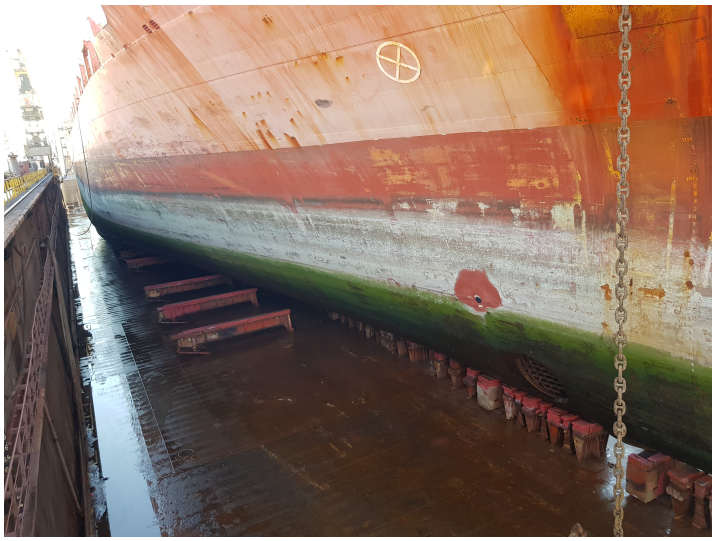

Figure 9.2: Fouling on the side

Figure 9.2 show the condition of the side of the hull. Here it is shown that a heavy slime layer and some hard fouling have developed on the hull. Schultz [2] made some predictions of the resistance due to fouling on a US Naval ship, the results are given in Table 3.2. Table 3.2 shows that a heavy slime layer and small calcareous fouling gives an added resistance are between 16 and 34 %. From the results in Table 9.1 gave Method 2 with the Admiralty coefficient an added power of 19 % and all the different methods gave added power between 19 and 30 %, which is consistent with Schultz predictions. Figure 9.3 shows the heavy slime layer at the bottom of the vessel.

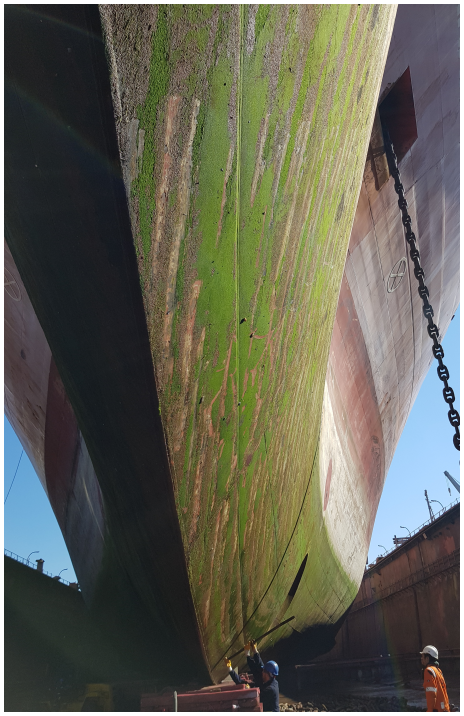

Figure 9.3: Fouling under

Chapter 10

Conclusions and Further Work

The main objective of this master thesis was to develop different methods to determine the added power of a ship by using in-service performance monitoring data. This topic is important for ship owners and operators as knowing the added power due to fouling gives them a better estimation for attainable speed and sea margin. It also gives them information regarding the hull condition, which can be used to optimize the time between hull and propeller cleanings. This optimization can give substantial economic savings and ensure more effective operations.

Performance monitoring data for a five year old 2500 TEU container vessel were acquired and used in the analysis. Location data were obtained from the AIS database, and environmental data were gathered from the ECMWF database. Some initial processing of the data was necessary in order to run the analysis. First, the data from the three different sources were combined, then some undesirable data points were removed, like when the vessel was accelerating. Some limitations to minimum speed, RPM, and draft were also applied as well as limitations to maximum significant wave height. During the relevant period, the vessel was subjected to three propeller cleanings and one hull cleaning.

In this thesis, three different methods have been developed to determine the added power due to fouling. Method 1 removes data points with bad weather in order to create a dataset that only contains values for calm water operations. Method 2 follows the weather restrictions given in ISO 15016 standard, and use the methods described in the standard to compensate for the environmental effects. Method 3 uses the same data set as Method 2, which means that Method 2 and 3 contained approximately 70 % more data than Method 1. Both Method 1 and 2 evaluate the change in the Admiralty and resistance coefficient over time to determine the added power due to fouling. Method 3 uses two different machine learning algorithms to predict the shaft power based on input data containing information about the loading condition, speed, and environmental condition. It was assumed that the fouling during the first year of operation was small, so the models were trained on this data. Thus, the change in relative prediction error over time could be used to determine added power due to fouling.

Trend lines between each event (propeller and hull cleanings), were made by reducing the mean square error based on the data points. It was found that the added power due to fouling was between -1 and 30 % for all methods, as per Munk's [3] experiences. He states that about 80 % of the world's ships have an added resistance between 0 and 40 % due to fouling. The vessel was dry-docked in March 2019, and it was found that it had a heavy slime layer as well as some hard fouling on the sides. The different methods estimated an added power due to fouling between 19 and 30 % for the vessel right before the dry dock. For comparison, Schultz has given similar predictions for a US Naval ship where added resistance due to fouling for a heavy slime layer with some small calcareous fouling was between 16 and 34 % [2].

However, there were some problems with the different methods as well. For Method 1, it was found that there were some periods where the available data points per day were low. Since the trend lines were based on reducing the mean square error, parts with many data points available were favored, which resulted in false trend lines for some cases for Method 1. The resistance coefficient model also gave initially an added power of about 8 %, which was found to be too large for a clean and newly delivered vessel. To interpret the relative prediction error in Method 3 as the added power directly was not the best assumption as there is some expected prediction error. Also, the regression models are trained on data for the first year with the assumption that the added power due to fouling is small. However, Method 1 and 2 gave an added power of about 10 % at the end of the first year. Additionally, the operation profile of the vessel changed over time, where the vessel was operating at higher speeds towards the end of the time series. The relative prediction error is then expected to increase with the new operation profile, as there were not that many data points with this operation profile in the training data. Thus, it can be concluded that Method 2 based on the Admiralty coefficient is the recommended method.

10.1 Further Work

A benchmark model that includes the effect of loading conditions such as variations in draft and trim should be made in order to improve the accuracy of both Method 1 and 2. Method 1 can be improved by re-sampling the dataset in order to reduce data clusters. One way to do this is to average data in the clusters over a period, so the amount of data in the clusters is reduced. Then the cluster's influence on trend lines is decreased. Another way to improve the accuracy of the model is to include the effects of temperature changes both in air and water. As stated in ISO 15016, change in the temperature will change the density and viscosity of the fluid, which both influence the resistance of the vessel. The method can also be developed further to determine the added power for the propeller and hull fouling separately.

In order to make the results more commercially attractive, a cost function should be developed based on the determined added power due to fouling. This cost function would give the potential cost savings for a hull or propeller cleaning. Other possible expansions are to include the methods proposed in this thesis, in algorithms to estimate the attainable speed or sea margin, which will make such estimates more accurate.

Bibliography

[1] R L Townsin. "The Ship Hull Fouling Penalty". In: *Biofouling* 19.sup1 (2003), pp. 9–15. ISSN: 0892-7014.

[2] Michael P. Schultz. "Effects of coating roughness and biofouling on ship resistance and powering". In: *Biofouling* 23.5 (2007), pp. 331–341. ISSN: 0892-7014.

[3] Torben Munk. "Fuel Conservation through Managing Hull Resistance". In: *Motorship Propulsion Conference, Copenhagen* (Apr. 2006).

[4] Dinis Oliveira and Lena Granhag. "Matching Forces Applied in Underwater Hull Cleaning with Adhesion Strength of Marine Organisms". In: *Journal of Marine Science and Engineering* 4.4 (2016). ISSN: 2077-1312. URL: http://search.proquest.com/docview/1858321348/.

[5] IMO. *Sulphur oxides (SOx) and Particulate Matter (PM) – Regulation 14*. Available at http://www.imo.org/en/OurWork/Environment/PollutionPrevention/AirPollution/Pages/Sulphur-oxides-(SOx)-\OT1\textendash-Regulation-14.aspx (2018/11/24).

[6] International Maritime Organization (IMO). "A Transparent and Reliable Hull and Propeller Performance Standard". In: *MEPC 63/4/8* (2011).

[7] John Carlton. *Marine Propellers and Propulsion*. eng. 2nd ed. Elsevier Science, 2007. ISBN: 0750681500.

[8] BMT SeaTech. *Safety and Performance Monitoring SMART*. Available at http://www.messe.no/ExhibitorDocuments/128183/2764/SMART%20Safety%20and%20Performance%20Monitoring.pdf (2018/11/23).

[9] T. W. P. Smith et al. *Third IMO GHG Study 2014*. London, UK: international maritime organization (IMO), April 2015.

[10] Kristian O. Ejdfors. *Use of in-service data to predict the added power of a ship due to fouling*. Norwegian University of Science and Technology (NTNU), 2018.

[11] A. F. Molland, S. R. Turnock, and D. A. Hudson. *Ship Resistance and Propulsion : Practical Estimation of Ship Propulsive Power*. Cambridge: Cambridge University Press, 2011. ISBN: 9780511974113.

[12] Propulsion Committee of 27th ITTC. *ITTC – Recommended Procedures and Guidelines, 1978 ITTC Performance Prediction Method*. Rev.03, 7.5–02 03–01.4. 2014.

[13] 26th ITTC Resistance Committee. *ITTC – Recommended Procedures and Guidelines, Resistance Test*. Rev.03, 7.5-02-02-01. 2011.

[14] MARIN. *Vessel owners join forces to set standards for sea trials*. Available at `http://www.marin.nl/web/JIPs-Networks/JIPs-public/STA.htm` (2018/10/23).

[15] Min-Guk Seo et al. "Comparative study on computation of ship added resistance in waves". eng. In: *Ocean Engineering* 73 (2013), pp. 1–15. ISSN: 0029-8018.

[16] ISO. *International Standard 15016, Ships and Marine technology - Guidelines for the Assessment of Speed and Power Performance by Analysis of Speed Trial Data*. Second edition. 2015.

[17] Hemrik van den Boom, Hans Huisman, and Frits Mennen. *New Guidelines for Speed/Power Trials Level playing field established for IMO EEDI*. Available at `http://www.marin.nl/web/JIPs-Networks/JIPs-public/STA.htm` (2018/11/16).

[18] Benjamin Pjedsted Pedersen et al. "Data-driven Vessel Performance Monitoring". PhD thesis. DTU, 2014.

[19] Dinis Oliveira. "The Enemy Below - Adhesion and Friction of Ship Hull Fouling". PhD thesis. Gotenburg, Sweden.

[20] Michael P. Schultz. "Turbulent boundary layers on surfaces covered with filamentous algae". In: *Journal of Fluids Engineering, Transactions of the ASME* 122.2 (2000), pp. 357–363. ISSN: 00982202.

[21] CleanHull. *CUT COST! A clean hull makes major savings*. Available at `http://www.cleanhull.no/doc//CleanHull_brochure%20new.pdf` (2018/12/04).

[22] Dinis Oliveira, Ann I. Larsson, and Lena Granhag. "Effect of ship hull form on the resistance penalty from biofouling". In: *Biofouling* 34.3 (2018), pp. 262–272. ISSN: 0892-7014.

[23] Odd M Faltinsen. *Hydrodynamics of high-speed marine vehicles*. Cambridge: Cambridge University Press, 2005. ISBN: 9780521845687.

[24] Bradford Samuel A. *Corrosion Control*. Boston, MA, 1993. ISBN: 1-4684-8845-7.

[25] IMO. *Anti-fouling systems*. Available at `http://www.imo.org/en/OurWork/Environment/Anti-foulingSystems/Pages/Default.aspx` (2018/11/20).

[26] Claire Hellio and Diego Yebra. *Advances in Marine Antifouling Coatings and Technologies*. Woodhead Publishing, 2009. ISBN: 978-1-84569-386-2.

[27] GloMEEP. *HULL CLEANING*. Available at `https://glomeep.imo.org/technology/hull-cleaning/` (2018/12/04).

[28] Martin Stopford. *Smart Shipping & The 4th Sea Transport Revolution*. Clarkson Research, 2016.

[29] Nicolas Bialystocki and Dimitris Konovessis. "On the estimation of ship's fuel consumption and speed curve: A statistical approach". In: *Journal of Ocean Engineering and Science* 1.2 (2016), pp. 157–166. ISSN: 2468-0133.

[30] Søren Vinther Hansen. "Performance monitoring of ships". PhD thesis. DTU, 2011.

[31] E. Vanem, A. Brandsæter, and O. Gramstad. "Regression models for the effect of environmental conditions on the efficiency of ship machinery systems". In: *Risk, Reliability and Safety: Innovating Theory and Practice - Proceedings of the 26th European Safety and Reliability Conference, ESREL 2016*. CRC Press/Balkema, 2017. ISBN: 9781138029972.

[32] Andreas Brandsæter and Erik Vanem. "Ship speed prediction based on full scale sensor measurements of shaft thrust and environmental conditions". eng. In: *Ocean Engineering* 162 (2018), pp. 316–330. ISSN: 0029-8018.

[33] Propulsion Dynamics. *About us*. Available at `http://www.propulsiondynamics.net/about-us.html` (2018/11/23).

[34] Daniel Kane. *Developing a more fuel efficient tonnage through blasting of hulls and timely in-water husbandry*. Available at `https://www.ship-efficiency.org/onTEAM/pdf/10-CASPER%20-%20Ship%20Efficiency%2004.pdf` (2018/11/23).

[35] Omer Soner, Emre Akyuz, and Metin Celik. "Statistical modelling of ship operational performance monitoring problem". In: *Journal of Marine Science and Technology* (June 2018). ISSN: 1437-8213. DOI: 10.1007/s00773-018-0574-y. URL: https://doi.org/10.1007/s00773-018-0574-y.

[36] Trevor J Hastie. *The elements of statistical learning : data mining, inference, and prediction*. eng. 2nd ed. Springer series in statistics. Corrected 12th printing - Jan 13, 2017. New York: Springer Science + Business Media, 2009.

[37] Christopher M Bishop. *Pattern recognition and machine learning*. eng. Information science and statistics. New York: Springer, 2006. ISBN: 0387310738.

[38] P. Berrisford et al. "The ERA-Interim archive Version 2.0". In: 1 (Nov. 2011), p. 23. URL: `https://www.ecmwf.int/node/8174`.

[39] Jørgen Amdahl et al. *TMR4105 Marin Teknikk Grunnlag Kompendium*. Vol. 5. Marin Teknisk Senter, NTNU: Akademika Forlag, 2014.

[40] C. E. Rasmussen and C. K. I. Williams. *Gaussian Processes for Machine Learning*. Cambridge, Massachusetts: MIT Press, 2006.

Appendices

Appendix A

Data Processing

A.1 Save_Variable.m

```
%--------------------------------------------------------------------------
% Creates a MATLAB data struct with the AIS data and performance monitoring
% data are combined combined, the performance monitoring data and AIS data
% are given as one .csv file per year
%--------------------------------------------------------------------------

%Path where raw data is located
folder = strcat(pwd,'/Data/');
%Years for the different datafiles
years = 2014:2018;

for a = 1:length(years)
    year = num2str(years(a));
    disp(year)
% Reading data - the order and content of the data are given below
% Timestamp, Speed (water), Speed (ground), Course, ME Shaft Power,
% ME RPM, Wind speed abs, Wind speed rel, wind dir, Draft fwd, draft aft
data = csvread(strcat(folder,year,'.csv'),1,0);
%Timestamp, Latitude, Longetude, Year
ais = csvread(strcat(folder,'AIS_',year,'.csv'));

%  Interpolating AIS data
lat = zeros(length(data),1); % pre-allocating
lon = zeros(length(data),1); % pre-allocating
timestamp = zeros(length(data),1); % pre-allocating

%Setting a limit of 1 hour time difference
limit = 60*60;
for j = 1:length(data)-1
%         Finds the minimum difference between the timestamp in the AIS
%         Data and Performance Data.
        [v_min,index] = min(abs(ais(:,1)-data(j,1)));
        if v_min < limit && index > 1 && index < length(ais)
            %Interpolating GPS position based on timestamp
            if data(j,1) > ais(index,1) && ais(index+1,1) - ais(index,1)...
                    < limit && ais(index,1) ≠ ais(index+1,1)
                lat(j) = interp1([ais(index,1) ais(index+1,1)],...
                    [ais(index,2) ais(index+1,2)], data(j,1));
                lon(j) = interp1([ais(index,1) ais(index+1,1)],...
                    [ais(index,3) ais(index+1,3)], data(j,1));
                timestamp(j) = data(j,1);
            elseif data(j,1) < ais(index,1) && ais(index,1) - ais(index-1,1)...
```

```
                    < limit && ais(index,1) ≠ ais(index-1,1)
                lat(j) = interp1([ais(index-1,1) ais(index,1)],...
                    [ais(index-1,2) ais(index,2)], data(j,1));
                lon(j) = interp1([ais(index-1,1) ais(index,1)],...
                    [ais(index-1,3) ais(index,3)], data(j,1));
                timestamp(j) = data(j,1);
            else
            lat(j) = nan;
            lon(j) = nan;
            timestamp(j) = nan;
            end
        else
            lat(j) = nan;
            lon(j) = nan;
            timestamp(j) = nan;
        end
end
%removing datapoints where GPS position was not obtained
lat(end) = nan;
lon(end) = nan;
index = isnan(lat+lon);
data(:,end+1) = lat;
data(:,end+1) = lon;
data(index,:) = [];
% Saving data to file as a MATLAB struct
Data.Timestamp      = data(:,1);
Data.STW            = data(:,2);
Data.SOG            = data(:,3);
Data.Course         = data(:,4);
Data.ShaftPower     = data(:,5);
Data.RPM            = data(:,6);
Data.WindSpeed      = data(:,7);
Data.RelWindSpeed   = data(:,8);
Data.RelWindDir     = data(:,9);
Data.DraftMid       = (data(:,10)+data(:,11))/2;
Data.Trim           = data(:,10)-data(:,11);
Data.Lat            = data(:,12);
Data.Lon            = data(:,13);

save(strcat(folder,'NAME_',year,'.mat'),'Data')
end
```

A.2 Combine_Data.m

```
%-------------------------------------------------------------------------
% Combine performance monitoring data and hindcast weather data from ECMWF
% The performance monitoring data are the out put of the script
% Save_Variable.m and the weather data are monthly .grib files
%-------------------------------------------------------------------------
clear; clc;
%Path where data is located
folder = strcat(pwd,'/Data/'); % folder for performance monitoring data
matDataFolder =strcat(pwd,'/Data/ECMWF/'); %folder for weather data
%Years for the different datafiles
years = 2014:2018;
for q = 1:length(years)
    year = num2str(years(q));
    %Load data
    load(strcat(folder,'NAME_',year,'.mat'));
    load(strcat(folder,'Data_w_Weather_empty','.mat'));
    %Converting from epoch to datetime
    Data.Time = datetime(Data.Timestamp,'ConvertFrom','posixtime');
    for g = 1:12
```

```
20          if strcmp(year,'2014')
21              g = g+3;
22              if g > 12
23                  break
24              end
25          end
26          disp(g)
27          Data_temp = Data;
28          % Retriving weather data from .grib files and create a data struct
29          % with the weter data for the ships location
30          [ECMWF, first, last] = Ship_ECMWF(matDataFolder,year,...
31              Data.Timestamp,Data.Lon,Data.Lat,folder,g);
32          %Working with weather data
33          names = fieldnames(Data_temp);
34          index = isnan(ECMWF.SignWaveHeight);
35          fprintf('\n Number of missing Hs values: %d \n\n\n',sum(index))
36              for i = 1:length(names)
37                  temp = Data_temp.(names{i});
38                  temp = temp(first:last);
39          %Removing values without information about significant wave height
40                   temp(index) = [];
41                  Data_temp.(names{i}) = temp;
42              end
43          names = fieldnames(ECMWF);
44              for i = 2:length(names)
45                  temp = ECMWF.(names{i});
46          %Removing values without information about significant wave height
47                   temp(index) = [];
48                   ECMWF.(names{i}) = temp;
49                  Data_temp.(names{i}) = temp;
50              end
51          %combining data
52          names = fieldnames(Data_temp);
53               for i = 1:length(names)
54                  Data_w_Weather.(names{i}) = [Data_w_Weather.(names{i})',...
55                      Data_temp.(names{i})'];
56              end
57          end
58  % Save data to file
59  save(strcat(folder,'Data_w_Weather_',year,'.mat'),'Data_w_Weather')
60  clear Data
61  clear Data_w_Weather
62  clear ECMWF
63  end
64  %-------------------------------------------------------------------------
65  % Load data by year and combine them to one large data struct with all data
66  %-------------------------------------------------------------------------
67  clear; clc;
68  %Path where raw data is located
69  folder = strcat(pwd,'/Data/');
70  %Years for the different datafiles
71  years = 2014:2018;
72  load(strcat(folder,'Data_w_Weather_empty','.mat'));
73  Data_w_Weather_tot = Data_w_Weather;
74  for a = 1:length(years)
75      year = num2str(years(a));
76      load(strcat(folder,'Data_w_Weather_',year,'.mat'));
77      names = fieldnames(Data_w_Weather);
78           for i = 1:length(names)
79              Data_w_Weather_tot.(names{i}) = [Data_w_Weather_tot.(names{i})',...
80                  Data_w_Weather.(names{i})'];
81           end
82  end
83  Data_w_Weather = Data_w_Weather_tot;
84  % Save data to file
85  save(strcat(folder,'Data_w_Weather_','tot','.mat'),'Data_w_Weather')
```

A.3 Ship_ECMWF.m

```
function [ECMWF, start, last] = ...
    Ship_ECMWF(matDataFolder,yearStr,TIMEMS,LON,LAT,SaveToFolder,g)
%--------------------------------------------------------------------------
% Creates a MATLAB data struct with weather data based on the vessel
% position and timestamp. The weater data are given as a .grib file
% containing information about both the wind and wave condition for 1 month
% Input parameters:
% matDataFolder - gives the folder where the weather data are stored
% yearStr - the dessired year as a string
% TIMEMS - the timestamp in seconds
% LON - longitude coordinate in -180 to 180 degrees
% LAT - latitiude coordinate in degrees
% SaveToFolder - folder where the output struct are saved
% g - number of the month
% output:
% ECMWF - MATLAB data struct with information about the wind and wave
% condition at the vessel's location
% start - index of the first timestamp for the given month
% last - index of the last timestamp for the given month
%--------------------------------------------------------------------------
% Created by:
% Oyvind Oksnes Dalheim
% Modified By:
% Kristian Ejdfors
%--------------------------------------------------------------------------
% converting Longetude from -180:180 to 0:360
for i = 1:length(LON)
    if LON(i) <0
        LON(i) = LON(i) + 360;
    end
end
%% GRIB data folder
ECMWFdataFolder = matDataFolder;
GRIBdataFolder  = strcat(ECMWFdataFolder,yearStr,'/');

%% GRIB file
tmp = dir(fullfile(GRIBdataFolder,'*grib')); GRIBfiles = {tmp.name}';...
    GRIBfiles(ismember(GRIBfiles,{'.','..','DS_Store'})) = [];

GRIBinputFile = strcat(GRIBdataFolder,GRIBfiles{g}); %selected GRIB file
tmp = dir(fullfile(SaveToFolder,'ECMWF/','*mat')); ...
    ECMWF_mat = {tmp.name}'; ...
    ECMWF_mat(ismember(ECMWF_mat,{'.','..','DS_Store'})) = [];

ECMWF_file = strcat('ECMWF_',yearStr,'_',num2str(g),'.mat');
%Loading pre existing weather file
a = logical(find(contains(ECMWF_mat,ECMWF_file)));
if a
    load(strcat(SaveToFolder,'ECMWF/',ECMWF_file));
    start = find(ECMWF.Time(1) == TIMEMS);
    last = find(ECMWF.Time(end) ≥ TIMEMS,1,'last');
    return
end
%% Collect GRIB data
weatherECMWF = ncdataset(GRIBinputFile);
%Checking content
weatherECMWF.variables;
%Finding dates included in the GRIB file
GRIBTimeInMS = days2ms(weatherECMWF.time('time'));
%Finding intervall in TIMEMS which correspond to GRIBTimeInMS
flag = 0;
for i=1:length(GRIBTimeInMS)
    start = find(GRIBTimeInMS(i) ≥ TIMEMS,1,'last');
    if start > 0
```

```
64          last = find(GRIBTimeInMS(end) ≥ TIMEMS,1,'last');
65          flag = 1;
66          break
67      end
68  end
69  if flag == 0
70      disp('vessel timestamp not in weather data')
71      return
72  end
73  % Deliting data outside desired intervall
74  TIMEMS(last:end) = [];
75  TIMEMS(1:start) = [];
76  LON(last:end) = [];
77  LON(1:start) = [];
78  LAT(last:end) = [];
79  LAT(1:start) = [];
80
81  %Preallocate
82  ECMWF_uW = zeros(length(TIMEMS),1);
83  ECMWF_vW = zeros(length(TIMEMS),1);
84  ECMWF_Hs = zeros(length(TIMEMS),1);
85  ECMWF_Wd = zeros(length(TIMEMS),1);
86  ECMWF_Ts = zeros(length(TIMEMS),1);
87  Beaufort = zeros(length(TIMEMS),1);
88  Wave_class = zeros(length(TIMEMS),1);
89
90  %Finding positions included in the GRIB file
91  GRIBlon = double(weatherECMWF.data('lon')); %Defining longtitude vector
92  GRIBlat = double(weatherECMWF.data('lat')); %Defining latitude vector
93
94  %Reading data
95  Uwind = double(weatherECMWF.data('10_metre_U_wind_component_surface'));
96  Vwind = double(weatherECMWF.data('10_metre_V_wind_component_surface'));
97  SWH   = double(weatherECMWF.data('Significant_wave_height_msl'));
98  MWD   = double(weatherECMWF.data('Mean_wave_direction_msl'));
99  MWP   = double(weatherECMWF.data('Mean_wave_period_msl'));
100
101 %Interpolating uWind at time, lat and lon
102 fprintf('%s\n','--> Collecting uWind data');
103 for i = 1:length(TIMEMS)
104     timeIDXtoInstantBefore = find(GRIBTimeInMS ≤ TIMEMS(i),1,'last');
105     timeIDXtoInstantAfter  = find(GRIBTimeInMS ≥ TIMEMS(i),1,'first');
106     timeBeforeAfter = [GRIBTimeInMS(timeIDXtoInstantBefore)...
107         GRIBTimeInMS(timeIDXtoInstantAfter)];
108
109     lonIDXWest  = find(GRIBlon ≤ LON(i),1,'last');
110     lonIDXEast  = find(GRIBlon ≥ LON(i),1,'first');
111
112     latIDXNorth = find(GRIBlat ≥ LAT(i),1,'last');
113     latIDXSouth = find(GRIBlat ≤ LAT(i),1,'first');
114
115     Xlat = repmat(GRIBlat(latIDXNorth:latIDXSouth),[1,2]);
116
117      if LON(i) > GRIBlon(end)
118         lonIDXWest = GRIBlon(1);
119         lonIDXEast = GRIBlon(end);
120         Xlon = [lonIDXWest lonIDXEast; lonIDXWest lonIDXEast];
121
122         %Concatenate
123         %(time,lat,lon) -> (lat,lon,time)
124         Cat    = cat(3,squeeze(Uwind(timeIDXtoInstantBefore,sort...
125             (latIDXNorth:latIDXSouth),[1 length(GRIBlon)])),...
126             squeeze(Uwind(timeIDXtoInstantAfter,sort(latIDXNorth:...
127             latIDXSouth),[1 length(GRIBlon)])));
128      else
129         Xlon = repmat(GRIBlon(lonIDXWest:lonIDXEast)',[2,1]);
130         %Concatenate
131         %(time,lat,lon) -> (lat,lon,time)
```

```
        Cat   = cat(3,squeeze(Uwind(timeIDXtoInstantBefore,sort...
            (latIDXNorth:latIDXSouth),sort(lonIDXWest:lonIDXEast))),...
            squeeze(Uwind(timeIDXtoInstantAfter,sort(latIDXNorth:...
            latIDXSouth),sort(lonIDXWest:lonIDXEast))));
     end
    %Permute to get interpolated dimension first
    %(lat,lon,time) -> (time,lat,lon)
    Per = permute(Cat,[3 1 2]);

    %Interpolate over time
    if timeIDXtoInstantBefore == timeIDXtoInstantAfter
        TwoDimInterp = squeeze(Per(1,:,:));
    else
        try
            TwoDimInterp = squeeze(interp1(timeBeforeAfter,Per,TIMEMS(i)));
        catch
            disp('Some error');
        end
    end

    %Interpolate over position
    ECMWF_uW(i) = interp2(Xlon,Xlat,TwoDimInterp,LON(i),LAT(i)); %U wind velocity
end

%Interpolating vWind time, lat and lon
fprintf('%s\n','--> Collecting vWind data');

for i = 1:length(TIMEMS)
    timeIDXtoInstantBefore = find(GRIBTimeInMS ≤ TIMEMS(i),1,'last');
    timeIDXtoInstantAfter  = find(GRIBTimeInMS ≥ TIMEMS(i),1,'first');
    timeBeforeAfter = [GRIBTimeInMS(timeIDXtoInstantBefore)...
        GRIBTimeInMS(timeIDXtoInstantAfter)];

    lonIDXWest  = find(GRIBlon ≤ LON(i),1,'last');
    lonIDXEast  = find(GRIBlon ≥ LON(i),1,'first');

    latIDXNorth = find(GRIBlat ≥ LAT(i),1,'last');
    latIDXSouth = find(GRIBlat ≤ LAT(i),1,'first');

    Xlat = repmat(GRIBlat(latIDXNorth:latIDXSouth),[1,2]);

     if LON(i) > GRIBlon(end)
        lonIDXWest = GRIBlon(1);
        lonIDXEast = GRIBlon(end);
        Xlon = [lonIDXWest lonIDXEast; lonIDXWest lonIDXEast];

        %Concatenate
        %(time,lat,lon) -> (lat,lon,time)
        Cat   = cat(3,squeeze(Vwind(timeIDXtoInstantBefore,sort(...
            latIDXNorth:latIDXSouth),[1 length(GRIBlon)])), ...
            squeeze(Vwind(timeIDXtoInstantAfter,sort(latIDXNorth:...
            latIDXSouth),[1 length(GRIBlon)])));
     else
        Xlon = repmat(GRIBlon(lonIDXWest:lonIDXEast)',[2,1]);
        %Concatenate
        %(time,lat,lon) -> (lat,lon,time)
        Cat   = cat(3,squeeze(Vwind(timeIDXtoInstantBefore,sort(...
            latIDXNorth:latIDXSouth),sort(lonIDXWest:lonIDXEast))), ...
            squeeze(Vwind(timeIDXtoInstantAfter,sort(latIDXNorth:...
            latIDXSouth),sort(lonIDXWest:lonIDXEast))));
     end
    %Permute to get interpolated dimension first
    %(lat,lon,time) -> (time,lat,lon)
    Per = permute(Cat,[3 1 2]);

    %Interpolate over time
    if timeIDXtoInstantBefore == timeIDXtoInstantAfter
        TwoDimInterp = squeeze(Per(1,:,:));
```

```
200     else
201         try
202             TwoDimInterp = squeeze(interp1(timeBeforeAfter,Per,TIMEMS(i)));
203         catch
204             disp('Some error');
205         end
206     end
207 
208     %Interpolate over position
209     ECMWF_vW(i) = interp2(Xlon,Xlat,TwoDimInterp,LON(i),LAT(i)); %V wind velocity
210 end
211 
212 %Interpolating Hs at time, lat and lon
213 fprintf('%s\n','--> Collecting Hs data');
214 
215 for i = 1:length(TIMEMS)
216     timeIDXtoInstantBefore = find(GRIBTimeInMS ≤ TIMEMS(i),1,'last');
217     timeIDXtoInstantAfter  = find(GRIBTimeInMS ≥ TIMEMS(i),1,'first');
218     timeBeforeAfter = [GRIBTimeInMS(timeIDXtoInstantBefore)...
219         GRIBTimeInMS(timeIDXtoInstantAfter)];
220 
221     lonIDXWest  = find(GRIBlon ≤ LON(i),1,'last');
222     lonIDXEast  = find(GRIBlon ≥ LON(i),1,'first');
223 
224     latIDXNorth = find(GRIBlat ≥ LAT(i),1,'last');
225     latIDXSouth = find(GRIBlat ≤ LAT(i),1,'first');
226 
227     Xlat = repmat(GRIBlat(latIDXNorth:latIDXSouth),[1,2]);
228 
229      if LON(i) > GRIBlon(end)
230         lonIDXWest = GRIBlon(1);
231         lonIDXEast = GRIBlon(end);
232         Xlon = [lonIDXWest lonIDXEast; lonIDXWest lonIDXEast];
233 
234         %Concatenate
235         %(time,lat,lon) -> (lat,lon,time)
236         Cat    = cat(3,squeeze(SWH(timeIDXtoInstantBefore,sort(...
237             latIDXNorth:latIDXSouth),[1 length(GRIBlon)])),...
238             squeeze(SWH(timeIDXtoInstantAfter,sort(...
239             latIDXNorth:latIDXSouth),[1 length(GRIBlon)])));
240      else
241         Xlon = repmat(GRIBlon(lonIDXWest:lonIDXEast)',[2,1]);
242         %Concatenate
243         %(time,lat,lon) -> (lat,lon,time)
244         Cat    = cat(3,squeeze(SWH(timeIDXtoInstantBefore,sort(...
245             latIDXNorth:latIDXSouth),sort(lonIDXWest:lonIDXEast))),...
246             squeeze(SWH(timeIDXtoInstantAfter,sort(latIDXNorth:...
247             latIDXSouth),sort(lonIDXWest:lonIDXEast))));
248      end
249     %Permute to get interpolated dimension first
250     %(lat,lon,time) -> (time,lat,lon)
251 
252     %Changing NaN values to mean of the other values
253     Cat(isnan(Cat(:,:,1))) = mean(Cat(not(isnan(Cat(:,:,1)))));
254     Cat2 = Cat(:,:,2);
255     Cat2(isnan(Cat2)) = mean(Cat2(not(isnan(Cat2))));
256     Cat(:,:,2) = Cat2;
257 
258 
259     Per = permute(Cat,[3 1 2]);
260 
261     %Interpolate over time
262     if timeIDXtoInstantBefore == timeIDXtoInstantAfter
263         TwoDimInterp = squeeze(Per(1,:,:));
264     else
265         try
266             TwoDimInterp = squeeze(interp1(timeBeforeAfter,Per,TIMEMS(i)));
267         catch
```

```
            disp('Some error');
        end
    end

    %Interpolate over position
    ECMWF_Hs(i) = interp2(Xlon,Xlat,TwoDimInterp,LON(i),LAT(i)); %Wave height
end

%Interpolating WaveDir at time, lat and lon
fprintf('%s\n','--> Collecting WaveDir data');
for i = 1:length(TIMEMS)
    timeIDXtoInstantBefore = find(GRIBTimeInMS ≤ TIMEMS(i),1,'last');
    timeIDXtoInstantAfter  = find(GRIBTimeInMS ≥ TIMEMS(i),1,'first');
    timeBeforeAfter = [GRIBTimeInMS(timeIDXtoInstantBefore) ...
        GRIBTimeInMS(timeIDXtoInstantAfter)];

    lonIDXWest  = find(GRIBlon ≤ LON(i),1,'last');
    lonIDXEast  = find(GRIBlon ≥ LON(i),1,'first');

    latIDXNorth = find(GRIBlat ≥ LAT(i),1,'last');
    latIDXSouth = find(GRIBlat ≤ LAT(i),1,'first');

    Xlat = repmat(GRIBlat(latIDXNorth:latIDXSouth),[1,2]);

     if LON(i) > GRIBlon(end)
        lonIDXWest = GRIBlon(1);
        lonIDXEast = GRIBlon(end);
        Xlon = [lonIDXWest lonIDXEast; lonIDXWest lonIDXEast];

        %Concatenate
        %(time,lat,lon) -> (lat,lon,time)
        Cat    = cat(3,squeeze(MWD(timeIDXtoInstantBefore,sort(...
            latIDXNorth:latIDXSouth),[1 length(GRIBlon)])),...
            squeeze(MWD(timeIDXtoInstantAfter,sort(latIDXNorth:...
            latIDXSouth),[1 length(GRIBlon)])));
     else
        Xlon = repmat(GRIBlon(lonIDXWest:lonIDXEast)',[2,1]);
        %Concatenate
        %(time,lat,lon) -> (lat,lon,time)
        Cat    = cat(3,squeeze(MWD(timeIDXtoInstantBefore,sort(...
            latIDXNorth:latIDXSouth),sort(lonIDXWest:lonIDXEast))),...
            squeeze(MWD(timeIDXtoInstantAfter,sort(latIDXNorth:...
            latIDXSouth),sort(lonIDXWest:lonIDXEast))));
     end
    %Permute to get interpolated dimension first
    %(lat,lon,time) -> (time,lat,lon)

    %Changing NaN values to mean of the other values
    Cat(isnan(Cat(:,:,1))) = mean(Cat(not(isnan(Cat(:,:,1)))));
    Cat2 = Cat(:,:,2);
    Cat2(isnan(Cat2)) = mean(Cat2(not(isnan(Cat2))));
    Cat(:,:,2) = Cat2;


    Per = permute(Cat,[3 1 2]);

    %Interpolate over time
    if timeIDXtoInstantBefore == timeIDXtoInstantAfter
        TwoDimInterp = squeeze(Per(1,:,:));
    else
        try
            TwoDimInterp = squeeze(interp1(timeBeforeAfter,Per,TIMEMS(i)));
        catch
            disp('Some error');
        end
    end

    %Interpolate over position
```

```
336     ECMWF_Wd(i) = interp2(Xlon,Xlat,TwoDimInterp,LON(i),LAT(i)); %Wave direction
337 end
338
339 %Interpolating WavePeriod at time, lat and lon
340 fprintf('%s\n','--> Collecting WavePeriod data');
341 for i = 1:length(TIMEMS)
342     timeIDXtoInstantBefore = find(GRIBTimeInMS ≤ TIMEMS(i),1,'last');
343     timeIDXtoInstantAfter  = find(GRIBTimeInMS ≥ TIMEMS(i),1,'first');
344     timeBeforeAfter = [GRIBTimeInMS(timeIDXtoInstantBefore) ...
345         GRIBTimeInMS(timeIDXtoInstantAfter)];
346
347     lonIDXWest  = find(GRIBlon ≤ LON(i),1,'last');
348     lonIDXEast  = find(GRIBlon ≥ LON(i),1,'first');
349
350     latIDXNorth = find(GRIBlat ≥ LAT(i),1,'last');
351     latIDXSouth = find(GRIBlat ≤ LAT(i),1,'first');
352
353     Xlat = repmat(GRIBlat(latIDXNorth:latIDXSouth),[1,2]);
354
355      if LON(i) > GRIBlon(end)
356         lonIDXWest = GRIBlon(1);
357         lonIDXEast = GRIBlon(end);
358         Xlon = [lonIDXWest lonIDXEast; lonIDXWest lonIDXEast];
359
360         %Concatenate
361         %(time,lat,lon) -> (lat,lon,time)
362         Cat    = cat(3,squeeze(MWP(timeIDXtoInstantBefore,sort(...
363             latIDXNorth:latIDXSouth),[1 length(GRIBlon)])),...
364             squeeze(MWP(timeIDXtoInstantAfter,sort(latIDXNorth:...
365             latIDXSouth),[1 length(GRIBlon)])));
366      else
367         Xlon = repmat(GRIBlon(lonIDXWest:lonIDXEast)',[2,1]);
368         %Concatenate
369         %(time,lat,lon) -> (lat,lon,time)
370         Cat    = cat(3,squeeze(MWP(timeIDXtoInstantBefore,sort(...
371             latIDXNorth:latIDXSouth),sort(lonIDXWest:lonIDXEast))),...
372             squeeze(MWP(timeIDXtoInstantAfter,sort(latIDXNorth:...
373             latIDXSouth),sort(lonIDXWest:lonIDXEast))));
374      end
375     %Permute to get interpolated dimension first
376     %(lat,lon,time) -> (time,lat,lon)
377
378     %Changing NaN values to mean of the other values
379     Cat(isnan(Cat(:,:,1))) = mean(Cat(not(isnan(Cat(:,:,1)))));
380     Cat2 = Cat(:,:,2);
381     Cat2(isnan(Cat2)) = mean(Cat2(not(isnan(Cat2))));
382     Cat(:,:,2) = Cat2;
383
384     Per = permute(Cat,[3 1 2]);
385
386     %Interpolate over time
387     if timeIDXtoInstantBefore == timeIDXtoInstantAfter
388         TwoDimInterp = squeeze(Per(1,:,:));
389     else
390         try
391             TwoDimInterp = squeeze(interp1(timeBeforeAfter,Per,TIMEMS(i)));
392         catch
393             disp('Some error');
394         end
395     end
396
397     %Interpolate over position
398     ECMWF_Ts(i) = interp2(Xlon,Xlat,TwoDimInterp,LON(i),LAT(i)); %Wave period
399 end
400
401 ECMWF.Time           = TIMEMS;
402 ECMWF.UwindVelocity  = ECMWF_uW;
403 ECMWF.VwindVelocity  = ECMWF_vW;
```

```
404 ECMWF.WindVelocity   = sqrt(ECMWF_uW.^2 + ECMWF_vW.^2);
405 ECMWF.WindDirection  = VesselECMWF_WindDirection(ECMWF_uW,ECMWF_vW);
406 ECMWF.SignWaveHeight = ECMWF_Hs;
407 ECMWF.WaveDirection  = ECMWF_Wd;
408 ECMWF.WavePeriod     = ECMWF_Ts;
409
410 %Beaufort number
411 for i =1:length(TIMEMS)
412     if ECMWF.WindVelocity(i) ≤ 0.2
413         Beaufort(i) = 0;
414     elseif ECMWF.WindVelocity(i) ≤ 1.5
415         Beaufort(i) = 1;
416     elseif ECMWF.WindVelocity(i) ≤ 3.3
417         Beaufort(i) = 2;
418     elseif ECMWF.WindVelocity(i) ≤ 5.4
419         Beaufort(i) = 3;
420     elseif ECMWF.WindVelocity(i) ≤ 7.9
421         Beaufort(i) = 4;
422     elseif ECMWF.WindVelocity(i) ≤ 10.7
423         Beaufort(i) = 5;
424     elseif ECMWF.WindVelocity(i) ≤ 13.8
425         Beaufort(i) = 6;
426     elseif ECMWF.WindVelocity(i) ≤ 17.1
427         Beaufort(i) = 7;
428     elseif ECMWF.WindVelocity(i) ≤ 20.7
429         Beaufort(i) = 8;
430     elseif ECMWF.WindVelocity(i) ≤ 24.4
431         Beaufort(i) = 9;
432     elseif ECMWF.WindVelocity(i) ≤ 28.4
433         Beaufort(i) = 10;
434     elseif ECMWF.WindVelocity(i) ≤ 36.6
435         Beaufort(i) = 11;
436     else
437         Beaufort(i) = 12;
438     end
439 end
440
441 ECMWF.Beaufort     = Beaufort;
442 filepath = strcat(SaveToFolder,'ECMWF/','ECMWF_',yearStr,'_',...
443     num2str(g),'.mat');
444 %Saving to file
445 save(filepath,'ECMWF');
446 end
```

Appendix B

Data Analysis

B.1 main.m

```
% -------------------------------------------------------------------------
% Main script for calculating added power due to fouling by using
% in-service performance monitoring data.
%
% The main path to the directory where the MATLAB struct are stored needs
% to be spesified in line 37 and 38 in order to use the script
%
% The MATLAB struct should be named Data_w_Weather and contains the
% performance monitoring data combined with the weather data.
%
% The data struct should contain the following fields:
% -Beaufort - Beaufort number
% -Course - compass course of the ship 0:360 degrees
% -DraftMid - Draft midships in meters
% -RPM - Shaft Rotations per minute
% -ShaftPower - Shaft power in kilo watts
% -SignWaveHeight - Significant wave height in meters
% -SOG - speed over ground in knots
% -STW - speed through water in knots
% -Time - Time as datetimevariable
% -Timestamp - Timestamp in epoch (seconds)
% -Trim - Trim in meters
% -WaveDirection - Mean wave direction using compass direction 0:360 degrees
% -WavePeriod - Mean wave period in seconds
% -WindDirection - Wind direction using compass direction 0:360 degrees
% -WindVelocity - Wind speed in m/s
% -------------------------------------------------------------------------
% Created by:
% Kristian Ejdfors
% Created:      19/01/2019
% Last updated: 04/06/2019
% -------------------------------------------------------------------------

% Clears the workspace
clear; close all; clc;

folder = strcat(pwd,'/Data/');  % Path to folder where the data are stored
filename = 'Data_w_Weather_tot';  % Name of the stored data struct

% Load data struct with performance monitoring data
load(strcat(folder,filename,'.mat'),'Data_w_Weather');
% Load constants for the vessel
```

```
constants;

% Creating a struct containing the original data
Data_org = Data_w_Weather;

%% Data processing
% Removing data points where the vessel is accelerating
index = false(length(Data_org.STW),1);
for i = 1:length(Data_org.SOG)-1
    if  Data_org.Timestamp(i+1) - Data_org.Timestamp(i) < 10*60
        index(i) = true;
        index(i+1) = true;
    elseif abs(Data_org.SOG(i) - Data_org.SOG(i+1)) > 0.5 && ...
           Data_org.Timestamp(i+1) - Data_org.Timestamp(i) < 30*60
        index(i) = true;
        index(i+1) = true;
    end
end
names = fieldnames(Data_w_Weather);
for i = 1:length(names)
    Data_w_Weather.(names{i})(index) = [];
end

% Removing vessel speed < 8 knots, draft < 6 meters, |Trim| > 4 meters,
% |STW-SOG| > 1.5 knots, Significant wave height > 3 meters and RPM < 50
index = logical(remove_under_threshold(Data_w_Weather.STW,8) ...
    + remove_under_threshold(Data_w_Weather.SOG,8) + ...
    remove_under_threshold(Data_w_Weather.DraftMid,6) + ...
    remove_under_threshold(Data_w_Weather.RPM,50)+ ...
    not(remove_under_threshold(...
    abs(Data_w_Weather.STW-Data_w_Weather.SOG),1.5))+ ...
    not(remove_under_threshold(abs(Data_w_Weather.Trim),4))+ ...
    not(remove_under_threshold(Data_w_Weather.SignWaveHeight,3)));
for i = 1:length(names)
    Data_w_Weather.(names{i})(index) = [];
end

% Create mean values for draft and trim
draft_mid = Data_w_Weather.DraftMid;
i = 1;
n = 10;
draft = 0;
trim = 0;
a = 0;
while i < length(Data_w_Weather.DraftMid)
    while Data_w_Weather.Timestamp(i+1) - Data_w_Weather.Timestamp(i) < 60*60*2
        draft = draft + Data_w_Weather.DraftMid(i);
        trim = trim + Data_w_Weather.Trim(i);
        a = a+1;
        i = i+1;
        if i == length(Data_w_Weather.DraftMid)
            break
        end
    end
    if a > 0
        draft = round(draft/a,2);
        trim = round(trim/a,2);
        Data_w_Weather.DraftMid(i-a:i) = draft;
        Data_w_Weather.Trim(i-a:i) = trim;
    end
    i = i+1;
    a = 0;
    draft = 0;
    trim = 0;
end
% Removing draft < 6 meters and |Trim| > 4 meters,
index = logical(remove_under_threshold(Data_w_Weather.DraftMid,6) + ...
    not(remove_under_threshold(abs(Data_w_Weather.Trim),4)));
```

```
111 for i = 1:length(names)
112     Data_w_Weather.(names{i})(index) = [];
113 end
114 
115 %% Calculating volumedisplacement
116 %assuming only changes in draft, all other patameters are constant i.e.
117 %vertical sides, Cb constant
118 Data_w_Weather.Displacement = B*l_pp*C_b*Data_w_Weather.DraftMid;
119 Data_org.Displacement = B*l_pp*C_b*Data_org.DraftMid;
120 
121 %% Calculating wetted surface
122 Data_w_Weather.WettedSurface = zeros(length(Data_w_Weather.DraftMid),1);
123 for i = 1:length(Data_w_Weather.DraftMid)
124 Data_w_Weather.WettedSurface(i) = estimate_wetted_surface(...
125     Data_w_Weather.DraftMid(i));
126 end
127 
128 %% Calculating Admiralty constant
129 Data_w_Weather.Admiralty = ((Data_w_Weather.Displacement.*1025).^(2/3)).* ...
130     ((Data_w_Weather.STW.*0.54444).^3)./(Data_w_Weather.ShaftPower*1000);
131 Data_org.Admiralty = ((Data_org.Displacement.*1025).^(2/3)).* ...
132     ((Data_org.STW.*0.54444).^3)./(Data_org.ShaftPower*1000);
133 
134 %% Create data struct with only calmwater data
135 Data_CW = Data_w_Weather; %Creating new data struct
136 % Removing data points with Beafourt wind class above 3 and
137 % significant wave height larger than 1 meters
138 index_wind = find(Data_CW.Beaufort ≤ 3);
139 names = fieldnames(Data_CW);
140 %Removing values with Beafourt number larger than 3
141  for i = 1:length(names)
142      Data_CW.(names{i}) = Data_w_Weather.(names{i})(index_wind);
143  end
144 % Removing data points with significant wave height larger than 1 meters
145 index_wave = find(Data_CW.SignWaveHeight ≤ 1);
146 %Removing values with Beafourt number larger than 3
147  for i = 1:length(names)
148      Data_CW.(names{i}) = Data_CW.(names{i})(index_wave);
149  end
150 
151 %% Benchmark model
152 [C,¬,¬] = unique(Data_CW.STW); %unique speeds
153 min_val = zeros(length(C),1);
154 % finds corresponding minimum shaft power and speed
155 for i = 1:length(C)
156     index = find(Data_CW.STW == C(i));
157     min_val(i) = min(Data_CW.ShaftPower(index));
158 end
159 % Creates the benchmark model
160  q = fit(C,min_val,'exp1');
161  q1 = 304.1*exp(0.192*C);
162 % Plotting benchmark PS-curve
163 figure()
164 hold on
165 grid on
166 grid minor
167 scatter(Data_CW.STW,Data_CW.ShaftPower)
168 plot(C,q1,'LineWidth',3)
169 xlabel('Speed through water [knots]')
170 ylabel('Shaft power [kW]')
171 legend('Data','304.1e^{0.192x}')
172 set(gca,'fontsize',20)
173 
174 %% Method 1
175 % Calculate added power based on Admiralty Coefficient
176 Data_CW.Added_power_Admiralty = added_power_admiralty(Data_CW,18);
177 % Calculate added power based on resistance coefficient
178 [Data_CW.AddedPower_res_coeff, Data_CW.Res_coeff] = ...
```

```
    added_power_resistance_coeff(Data_CW);
% Plotting added resistance diagram for Method 1
figure()
added_res_diagram(Data_CW.Time,Data_CW.Timestamp,...
    Data_CW.Added_power_Admiralty,false)
ylim([-50 150])
ylabel('Increase of shaft power [%]')
xlabel('Time')
set(gca,'fontsize',20)

figure()
added_res_diagram(Data_CW.Time,Data_CW.Timestamp,...
    Data_CW.AddedPower_res_coeff,false)
set(gca,'fontsize',20)
ylabel('Increase of shaft power [%]')
xlabel('Time')

%% Method 2
% Calculating added power due to wind and waves
R_aa = zeros(length(Data_w_Weather.Timestamp),1);
R_aw = zeros(length(Data_w_Weather.Timestamp),1);
for i = 1:length(Data_w_Weather.STW)
% Calculating wind resistance
R_aa(i) = Wind_resistance(Data_w_Weather.WindVelocity(i), ...
    Data_w_Weather.WindDirection(i), Data_w_Weather.Course(i));
% Calculating wave resistance
R_aw(i) = Wave_resistance(Data_w_Weather.SignWaveHeight(i), ...
    Data_w_Weather.WaveDirection(i), Data_w_Weather.WavePeriod(i), ...
    Data_w_Weather.DraftMid(i),Data_w_Weather.STW(i), ...
    Data_w_Weather.Course(i));
end
% Converting added resistance due to wind and waves to added power in kW
d_power = ((R_aa + R_aw).*(Data_w_Weather.STW*0.51444))./1000;
Data_mod = Data_w_Weather;  %creating a new data struct for Method 2

%Removing effect from enviromental forces
Data_mod.ShaftPower = Data_mod.ShaftPower - d_power;
Data_mod.Admiralty = ((Data_mod.Displacement.*1025).^(2/3)).* ...
    ((Data_mod.STW.*0.54444).^3)./(Data_mod.ShaftPower*1000);

% Calculate added power based on Admiralty Coefficient
Data_mod.AddedPower_Admiralty = added_power_admiralty(Data_mod,18);
% Calculate added power based on resistance coefficient
[Data_mod.AddedPower_res_coeff,Data_mod.Res_coeff] = ...
    added_power_resistance_coeff(Data_mod);

% Plotting added resistance diagram for Method 2
figure()
added_res_diagram(Data_mod.Time,Data_mod.Timestamp,...
    Data_mod.AddedPower_Admiralty,false)
set(gca,'fontsize',20)
ylim([-50 150])
ylabel('Increase of shaft power [%]')
xlabel('Time')

figure()
added_res_diagram(Data_mod.Time,Data_mod.Timestamp,...
    Data_mod.AddedPower_res_coeff,false)
set(gca,'fontsize',20)
ylim([-20 100])
ylabel('Increase of shaft power [%]')
xlabel('Time')

%% Method 3
% Creating new data struct to be used in training the model
ML_data = Data_w_Weather;
% Creating new data struct without the training data to be used in the
% Analysis
```

```
247 data_without_training_data = Data_w_Weather;
248
249 time_val = 1429048800; %Timestamp for 1 year after delivery
250 index_time1 = find(ML_data.Timestamp > time_val);
251 index_time2 = find(Data_w_Weather.Timestamp < time_val);
252 names = fieldnames(ML_data);
253 for i=1:length(names)
254     % Data for the first year of operation
255     ML_data.(names{i})(index_time1) = [];
256     % Data witout the first year of operation
257     data_without_training_data.(names{i})(index_time2) = [];
258 end
259
260 % Calculate relative wind and wave angle
261 ML_data.WindDirection(ML_data.WindDirection > 180) = ...
262     ML_data.WindDirection(ML_data.WindDirection > 180) - 360;
263 ML_data.WaveDirection(ML_data.WaveDirection > 180) = ...
264     ML_data.WaveDirection(ML_data.WaveDirection > 180) - 360;
265 ML_data.Course(ML_data.Course > 180) = ...
266     ML_data.Course(ML_data.Course > 180) - 360;
267 ML_data.rel_wind_dir = zeros(length(ML_data.Course),1);
268 ML_data.rel_wave_dir = zeros(length(ML_data.Course),1);
269 for i = 1:length(ML_data.Course)
270     if ML_data.WindDirection(i) > 0 && ML_data.Course(i) > 0
271         ML_data.rel_wind_dir(i) = abs(ML_data.WindDirection(i) - ML_data.Course(i));
272     elseif ML_data.WindDirection(i) < 0 && ML_data.Course(i) < 0
273         ML_data.rel_wind_dir(i) = abs(ML_data.WindDirection(i) - ML_data.Course(i));
274     elseif ML_data.WindDirection(i) < 0 && ML_data.Course(i) > 0
275         ML_data.rel_wind_dir(i) = abs(ML_data.WindDirection(i) + ML_data.Course(i));
276     elseif ML_data.WindDirection(i) > 0 && ML_data.Course(i) < 0
277         ML_data.rel_wind_dir(i) = abs(ML_data.WindDirection(i) + ML_data.Course(i));
278     end
279
280     if ML_data.WaveDirection(i) > 0 && ML_data.Course(i) > 0
281         ML_data.rel_wave_dir(i) = abs(ML_data.WaveDirection(i) - ML_data.Course(i));
282     elseif ML_data.WaveDirection(i) < 0 && ML_data.Course(i) < 0
283         ML_data.rel_wave_dir(i) = abs(ML_data.WaveDirection(i) - ML_data.Course(i));
284     elseif ML_data.WaveDirection(i) < 0 && ML_data.Course(i) > 0
285         ML_data.rel_wave_dir(i) = abs(ML_data.WaveDirection(i) + ML_data.Course(i));
286     elseif ML_data.WaveDirection(i) > 0 && ML_data.Course(i) < 0
287         ML_data.rel_wave_dir(i) = abs(ML_data.WaveDirection(i) + ML_data.Course(i));
288     end
289 end
290
291 % Creating index to split the data for the first year into a training and
292 % validation set
293 amount_trainingData = round(0.8*length(ML_data.ShaftPower));
294 random_index = randperm(length(ML_data.ShaftPower),amount_trainingData);
295
296 %Time from delivery
297 ML_data.d_time = ML_data.Timestamp - ML_data.Timestamp(1);
298
299 % Training models and finding relative prediction error for the different
300 % input sets
301 for k = 1:7
302 names = defining_input_param(k);
303 clear data_2_trainingSet
304 clear data_2_validationSet
305 temp = ML_data;
306 for i = 1:length(names)
307     data_2_trainingSet.(names{i}) = ...
308         ML_data.(names{i})(random_index); %Training data
309     temp.(names{i})(random_index) = [];
310     if i == length(names)
311         y_val = temp.(names{i}); %True value for validation set
312          break
313     end
314     data_2_validationSet.(names{i}) = temp.(names{i});
```

```
end

%Struct to Table in order to use ML model
training_set = struct2table(data_2_trainingSet);
validation_set = struct2table(data_2_validationSet);

% Gaussian Regression model
gprMdl_bench = fitrgp(training_set,'ShaftPower',...
    'KernelFunction','squaredexponential');
% Predict values from Gaussian Regression model
GR_shaftpower_pred = predict(gprMdl_bench,validation_set);
% mean prediction error for the inputset number k
mean_pred_error_GR(k) = mean(abs((y_val-GR_shaftpower_pred)./y_val))*100;

% Linear Regression model
mdl = fitlm(training_set);
%Predict values from Linear Regression model
LR_shaftpower_pred = predict(mdl,validation_set);
% mean prediction error for the inputset number k
mean_pred_error_LR(k) = mean((abs(y_val-LR_shaftpower_pred)./y_val))*100;

% Custom Linear Regression model
training_set_custom = training_set;
validation_set_custom = validation_set;
for i =1:length(names)
    if strcmp(names{i},'DraftMid')
        training_set_custom.(names{i}) = training_set_custom.(names{i}).^(2/3);
        validation_set_custom.(names{i}) = validation_set_custom.(names{i}).^(2/3);
    elseif strcmp(names{i},'STW')
        training_set_custom.(names{i}) = training_set_custom.(names{i}).^3;
        validation_set_custom.(names{i}) = validation_set_custom.(names{i}).^3;
    elseif strcmp(names{i},'RPM')
        training_set_custom.(names{i}) = training_set_custom.(names{i}).^3;
        validation_set_custom.(names{i}) = validation_set_custom.(names{i}).^3;
    end
end
mdl_custom = fitlm(training_set_custom);
LR_custom_shaftpower_pred = predict(mdl_custom,validation_set_custom);
% mean prediction error for the inputset number k
mean_pred_error_LR_custom(k) = mean(abs((y_val-LR_custom_shaftpower_pred)./y_val))*100;
end

% Plot the mean prediction error for the input sets
figure()
hold on
bar([1:k],[mean_pred_error_LR;mean_pred_error_LR_custom;mean_pred_error_GR]')
legend('Linear Regression','Custom Linear Regression','Gaussian Regression')
xlabel('Input set')
ylabel('Mean prediction error [%]')
ylim([0.9*min(mean_pred_error_GR) 1.05*max(mean_pred_error_LR)])
set(gca,'FontSize',20)

% Analysis

% Load Machine learning model for input set 4
filename_GR = strcat(folder,'GR_input_4.mat');
filenime_CLR = strcat(folder,'CLR_input_4.mat');
load(filename_GR);
load(filenime_CLR);

GR_model = gprMdl2;
LR_model = mdl_custom;

% Create data set that can be used in the analysis, which means that it
% contains values only for input set 4 and without the first year of
% operation
Data_method3 = data_without_training_data;
input_no = 4;
```

```
input_predictions_GR = input_to_Method3(Data_method3,input_no);

% Custom Linear Regression
input_predictions_custom_LR = input_predictions_GR;
names = defining_input_param(4);
for i =1:length(names)
    if strcmp(names{i},'DraftMid')
        input_predictions_custom_LR.(names{i}) = ...
            input_predictions_custom_LR.(names{i}).^(2/3);
    elseif strcmp(names{i},'STW')
        input_predictions_custom_LR.(names{i}) = ...
            input_predictions_custom_LR.(names{i}).^3;
    elseif strcmp(names{i},'RPM')
        input_predictions_custom_LR.(names{i}) = ...
            input_predictions_custom_LR.(names{i}).^3;
    end
end
% Shaft power predictions
GR_ShaftPower = predict(GR_model,input_predictions_GR);
LR_custom_ShaftPower = predict(LR_model,input_predictions_custom_LR);

% Relative prediction error
pred_error_GR = ((data_without_training_data.ShaftPower-GR_ShaftPower)./...
    data_without_training_data.ShaftPower)*100;
pred_error_LR = ((data_without_training_data.ShaftPower-...
    LR_custom_ShaftPower)./data_without_training_data.ShaftPower)*100;

% Plotting relative prediction error over time
figure()
added_res_diagram(data_without_training_data.Time,...
    data_without_training_data.Timestamp,pred_error_LR,false)
ylabel('Relative prediction error [%]')
xlabel('Time')
ylim([-50 100])
set(gca,'fontsize',20)

figure()
added_res_diagram(data_without_training_data.Time,...
    data_without_training_data.Timestamp,pred_error_GR,false)
ylabel('Relative prediction error [%]')
xlabel('Time')
set(gca,'fontsize',20)
```

B.2 constants.m

```
%-------------------------------------------------------------------------
%  This file contains constant parameters to be used in calculations
%-------------------------------------------------------------------------

% The mass density of air in kg/m^3:
rho_a = 1.225;
% The gravitational acceleration in m/ s ^2:
g = 9.81;
% The water densisty in kg/m^3
rho_s = 1025.89;
% Kinematic viscosity for 15 degrees celsius
nu = 1.18830 * 10^-6;

% Dates for Propeller polish
Propell_polish = datetime({'18-11-2015','02-07-2016','10-02-2017'},...
    'InputFormat','dd-MM-yyyy');
Propell_polish_timestamp = [1447804800; 1467417600; 1486684800];
% Dates for Hull cleaning
```

```
Hull_cleaning = datetime('26-09-2017','InputFormat','dd-MM-yyyy');
Hull_cleaning_timestamp = 1506384000;
%Propulsion efficiancy
eta_d = 0.7;

%----------Ship parameters ----------%
%length overall in meters
l_oa = 208.9;
%length between perpendiculars in meters
l_pp = 196.90;
%Breath in meters
B = 29.8;
%Design Draught in meters
T_d = 10.10;
%Design displacement [m^3]
Volume_d = 37718.6;
%Block coefficient
C_b = Volume_d/(l_pp*B*T_d);
%bow distance to 95% of max breadth
l_bwl = 25;
%Transverse area above waterline
A_XV = 580;
%Design Wetted Surface (estimated)
wetted_surface_design = 6922.044023317390;
```

B.3 estimate_wetted_surface.m

```
function S = estimate_wetted_surface(draft)
%------------------------------------------------------------------------
% Returns estimate the wetted surface in square meters
% input: draft midship in meter
%------------------------------------------------------------------------

% Load constants
constants;
B_T_ratio = B/draft;
volume_displacement = B*draft*l_pp*C_b;
% Values for Cm 0.9 based on figure from TMR4105 Marin Teknikk Grunnlag
% compendium
k_vec = [2.75 2.7 2.65 2.62 2.60 2.58 2.56 2.54...
    2.54 2.56 2.58 2.60 2.62 2.65];
B_T_ratio_vec = [1.684 1.868 2.040 2.158 2.250 2.355 2.48 2.55 ...
    3.42 3.50 3.684 3.868 4.05 4.342];
if B_T_ratio < B_T_ratio_vec(1)
    k = k_vec(1);
elseif B_T_ratio > B_T_ratio_vec(end)
    k = k_vec(end);
else
    k = interp1(B_T_ratio_vec,k_vec,B_T_ratio);
end
S = k*sqrt(volume_displacement*l_pp);
end
```

B.4 added_power_admiralty.m

```
function added_power = added_power_admiralty(data,velocity)
%------------------------------------------------------------------------
```

```
% Returns the added power in percent based on the Admiralty coefficient
% Input parameters:
% data - MATLAB struct containing Admiralty coefficient for the vessel
% velocity - desired velocity in knots
%--------------------------------------------------------------------------

%load constants
constants;
% Estimated power based on the Admiralty coefficient
est_power = ((((Volume_d*1025)^(2/3)*(velocity*0.5144)^3)./...
    data.Admiralty))./1000;
% Design power from benchmark
design_power = (304.1*exp(0.192*velocity));
% Added power
added_power = -((design_power- (est_power))./design_power)*100;
end
```

B.5 added_power_resistance_coeff.m

```
function [added_power, dC_f] = added_power_resistance_coeff(data)
%--------------------------------------------------------------------------
% Returns the added power in percent based on the Resistance coefficient
% and the resistance coefficient
% Input parameters:
% data - MATLAB struct containing the following fields
% ShaftPower - Shaft power in kW
% STW - Speed through water in knots
% WettedSurface - Wetted surface area in square meters
%--------------------------------------------------------------------------
%load constants
constants;
%Calculate resistance coefficient
R_Ts_meassured = data.ShaftPower.*eta_d./(data.STW*0.5144);
R_Ts_bench = (304.1*exp(0.192*data.STW)).*eta_d./(data.STW*0.5144);
C_Ts_meassured = R_Ts_meassured./(0.5*rho_s*((data.STW*0.5144).^2).*...
    data.WettedSurface);
C_Ts_bench = R_Ts_bench./(0.5*rho_s*((data.STW*0.5144).^2).*...
    wetted_surface_design);
dC_f = C_Ts_meassured - C_Ts_bench;

added_power = ((dC_f.*0.5.*rho_s.*data.WettedSurface.*eta_d.*...
    ((data.STW*0.5144).^3))./(304.1*exp(0.192*data.STW)))*100;
end
```

B.6 Wind_resistance.m

```
function R_aa = Wind_resistance(wind_vel,wind_dir,heading)
%--------------------------------------------------------------------------
% Calculating wind resistance based on the method described in ISO 15016
% returns the wind resistance in Newtons
% Input parameters:
% wind_vel - Wind speed in m/s
% wind_dir - Wind direction using compass direction 0:360 degrees
% heading - compass course of the ship 0:360 degrees
%--------------------------------------------------------------------------
constants;  %loading constants
% Calculating relative wind direction between 0-180 degrees
```

```
wind_dir(wind_dir > 180) = ...
    wind_dir(wind_dir > 180) - 360;
heading(heading > 180) = ...
    heading(heading > 180) - 360;
rel_wind_dir = zeros(length(heading),1);
for i = 1:length(heading)
    if wind_dir(i) > 0 && heading(i) > 0
        rel_wind_dir(i) = abs(wind_dir(i) - heading(i));
    elseif wind_dir(i) < 0 && heading(i) < 0
        rel_wind_dir(i) = abs(wind_dir(i) - heading(i));
    elseif wind_dir(i) < 0 && heading(i) > 0
        rel_wind_dir(i) = abs(wind_dir(i) + heading(i));
    elseif wind_dir(i) > 0 && heading(i) < 0
        rel_wind_dir(i) = abs(wind_dir(i) + heading(i));
    end
end

% C_AA values taken from figure C.2 in ISO 15016
C_AA = [-0.6565 -0.7139 -0.7408 -0.7070 -0.6433 -0.3939 -0.2458 -0.2190 ...
    -0.2832 -0.0544 0.3361 0.6459 0.8646 0.8109 0.6358];
% Angle of attack for C_AA values
aoa = [0 8.25 15.75 23.56 30.34 45.91 60.83 75.46 90.11 104.66 119.50 ...
    134.71 149.26 164.59 180];
% interpolating to find C_aa values
C_aa = -interp1(aoa,C_AA,rel_wind_dir);
% Calculate wind resistance
R_aa = 0.5*rho_a*C_aa*A_XV*(wind_vel*cosd(rel_wind_dir))^2;
end
```

B.7 Wave_resistance.m

```
function R_aw = Wave_resistance(H_s,wave_dir,T_01,T_m,V_s,heading)
%-------------------------------------------------------------------------
%Calculating wave resistance based on the method described in ISO 15016
%returns the wave resistance in Newtons
% Input parameters:
% H_s - Significant wave height in meters
% wave_dir - Mean wave direction using compass direction 0:360 degrees
% T_01 - Mean wave period in seconds
% T_m - Draft midships in meters
% V_s - Speed through water in knots
% heading - compass course of the ship 0:360 degrees
%-------------------------------------------------------------------------
%load constants and ship characteristics
constants;

%finding relative wave direction
wave_dir(wave_dir > 180) = ...
    wave_dir(wave_dir > 180) - 360;
heading(heading > 180) = ...
    heading(heading > 180) - 360;
rel_wave_dir = zeros(length(heading),1);
for i = 1:length(heading)
    if wave_dir(i) > 0 && heading(i) > 0
        rel_wave_dir(i) = abs(wave_dir(i) - heading(i));
    elseif wave_dir(i) < 0 && heading(i) < 0
        rel_wave_dir(i) = abs(wave_dir(i) - heading(i));
    elseif wave_dir(i) < 0 && heading(i) > 0
        rel_wave_dir(i) = abs(wave_dir(i) + heading(i));
    elseif wave_dir(i) > 0 && heading(i) < 0
        rel_wave_dir(i) = abs(wave_dir(i) + heading(i));
    end
end
```

```
33
34 %Convert from knots to m/s
35 V_s = V_s * (1852/3600);
36 %Calculate Froude number
37 Fr = V_s/sqrt(g*l_pp);
38
39 R_aw = 0;
40
41 %Defining integration intervall
42 om_start  = 2*pi/25;
43 om_stop = 2*pi/4;
44 d_om = 0.1;
45 %Criteria to use STAWAVE 1
46 crit = 2.25*sqrt(l_pp/100);
47
48 %Criteria to use STAWAVE 2
49 if (2.2 < B/T_m && B/T_m < 9) && (0.1 < Fr && Fr < 0.3)
50     crit_STAWAVE_2 = true;
51 else
52     crit_STAWAVE_2 = false;
53 end
54
55 %STAWAVE-1 calculations
56 if H_s ≤ crit && rel_wave_dir ≤ 45
57     R_aw = 1/16 * rho_s * g * H_s^2 * B * sqrt(B/l_bwl);
58 elseif H_s ≤ crit && rel_wave_dir > 45
59     R_aw = 0;
60
61 %STAWAVE-2 calculations
62 elseif H_s > crit && rel_wave_dir ≤ 45 && crit_STAWAVE_2
63
64     for omega = om_start:d_om:om_stop
65         [R_wave, S_eta] = STAWAVE_2(omega,T_01,H_s,V_s,T_m);
66         a = 2*(R_wave)*S_eta*d_om;
67         R_aw = R_aw + a;
68     end
69
70 elseif  H_s > crit && rel_wave_dir > 45 && crit_STAWAVE_2
71     R_aw = 0;
72 end
73 end
```

B.8 STAWAVE_2.m

```
1  function [R_wave, S_eta] = STAWAVE_2(omega,T_01,H_s,V_s,T_m)
2  %------------------------------------------------------------------------
3  % STAWAVE-2 Calculations as defined in ISO 15016
4  % returns:
5  % R_wave - mean resistance in regular waves in newtons
6  % S_eta - is the frequency spectrum in square meters seconds, for the given
7  % omega
8  % Input parameters:
9  % omega - circular frequency of regular waves in radians per second
10 % T_01 - Mean wave period in seconds
11 % H_s - Significant wave height in meters
12 % V_s - Speed through water in knots
13 % T_m - Draft mid in meters
14 %------------------------------------------------------------------------
15
16 %load constants and ship characteristics
17 constants;
18 %Convert from knots to m/s
19 V_s = V_s * (1852/3600);
```

```
Fr = V_s/sqrt(g*l_pp);
% The non dimensional radius of gyration in the lateraldirection:
k_yy = 0.25*l_pp;
%Wave numer in rad/s
k = omega^2/g;

omega_bar = ((sqrt(l_pp/g)*k_yy^(1/3))/(1.17*Fr^(-0.143)))*omega;
if omega_bar < 1
    b_1 = 11;
    d_1 = 14;
else
    b_1 = -8.50;
    d_1 = -566*(l_pp/B)^-2.66;
end
a_1 = 60.3*C_b^1.34;
r_aw = omega_bar^b_1 * exp(b_1/d_1 * (1 - omega_bar^d_1)) * a_1*Fr^1.5 ...
    * exp(-3.5*Fr);
R_awml = 4 * rho_s * g * (B^2/l_pp) * r_aw;
f_1 = 0.692*((V_s/(sqrt(T_m * g)))^0.769) * 1.81*C_b^6.95;
% The modified bessel function of the f i r s t kind of order 1:
I_1 = besseli(1,1.5*k*T_m);
% The modified bessel function of the second kind of order 1:
K_1 = besselk(1,1.5*k*T_m);
alpha_1 = ((pi^2 * I_1^2)/(pi^2 * I_1^2 + K_1^2))*f_1;
R_awrl = 0.5* rho_s * g * B * alpha_1;

R_wave = R_awml + R_awrl;

%Pierson-Moskowitz Wave spectrum
A_fw = 173 * (H_s^2/(T_01^4));
B_fw = 691/(T_01^4);
S_eta = A_fw/(omega^5) * exp(-B_fw/(omega^4));
end
```

B.9 defining_input_param.m

```
function input_set = defining_input_param(input_set_no)
%-------------------------------------------------------------------------
% Gives names of input parameters to Method 3 based the input set number
%-------------------------------------------------------------------------
switch input_set_no
    case 1
        input_set = {'STW','DraftMid','Trim','ShaftPower'};
    case 2
        input_set = {'STW','DraftMid','Trim','WindVelocity',...
            'rel_wind_dir','ShaftPower'};
    case 3
        input_set = {'STW','DraftMid','Trim','SignWaveHeight',...
            'rel_wave_dir','WavePeriod','ShaftPower'};
    case 4
        input_set = {'STW','DraftMid','Trim','WindVelocity',...
            'rel_wind_dir','SignWaveHeight','rel_wave_dir',...
            'WavePeriod','ShaftPower'};
    case 5
        input_set = {'d_time','STW','DraftMid','Trim','ShaftPower'};
    case 6
        input_set = {'STW','DraftMid','ShaftPower'};
    case 7
        input_set = {'d_time','STW','DraftMid','Trim','WindVelocity',...
            'rel_wind_dir','SignWaveHeight','rel_wave_dir','WavePeriod',...
            'ShaftPower'};
end
```

B.10 input_to_Method3.m

```
function [input_to_ML] = input_to_Method3(Data,input_set_no)
%-------------------------------------------------------------------------
% Creates a table containing input variables to be used in Method 3
%-------------------------------------------------------------------------

% Calculating relative wind and wave angle
Data.WindDirection(Data.WindDirection > 180) = ...
    Data.WindDirection(Data.WindDirection > 180) - 360;
Data.WaveDirection(Data.WaveDirection > 180) = ...
    Data.WaveDirection(Data.WaveDirection > 180) - 360;
Data.Course(Data.Course > 180) = ...
    Data.Course(Data.Course > 180) - 360;

Data.rel_wind_dir = zeros(length(Data.Course),1);
Data.rel_wave_dir = zeros(length(Data.Course),1);

for i = 1:length(Data.Course)
    if Data.WindDirection(i) > 0 && Data.Course(i) > 0
        Data.rel_wind_dir(i) = abs(Data.WindDirection(i) - Data.Course(i));
    elseif Data.WindDirection(i) < 0 && Data.Course(i) < 0
        Data.rel_wind_dir(i) = abs(Data.WindDirection(i) - Data.Course(i));
    elseif Data.WindDirection(i) < 0 && Data.Course(i) > 0
        Data.rel_wind_dir(i) = abs(Data.WindDirection(i) + Data.Course(i));
    elseif Data.WindDirection(i) > 0 && Data.Course(i) < 0
        Data.rel_wind_dir(i) = abs(Data.WindDirection(i) + Data.Course(i));
    end

    if Data.WaveDirection(i) > 0 && Data.Course(i) > 0
        Data.rel_wave_dir(i) = abs(Data.WaveDirection(i) - Data.Course(i));
    elseif Data.WaveDirection(i) < 0 && Data.Course(i) < 0
        Data.rel_wave_dir(i) = abs(Data.WaveDirection(i) - Data.Course(i));
    elseif Data.WaveDirection(i) < 0 && Data.Course(i) > 0
        Data.rel_wave_dir(i) = abs(Data.WaveDirection(i) + Data.Course(i));
    elseif Data.WaveDirection(i) > 0 && Data.Course(i) < 0
        Data.rel_wave_dir(i) = abs(Data.WaveDirection(i) + Data.Course(i));
    end

end

%Defining input parameters for model
names = defining_input_param(input_set_no);
for i = 1:length(names)-1
    data_2_input.(names{i}) = ...
        Data.(names{i});
end
%Struct to Table in order to use ML model
input_to_ML = struct2table(data_2_input);
end
```

Kristian Olof Ejdfors

Use of in-service data to determine the added power of a ship due to fouling

NTNU
Norwegian University of
Science and Technology